Josef Bauchinger, BSc

Mission Analysis for a Passive Reflectometry Mission

Master's Thesis

zur Erlangung des akademischen Grades
Master of Science

eingereicht an der
Graz University of Technology

Betreuer
Univ.-Prof. Dipl.-Ing. Dr.techn. Otto Koudelka

Institut für Kommunikationsnetze und Satellitenkommunikation

Graz, April 2018

Statutory Declaration

I declare that I have authored this thesis independently, that I have not used other than the declared sources/resources, and that I have explicitly marked all material which has been quoted either literally or by content from the used sources.

Graz, _____   _____

  Date   Signature

Abstract

There are more than enough reasons for science (e.g. climate change research) and economy (e.g. shipping) to know the exact altitude of sea and ice areas. Equally interesting as the altitudes are some characteristics such as roughness, wind direction and wind speed for sea areas or thickness and surface roughness for ice surfaces. Of course, it would be the best to obtain all these information simultaneously for the whole Earth. A good way to obtain these information on a global level is satellite remote sensing. In satellite remote sensing, one or more satellites orbit the Earth and, by using a wide variety of measurement techniques, acquire diverse types of information about the Earth. One of these measurement techniques is passive reflectometry. Passive reflectometry measures and compares the direct and the earth-reflected electromagnetic signal of an already existing source (e.g. a satellite of a global navigation satellite system). Out of the comparison, information (e.g. altitude) about the area where the signal was reflected can be obtained. This thesis deals with satellite missions which use passive reflectometry to gain information about the altitudes and characteristics of sea and ice areas. In order to conduct correct measurements, such missions have to gauge the approximate location of the reflection point of the electromagnetic signal before they can perform the measurements. The approximate reflection point is calculated by the use of the position data of the satellites and an model of the Earth. Different already existing and new methods to calculate the approximate reflection point are explained and discussed in this thesis. Furthermore, three of the methods discussed were evaluated with regard to their performance on board a satellite. Preliminary to the investigation of the reflection point calculation, the influence of the atmosphere on the refraction of an electromagnetic signal propagating through it was investigated. This was done in order to be able to estimate the influence of the refraction on the reflection point calculation and, if necessary, to take this influence into account for the evaluation. One conclusion of this thesis is, why only two of the three methods discussed are appropriate to calculate the reflection point on-board a cube satellite. A

second conclusion is why the refraction of an electromagnetic signal caused by the atmosphere can be neglected.

Key words:
reflectometry, reflection point calculation, GNSS-R, Binary Search for reflection point calculation, atmospheric refraction of an electromagnetic signal, cube satellite

Contents

Contents

Contents

x

1. Introduction

For the scientific research, like the research of climate change, it is of great interest to know the altitude changes of sea and ice areas. Additionally it is useful to have information on the thickness of ice areas. For the economy like shipping in turn, it is handy to have information on the wind speed and the wind direction of open sea areas. This information eases shipping in such areas. To obtain all these information on a global scale, one way would be to travel to all these destinations and perform measurements. Which is very difficult, costly and dangerous. Another way to gain these information on a global level is satellite remote sensing. The PRETTY (Passive REflectomeTry and dosimeTrY) mission is an upcoming European Space Agency (ESA) science mission, which is intended to perform sea and ice level altimetry with satellites of a global navigation satellite system (GNSS) as measurement signal source. PRETTY will be a three unit cube satellite planned, produced and operated under cooperation of RUAG Space, Graz University of Technology and Seibersdorf Laboratories.

In the following, the introductory chapter explains reflectometry in general, with a specific focus on passive reflectometry. It continuous with a description of global navigation satellite system reflectometry (GNSS-R) and some of its possible applications. After a brief explanation of the PRETTY mission, the chapter finally specifies the objective of the thesis.

1.1. Overview of reflectometry

In general, the term reflectometry refers to the measurement of signals reflected at an object. Basically, a transmitter emits a signal which is reflected at an object and the reflected signal is measured by a receiver. The measurements are evaluated to detect as well as describe and characterize the reflecting object. Measurement signals can be any kind of travelling waves, such as sonic waves under water or electromagnetic waves in free

space. The variety of existing reflectometry methods can be classified in terms of radiation form, measurement geometry, application, wave length and so on.

Since this thesis refers to the PRETTY mission, the used reflectometry method is assigned to the application class of satellite remote sensing. Satellite remote sensing uses electromagnetic waves as measurement signals. Furthermore, satellite remote sensing can be divided into active and passive satellite remote sensing, respectively reflectometry. According to Gleason and Gebre-Egziabher (2009, chapter 16), active and passive reflectometry differ with respect to the source of the measurement signal. Whereas in active reflectometry, a signal is deliberately emitted and its reflection measured, passive reflectometry detects the reflections of already existing sources. Figure 1.1 shows schemes of active and passive reflectometry. A simple and easily imaginable example for active reflectometry is radar or sonar on a boat. The sonar device in the hulk, for example, emits the sonic wave in the water and measures its reflection to determine the depth of the water. Human vision on the other hand is a good example for passive reflectometry. The sun or a light bulb is the signal source and the eye is the receiver for the reflected light. An object which appears completely black for example, simply does not reflect any light. An object which appears red, only reflects light in the specific wave length of red. With respect to satellite remote sensing, this means that missions using active reflectometry carry both the transmitter and the receiver on board. Whereas, missions using passive reflectometry only carry the receiver. Therefore, for passive reflectometry a sufficiently strong measuring signal source covering the areas to be investigated must be available. Possible sources could be television broadcasting satellites or satellites from a global navigation satellite system. Because of the global coverage and the rather high number of satellites, GNSS satellites are good choices as signal sources. The method to use GNSS satellites for passive reflectometry remote sensing satellite missions is called GNSS-R .

1.2. GNSS-R and some of its possible applications

GNSS-R was first introduced by Martin-Neira (1993) under the name PARIS (Passive Reflectometry and Interferometry System). The idea was to perform altimetry from space that covers large areas of sea or ice surfaces with some form of multi-beam measurement. Therefore, a GNSS-R mission measures
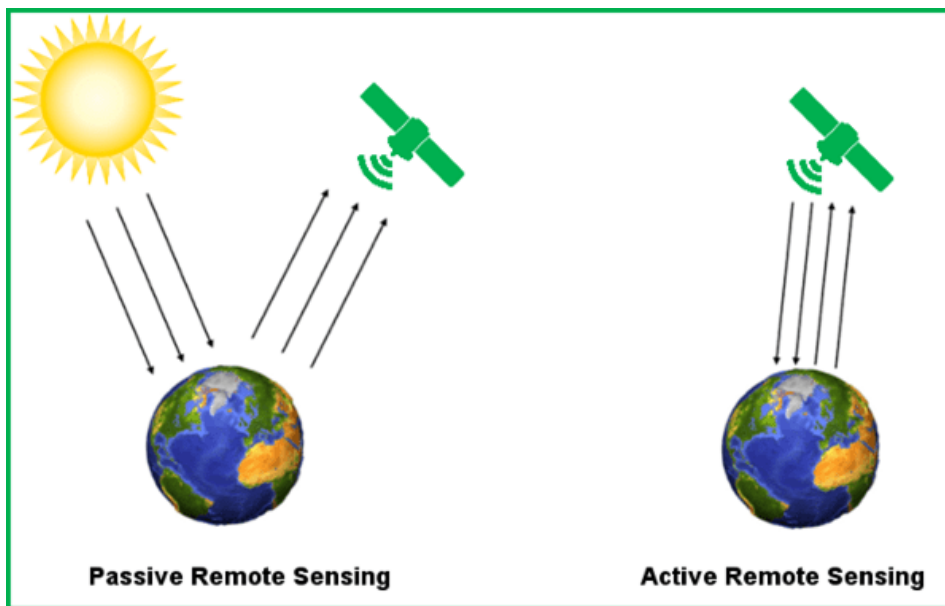
Figure 1.1.: Scheme of active and passive remote sensing (GrindGIS, 2017)

the directly received GNSS signal and the GNSS signal reflected by the Earth's surface, compares them and calculates the delay of the reflected signal. From this delay it is possible to gauge the altitude of the sea surface. Compared to the nadir looking active remote sensing method, GNSS-R is able to perform measurements also in other directions than nadir due to the use of reflected GNSS signals. Due to this ability, GNSS-R is directed towards the multi-beam measurement objective. Of course, with one GNSS receiver, GNSS-R can only measure one reflection point per processing chain. Another advantage of GNSS-R compared to active reflectometry is the absence of the transmitter for the measurement signal. This results in lower energy and space demand on board the satellite.

The biggest potential of GNSS-R applications is in the field of oceanographic research. Here, Martin-Neira (1993) and Gleason and Gebre-Egziabher (2009, chapter 16) do not only write about large scale ocean altimetry, they also mention the possibility to determine properties of the sea surface such as roughness, wind speed and wind direction. For more information refer to Martin-Neira (1993). In addition to measurements of sea surfaces, measurements of ice and land surface can be carried out too. Again, not only the altitudes of land and ice surfaces can be measured, parameters such as thickness, concentration or surface roughness can be obtained too

(see Zhu (2017) and Kostelecký, Klokocník, and Wagner (2005)). This is possible due to the measurement signal penetrating through the ice layer and generating additional reflections at subsurfaces. These parameters can be used to characterize different ice types such as new ice, thin first year ice or multiyear ice. On land surfaces, the reflected measurement signal has different characteristics, depending on the surface condition. These characteristics provide various information about the surface, such as ground vegetation or soil moisture.

1.3. The PRETTY mission

The PRETTY mission is a GNSS-R mission to perform sea and ice area altimetry from a satellite operating in a Low Earth Orbit (LEO). PRETTY uses one antenna to receive both the direct and the reflected signal. The advantage of this design is that both signals have to go through the same system path and therefore get influenced by the same inaccuracies. On the other hand, the design limits the possible measurement constellations for PRETTY. Due to the use of only one GNSS antenna, the antenna must be able to detect the direct and the reflected signal. Therefore, an elevation of the satellites above the horizontal plane is narrowed to approximately $0° \lessapprox ele \lessapprox 15°$. The horizontal plane is the plane which is tangential to the reflection point on the earth surface.

As described in the section above, to obtain the altitude of a surface, the GNSS-R mission has to calculate the delay of the earth-reflected GNSS signal compared to the direct GNSS signal. One way, as stated in Wickert (2016), to obtain the delay is to correlate the pseudo random noise (PRN) modulation of the direct and the earth-reflected signal with a local code replica of the PRN code of the GNSS signal. The correlation yields the code delay, related to the local code replica, for each signal and the difference of these code delays is the delay of the earth-reflected signal. The local code replicas necessary for the correlation are generated on-board the satellite. For the method using local code replicas, only the known modulations of the GNSS signal can be used for the correlation. Another way, which is used on-board PRETTY, is called interferometric approach. With the interferometric approach, the direct and the earth-reflected signal are correlated. Hence, no local code replica is necessary and the correlation directly yields the delay of the earth-reflected signal. The advantage of this method is that

unknown PRN modulations (e.g. military codes) of the GNSS signal still contribute to the signal power. To correlate the direct and the reflected signal the correlator has to know the approximate delay of the reflected signal. Otherwise it would have to store the whole direct signal and compare it with the whole reflected signal to determine the exact delay of the reflected signal. This is not possible due to the limited resources on-board a satellite.

1.4. Objective of the thesis

The objectives of this thesis are itemised below. Additionally, this section provides some input on these objectives.

Objectives:

- Investigation of the influence of the atmosphere on the refraction of an electromagnetic signal and its associated effects on the reflection point calculation.
- Find and discuss methods to calculate the reflection point for a snapshot of the measurement constellation.
- Implement and evaluate some of these methods.

As stated in the section above, the PRETTY mission has to gauge the approximate delay of the earth-reflected signal compared to the direct signal to perform correct measurements. Therefore, the reflection point of the earth-reflected signal has to be calculated on-board the satellite before the measurement is performed. The objective of this thesis is to find methods to calculate this reflection point. The methods should be able to perform the reflection point calculation for a snapshot of the measurement constellation and a model of the Earth. A snapshot of the measurement constellation means that the satellites are frozen in time. Hence, the satellites have fixed positions in relation to the earth model. The earth model to be used in this thesis shall be the World Geodetic System 1984 (WGS 84). Figure 1.2 shows a scheme of a possible GNSS-R measurement constellation on the northern hemisphere of the WGS 84. T is the transmitter satellite, R is the receiver satellite and S is the reflection point. Depending on the literature, the reflection point is also referred to as specular point. The solid line represents the direct signal path (SP_d) and the dotted line represents the reflected signal path (SP_r). For better visibility, the scheme is not true to scale.

Due to the changing conditions in the atmosphere (e.g. electron density, temperature), the propagation velocity of the electromagnetic signal changes. Therefore, the signal propagating through the atmosphere is delayed. This delay is caused mainly by the ionosphere (ionospheric delay) and can go up to 15 m. Additionally, the change of the propagation velocity causes a refraction of the electromagnetic signal. This refraction can influence the location of the reflection point and thereby cause a deviation of the signal path of the measurement signal. This deviation results an additional delay of the signal. Therefore, in addition to the reflection point calculation, this thesis also investigates the influence of the atmosphere on the refraction of an electromagnetic signal and the associated effects on the reflection point calculation. This is done in order to clarify, how much additional delay is caused by the influence of the atmosphere on the refraction of an electromagnetic signal and if this influence has to be taken into account for the reflection point calculation. Since the reflection point calculation in this thesis is performed for a snapshot of the measurement constellation, it does not matter when but only where (reflection point) the signal hits the Earth. Therefore, the ionospheric delay, although it occurs also for the snapshot of the measurement constellation, is neither investigated nor considered in this thesis. However, to set up the approximate delay for the comparison of the direct and the earth-reflected signal on-board the satellite, the ionospheric delay has to be taken into account.

According to section 1.3 and the text above, the method to calculate the reflection point has to fulfil the following requirements.

Requirements:

- The calculation method has to be applicable for a snapshot of the measurement constellation with the WGS 84 as earth model.
- The altitude of the transmitter satellite is $h_T = 20,000$ km.
- The altitude of the receiver satellite is $h_R = 600$ km.
- The elevation angle *ele* of the satellites over the horizontal plane has to be within $0° < ele < 15°$.
- The signal path difference (SP_{diff}) between the true reflected signal path (SP_r) and the calculated reflected signal path (SP_{rcalc}) is allowed to reach a maximum of 10 m $\rightarrow SP_{diff} < 10$ m.
- The calculation should require as little calculation time as possible.

The altitudes of the satellites are given by the operating altitude of global navigation satellite systems and the planned LEO for the PRETTY mission. *ele* is determined by the use of one GNSS antenna to receive both the direct
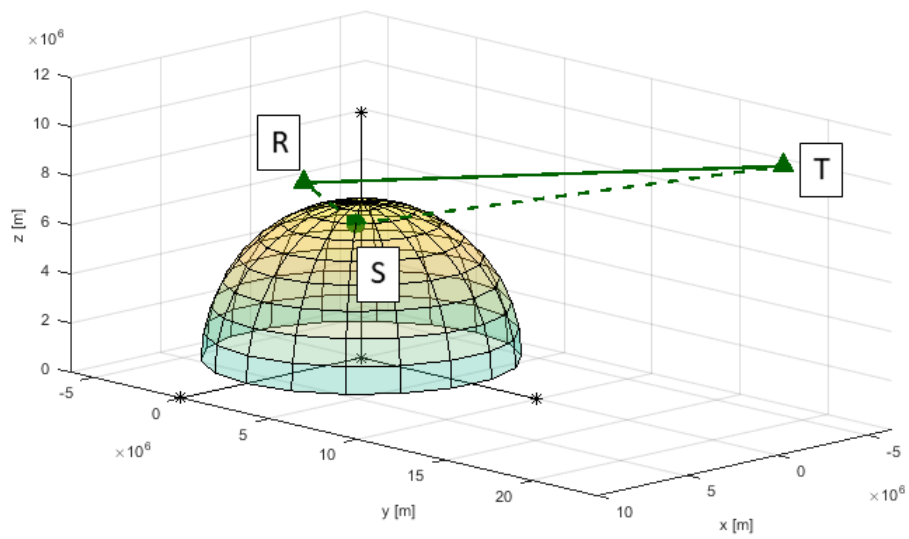
Figure 1.2.: Scheme of a GNSS-R measurement constellation for the northern hemisphere of WGS 84 with transmitter satellite (T), receiver satellite (R) and reflection point (S)

and the reflected signal. The maximum signal path difference is given by the correlator, as it has to gauge the delay of the reflected signal compared to the direct signal within a margin of $\pm 200\,\text{m}$. Since the deviation of the reflection point calculation is not the only error source (e.g. delay of electromagnetic signal caused by ionosphere), the maximum difference between the reflected and the non-reflected signal path is allowed to be at most $10\,\text{m}$. Due to the limited hardware on board a the satellite, the calculation should be as fast as possible.

2. Theory

The theory chapter provides information to understand the calculations executed in this thesis and explains the models and algorithms used. The structure of this chapter is to first explain the theoretical background of the influence of the atmosphere on the refraction of an electromagnetic signal. It continuous with the description of the geometry necessary to calculate a reflection point and an explanation of the earth models used. At the end of this chapter, the basic physics and algorithms for the reflection point calculation are explained.

2.1. Influence of the atmosphere on the refraction of an electromagnetic signal

The influence of the atmosphere on an electromagnetic signal propagating through it causes changes for several parameters of the electromagnetic signal. Like its phase, amplitude, polarisation and/or propagation velocity (see Alizadeh et al. (2013, chapter 1,2 and 3) and Heise (2002, chapter 2)). Changes of the propagation velocity for example can cause signal delay and refraction. Changes of the amplitude and the polarisation on the other hand influence for instance the signal to noise ratio (SNR). For the reflection point calculation the most interesting influence is the change of the propagation velocity or more precise the ionospheric signal delay and the refraction of the signal. The ionospheric delay is proportional to the total electron count of the ionosphere (TEC) and can go up to more than $15\,\mathrm{m}$ path delay. The refraction of the signal also depends on the electron count and has additional dependencies on parameters of the neutral atmosphere. As stated in section 1.4, this thesis deals with a snapshot of the measurement constellation. Hence, the ionospheric signal delay occurs, but, does not effect the reflection point calculation in this thesis (see 1.4). Therefore, the influence

of the atmosphere which is described in this section is the influence of the atmosphere on the refraction of an electromagnetic signal.

As mentioned in Heise (2002, chapter 2.4.1) the refraction of an electromagnetic wave is given by the refraction index n.

$$n = \frac{c}{v} \qquad (2.1)$$

Where:
  c speed of light in vacuum in m/s
  v speed of light in a specific medium in m/s

As described in Hofmann-Wellenhof, Legat, and Wieser (2003, chapter 4.2) the refractivity of the atmosphere can be divided into the the refractivitiy of the troposphere and the refractivity of the ionosphere. A distribution of the atmosphere with respect to its electromagnetic properties is described too. For this distribution, the refractivity of the atmosphere is divided into the refractivity of the neutral atmosphere including the troposphere and the stratosphere up to approximately 50 km above the earth surface and the refractivity of the ionosphere, which is everything above this 50 km up to something between 500 km and 1000 km.

2.1.1. Refractivity of the neutral atmosphere

The refraction index of the neutral atmosphere is denoted as n_{natmos} and is affected by the parameters temperature distribution, pressure distribution and water vapour distribution of the atmosphere. By combining equation one and seven from ITU-R P.453 (2017, chapter 1) a sufficient approach for n_{natmos} is given with equation 2.2.

$$n_{natmos}(h) = 1 + \frac{7.76 \times 10^{-6}}{T_{atmos}(h)} \left(p(h) + 4810 \cdot \frac{p_w(h)}{T(h)} \right) \qquad (2.2)$$

Where:
  p is the atmospheric pressure in hPa
  p_w is the water vapour pressure of the atmosphere in hPa
  T_{atmos} is the absolute temperature of the atmosphere in K
  h is the height above the earth surface in km

Equation 2.2 shows that the refraction index for the neutral atmosphere is always higher than one. Therefore the propagation velocity of the electromagnetic signal in the neutral atmosphere is slower than the speed of light.

To calculate the refraction index the distribution of the temperature, of the atmospheric pressure and of the water vapour pressure over the height above the earth surface is required. Since the atmosphere is a highly dynamical system it is not possible to state the exact distributions. Therefore the mean annual global reference atmosphere provided by ITU-R P.835 (2017) is used. The equations 2.4 to 2.6 state the distribution of the temperature, the atmospheric pressure and the water vapour pressure as given in ITU-R P.835 (2017, chapter 1.1 and 1.2). In the equations 2.4 and 2.5, ITU-R P.835 (2017) uses so called geopotential heights (h', given in km$'$) instead of geometric heights (h, given in km) for $h < 86$ km. This is because the equations 2.4 and 2.5 include statistically determined factors which best work with geopotential heights. Geopotential heights are calculated with equation 2.3. A geometric height of $h = 86$ km corresponds to a geopotential height of $h' = 84.852$ km$'$. The factors in the equations 2.4 to 2.6 are statistically determined and therefore do not have units.

$$h' = \frac{6356.766 \cdot h}{6356.766 + h} \tag{2.3}$$

Temperature distribution:

$$
\begin{aligned}
T_{atmos}(h') &= 288.15\,\text{K} - 6.5 \cdot h'; & 0\,\text{km}' &\leq h' \leq 11\,\text{km}' \\
T_{atmos}(h') &= 216.65\,\text{K}; & 11\,\text{km}' &< h' \leq 20\,\text{km}' \\
T_{atmos}(h') &= 216.65\,\text{K} + (h' - 20\,\text{km}'); & 20\,\text{km}' &< h' \leq 32\,\text{km}' \\
T_{atmos}(h') &= 228.65\,\text{K} + 2.8 \cdot (h' - 32\,\text{km}'); & 32\,\text{km}' &< h' \leq 47\,\text{km}' \\
T_{atmos}(h') &= 270.65\,\text{K}; & 47\,\text{km}' &< h' \leq 51\,\text{km}' \\
T_{atmos}(h') &= 270.65\,\text{K} - 2.8 \cdot (h' - 51\,\text{km}'); & 51\,\text{km}' &< h' \leq 71\,\text{km}' \\
T_{atmos}(h') &= 214.65\,\text{K} - 2.0 \cdot (h' - 71\,\text{km}'); & 71\,\text{km}' &< h' \leq 84.852\,\text{km}' \\
T_{atmos}(h) &= 186.8673; & 86\,\text{km} &< h \leq 91\,\text{km}
\end{aligned}
$$

$$T_{atmos}(h) = 263.1905 - 76.3232 \cdot \sqrt{1 - \left(\frac{h - 91\,\text{km}}{19.9429}\right)^2}; \quad 91\,\text{km} < h \leq 100\,\text{km} \tag{2.4}$$

2. Theory

Pressure distribution:

$$p(h') = 1013.25\,\text{hPa} \cdot \left(\frac{288.15\,\text{K}}{T_{atmos}(h')} \right)^{\frac{-34.1632}{6.5}} ; \qquad\qquad 0\,\text{km}' \leq h' \leq 11\,\text{km}'$$

$$p(h') = 226.3226\,\text{hPa} \cdot \exp\left(\frac{-34.1632 \cdot (h' - 11\,\text{km})}{T_{atmos}(h')} \right) ; \quad 11\,\text{km}' < h' \leq 20\,\text{km}'$$

$$p(h') = 54.7498\,\text{hPa} \cdot \left(\frac{216.65\,\text{K}}{T_{atmos}(h')} \right)^{34.1632} ; \qquad\qquad 20\,\text{km}' < h \leq 32\,\text{km}'$$

$$p(h') = 8.680422\,\text{hPa} \cdot \left(\frac{228.65\,\text{K}}{T_{atmos}(h')} \right)^{\frac{34.1632}{2.8}} ; \qquad\qquad 32\,\text{km}' < h' \leq 47\,\text{km}'$$

$$p(h') = 1.109106\,\text{hPa} \cdot \exp\left(\frac{-34.1632 \cdot (h' - 47\,\text{km})}{T_{atmos}(h')} \right) ; \quad 47\,\text{km}' < h' \leq 51\,\text{km}'$$

$$p(h') = 0.6694167\,\text{hPa} \cdot \left(\frac{270.65\,\text{K}}{T_{atmos}(h')} \right)^{\frac{-34.1632}{2.8}} ; \qquad 51\,\text{km}' < h' \leq 71\,\text{km}'$$

$$p(h') = 0.03956649\,\text{hPa} \cdot \left(\frac{214.65\,\text{K}}{T_{atmos}(h')} \right)^{\frac{-34.1632}{2.0}} ; \qquad 71\,\text{km}' < h' \leq 84.852\,\text{km}'$$

$$p(h) = \exp\left(a_0 + a_1 \cdot h + a_2 \cdot h^2 + a_3 \cdot h^3 + a_4 \cdot h^4 \right) ; \qquad 86\,\text{km} < h \leq 100\,\text{km}$$

$$(2.5)$$

With:

$$a_0 = 95.5718599$$
$$a_1 = -4.011801$$
$$a_2 = 6.424731 \times 10^{-2}$$
$$a_3 = -4.78966 \times 10^{-4}$$
$$a_4 = 1.340543 \times 10^{-6}$$

Water vapour pressure distribution:

$$p_w(h) = \frac{\rho(h) \cdot T_{atmos}(h)}{216.7} \qquad\qquad (2.6)$$

With:

$$\rho(h) = \rho_0 \cdot \exp\left(\frac{-h}{h_0} \right)$$
$$h_0 = 2\,\text{km}$$
$$\rho_0 = 7.5\,\text{g/m}^3$$
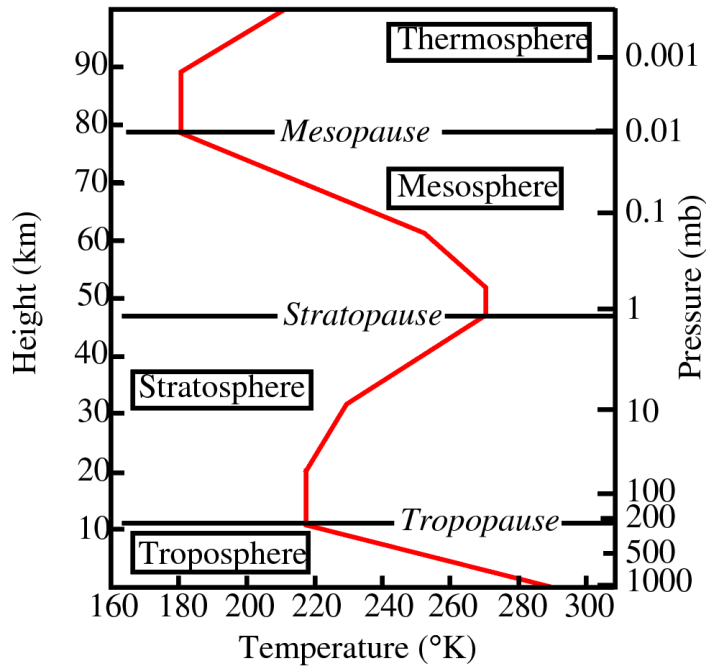
Figure 2.1.: Temperature distribution of earth atmosphere (Hakim, 2017)

Where:
ρ is the density of the atmosphere in g/m^3
ρ_0 is the standard ground level water vapour density
h_0 is the scale height in

According to ITU-R P.835 (2017, chapter 1.2) the water vapour density decreases with increasing altitude until a certain altitude at which the mixing ratio $\frac{p_w(h)}{p(h)} = 2 \times 10^{-6}$. Above this certain altitude $\frac{p_w(h)}{p(h)}$ is assumed constant. Similarly the atmospheric pressure decreases with increasing altitude. Thus, both the atmospheric pressure and the water vapour pressure decrease with increasing altitude. Hence, the refraction index of the neutral atmosphere approaches the value of one with increasing altitude.

2.1.2. Refractivity of the ionosphere

The refraction index of the ionosphere is denoted as n_{ion}. As stated in Alizadeh et al. (2013, chapter 2) and Heise (2002, chapter 2.4.1) it is dispersive and generally a complex value. Although, for electromagnetic waves with a

frequency higher than 100 Hz the refraction index can be seen as a real value which is determined by the frequency of the electromagnetic wave and the electron density of the ionosphere (Heise, 2002, chapter 2.4.1). As stated by Heise (2002, chapter 2.4.1), n_{ion} can be represented as a development after the inverse power of the frequency. Since the terms with order higher than 2 are much smaller than the terms with order one and two the refraction index of the ionosphere can be written as

$$n_{ion}(h) = 1 - K \cdot \frac{N_e(h)}{v^2}. \tag{2.7}$$

With:

$$K = \frac{C_x}{2} = 40.3 \, \frac{\text{m}^3}{\text{s}^2}$$

Where:
N_e is the electron density in e^-/m^3
v is the frequency of the electromagnetic wave (GNSS signal) in Hz

As can be seen in equation 2.7 the refraction index of the ionosphere is indirect proportional to the square of the frequency of the electromagnetic wave. Furthermore $n_{ion} < 1$ which indicates that the phase velocity of an electromagnetic wave in the ionosphere is faster than the speed of light in vacuum. With rising frequencies the refraction of the ionosphere loses relevance until over 10 GHz it can be neglected. However, for GNSS signals (e.g. GPS: $v_1 = 1,575.42 \, \text{MHz}, v_2 = 1,227.60 \, \text{MHz}$) it is significant. In case of a signal modulated on a carrier frequency instead of n_{ion} the group refraction index n_{Gion} of the ionosphere must be considered (see Heise (2002) or Alizadeh et al. (2013)).

$$n_{Gion}(h) = 1 + K \cdot \frac{N_e(h)}{v^2} \tag{2.8}$$

According to equation 2.8, n_{Gion} is always bigger than 1. Hence, the velocity of a modulated signal is always smaller than the speed of light. Since GNSS signals are modulated signals, equation 2.8 describes the refraction index of the ionosphere for GNSS signal propagating through it.

In equation 2.8 all parameters except N_e are known. Referred to Figure 2.2 the electron density distribution changes from day to night. Additionally it changes daily and has local variations and a height dependency. There are several models to calculate an approximated N_e distribution. The one used in this thesis is the International Reference Ionosphere provieded by NASA (2012) where the N_e distribution for a given date and location can be downloaded.
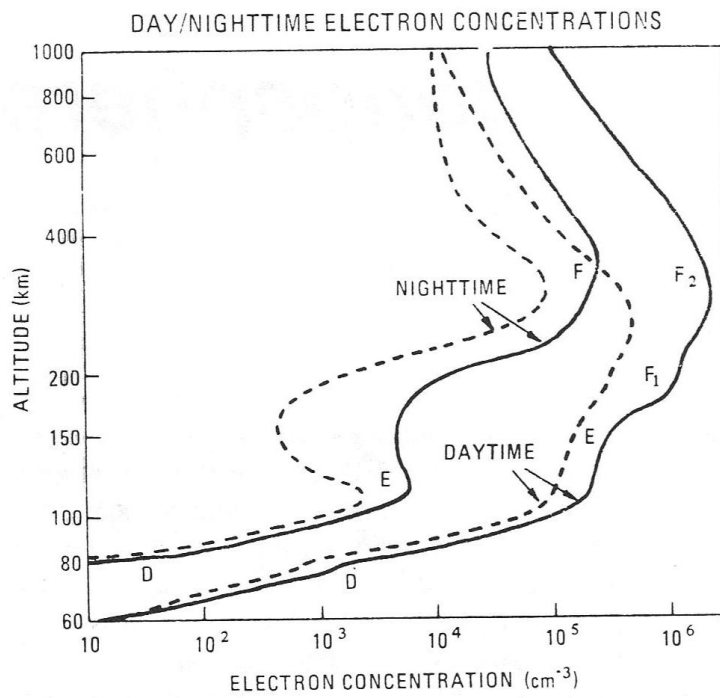
Figure 2.2.: Electron density distribution of the ionosphere, solid lines: solar maximum, dashed lines: solar minimum (PoleCATS, 2017)

2.1.3. Geometry for refraction

The geometry needed to calculate the propagation path of a refracted signal through mediums with different refraction indices is explained in this section.

Refraction on straight interface / Snell's law

An electromagnetic wave which propagates from a medium with a lower refraction index into a medium with a higher refraction index ($n_1 < n_2$) is refracted towards the normal on the interface. This is called Snell's law and is described by equation 2.9 and shown in Figure 2.3.

$$\frac{\sin(\alpha)}{\sin(\beta)} = \frac{n_2}{n_1} = \frac{v_1}{v_2} \tag{2.9}$$

Where:
- α is the angle of incidence in rd
- β is the angle of refraction in rd
- n_1 is the refraction index for medium one
- n_2 is the refraction index for medium two
- v_1 is the wave propagation velocity for media one in m/s
- v_2 is the wave propagation velocity for media two in m/s

Refraction on a radially bent interface

To calculate the refraction on a radially bent interface some more geometry is necessary. It is explicitly described in Mangum and Wallace (2015) and a short description is given below.

Figure 2.4 shows the propagation of an electromagnetic wave through media with different refraction indices ($n_1 < n_2 < n_3$) and radially bent interfaces. h_1 and h_2 denote arbitrarily selected interface boundaries. The heights for these boundaries are related to the centre of the radially bent interfaces (e.g. centre of the Earth for spherical earth model with radially bent layers of atmosphere) and are selected according to the problem to be discussed. Assumed angle α_1 is given, α_2 is calculated as follows.
Snell's law

$$\sin(\alpha_1) \cdot n_1 = \sin(\beta) \cdot n_2 \tag{2.10}$$

2.1. Influence of the atmosphere on the refraction of an electromagnetic signal
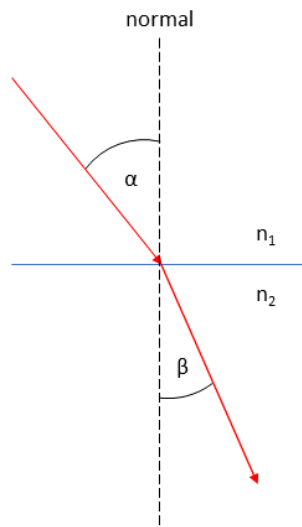
Figure 2.3.: Illustration of Snell's law
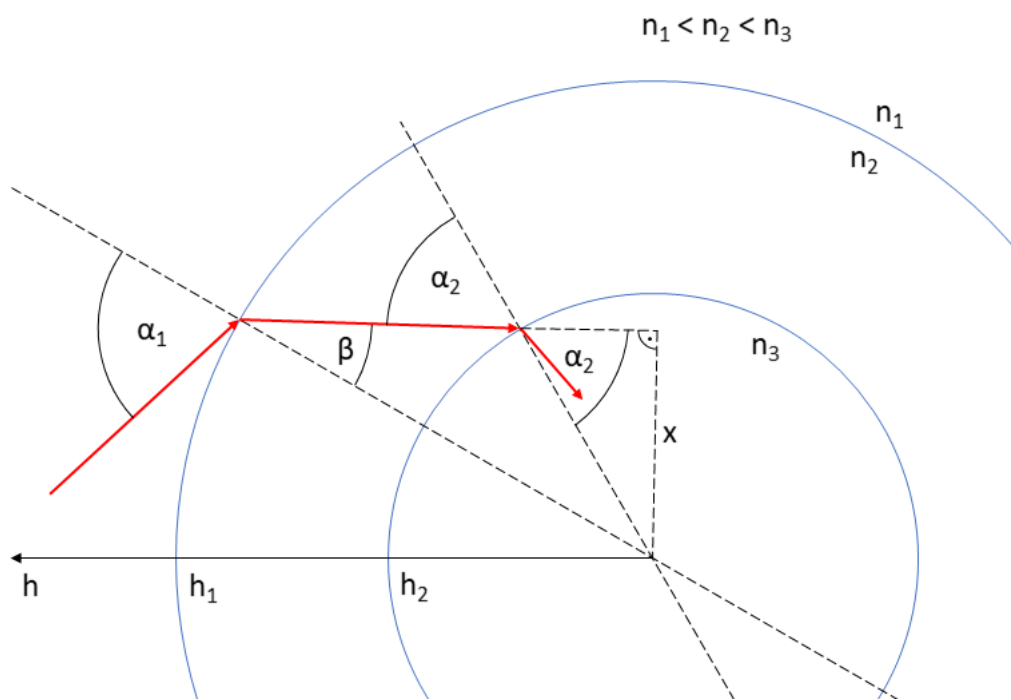
Figure 2.4.: Illustration of refraction on a radially bent interface

and the fact that

$$\sin(\beta) \cdot h_1 = \sin(\alpha_2) \cdot h_2 = x \tag{2.11}$$

can be set equal for $\sin(\beta)$ to

$$\sin(\alpha_1) \cdot n_1 \cdot h_1 = \sin(\alpha_2) \cdot n_2 \cdot h_2. \tag{2.12}$$

Equation 2.12 can be transformed into equation 2.13 to calculate α_2.

$$\alpha_2 = \arcsin\left(\frac{\sin(\alpha_1) \cdot n_1 \cdot h_1}{n_2 \cdot h_2}\right) \tag{2.13}$$

2.2. Geometry necessary for the reflection point calculation

The calculation of a reflection point is basically part of the field of analytical geometry. Since analytical geometry is a very wide field, this section describes the basics and advanced methods of analytical geometry used in this thesis.

2.2.1. Basics

To enable a better understanding, the equations and characteristics of the geometric objects used in this thesis are given in this section.

Ellipse in $\mathbb{R}^2$

As stated in Fischer (2017, chapter 5.5.1 and 5.5.2), the implicit form of an ellipse in $\mathbb{R}^2$ is

$$\frac{x^2}{a^2} + \frac{y^2}{b^2} = 1 \tag{2.14}$$

Where:
  a and b are the semi axes of the ellipsoid

Figure 2.5 shows some more parameters of an ellipse.

M	is the centre of the ellipse
T and R	are the foci of the ellipse
S	is a point on the circumference of the ellipse
e	is the linear eccentricity
$p_{ellipse}$	is the semi-latus rectum of an ellipse

With the following relations:

$$e = \sqrt{a^2 - b^2} \qquad (2.15)$$

$$\epsilon = \frac{e}{a} \qquad (2.16)$$

$$f = \frac{a - b}{a} \qquad (2.17)$$

$$p = \frac{b^2}{a} \qquad (2.18)$$

Where:

ϵ	is the numerical eccentricity
f	is the flattening

An important characteristic of an ellipse is that the length of a beam from one focus to the other reflected by the circumference of the ellipse is twice the length of the semi major axis.

$$SP_r = a + a \qquad (2.19)$$

Straight line in $\mathbb{R}^3$

As stated in Lang and Pucker (2005, chapter 3.3.3), the parameter form of a straight line $\vec{s}$ in $\mathbb{R}^n$ is illustrated as follows.

$$\vec{s}(k) = S + k \cdot \vec{r} \qquad (2.20)$$

Where:

S	is the so called space point
$\vec{r}$	is the direction vector specifying the direction of the straight line
k	is the parameter used to define any point lying on the straight line

Equation 2.20 can be rewritten in $\mathbb{R}^3$ as

$$\begin{pmatrix} x_s \\ y_s \\ z_s \end{pmatrix} = \begin{pmatrix} x_S \\ y_S \\ z_S \end{pmatrix} + k \cdot \begin{pmatrix} x_r \\ y_r \\ z_r \end{pmatrix}. \qquad (2.21)$$
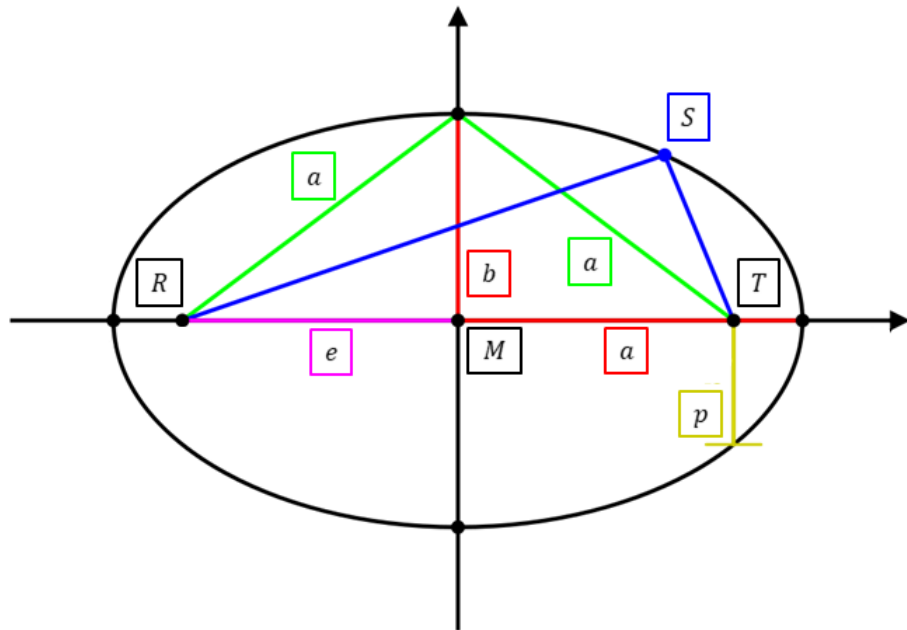
Figure 2.5.: Parameters of an ellipse

Plane in $\mathbb{R}^3$

As stated in Lang and Pucker (2005, chapter 3.3.3), a plane in the $\mathbb{R}^3$ can be illustrated by the following three forms.

- Three different points
- One point and two directions.
- One point and one vector normal to the plane

All three variations are associated. The difference between the three points R, S and T of the first variant result in the two directions $\vec{r}$ and $\vec{t}$ and the point S for the second variant.

$$\vec{p}(k,l) = S + k \cdot \left(\overrightarrow{R - S} \right) + l \cdot \left(\overrightarrow{T - S} \right) = S + k \cdot \vec{r} + l \cdot \vec{t} \tag{2.22}$$

Where:
$\vec{p}$	is the plane
k and l	are the parameters used to define any point on the plane (p) by the use of the directions $\vec{r}$ and $\vec{t}$

Equation 2.22 is the parameter form of a plane and can be written in $\mathbb{R}^3$ as

$$\begin{pmatrix} x_p \\ y_p \\ z_p \end{pmatrix} = \begin{pmatrix} x_S \\ y_S \\ z_S \end{pmatrix} + k \cdot \begin{pmatrix} x_r \\ y_r \\ z_r \end{pmatrix} + l \cdot \begin{pmatrix} x_t \\ y_t \\ z_t \end{pmatrix}. \tag{2.23}$$

The cross product of the two direction vectors $\vec{r}$ and $\vec{t}$ of the second variation yields the normal vector $\vec{n}$ on the plane $\vec{p}$ for the third variant.

$$\vec{n} = \vec{r} \times \vec{t} \tag{2.24}$$

Ellipsoid and spheroid in $\mathbb{R}^3$

As stated in Bronstein et al. (2008, chapter 3.5.3.10), the implicit form of an ellipsoid in the $\mathbb{R}^3$ is

$$\frac{x^2}{a^2} + \frac{y^2}{b^2} + \frac{z^2}{c^2} = 1. \tag{2.25}$$

Where:
a, b and c are the semi axes of the ellipsoid

Equation 2.25 can be rewritten in the parameter form as

$$x = a \cdot \cos \phi \cdot \cos \lambda \tag{2.26}$$
$$y = b \cdot \cos \phi \cdot \sin \lambda \tag{2.27}$$
$$z = c \cdot \sin \phi \tag{2.28}$$

With:

$$-\frac{\pi}{2} \leq \phi \leq \frac{\pi}{2}$$
$$-\pi \leq \lambda \leq +\pi$$

Where:
ϕ and λ are the angles that are used to perform a coordinate transformation from spherical coordinates to Cartesian coordinates

In case of the WGS 84 model of the Earth, the ellipsoid becomes a spheroid where equation 2.25 becomes

$$\frac{x^2}{a^2} + \frac{y^2}{a^2} + \frac{z^2}{b^2} = 1. \tag{2.29}$$

With only the semi major axis a and the semi minor axis b of en ellipse left. The equations 2.26, 2.27 and 2.28 than become

$$x = a \cdot \cos \phi \cdot \cos \lambda \qquad (2.30)$$
$$y = a \cdot \cos \phi \cdot \sin \lambda \qquad (2.31)$$
$$z = b \cdot \sin \phi. \qquad (2.32)$$

2.2.2. Angle between to vectors $\mathbb{R}^3$

As stated in Bronstein et al. (2008, chapter 3.5.3.9), a angle ζ between two vectors is calculated as follows.

$$\cos(\zeta) = \frac{\vec{r} \cdot \vec{t}}{|\vec{r}| \cdot |\vec{t}|} \Rightarrow \zeta = \cos^{-1} \left(\frac{\vec{r} \cdot \vec{t}}{|\vec{r}| \cdot |\vec{t}|} \right) \qquad (2.33)$$

2.2.3. Surface normal on an ellipsoid

As stated in Lang and Pucker (2005, chapter 7.4), the normal on a surface described by a function $f(x, y, z)$ can be calculated by forming the gradient of this function.

$$\nabla f = \begin{pmatrix} \frac{\delta f}{\delta x} \\ \frac{\delta f}{\delta y} \\ \frac{\delta f}{\delta z} \end{pmatrix} \qquad (2.34)$$

For the function of an ellipsoid the gradient of equation 2.25 is

$$\nabla f = \begin{pmatrix} \frac{2x}{a^2} \\ \frac{2y}{b^2} \\ \frac{2z}{c^2} \end{pmatrix}. \qquad (2.35)$$

To determine the surface normal for a given point S with the coordinates (x_S, y_S, z_S) enter the point S in equation 2.35.

2.2.4. Intersection of a straight line and an ellipsoid

To calculate the intersection of a straight line and an ellipsoid, equation 2.21 of a straight line has to be insert into equation 2.25 of the ellipsoid.

$$\frac{(x_S + k \cdot x_R)^2}{a^2} + \frac{(y_S + k \cdot y_R)^2}{b^2} + \frac{(z_S + k \cdot z_R)^2}{c^2} = 1. \qquad (2.36)$$

Equation 2.36 must be transformed to receive k.

$$\begin{aligned}
&k^2 \cdot (b^2 \cdot c^2 \cdot x_R^2 + a^2 \cdot c^2 \cdot y_R^2 + a^2 \cdot b^2 \cdot z_R^2) + \\
&k \cdot (2 \cdot c^2 \cdot b^2 \cdot x_S \cdot x_R + 2 \cdot a^2 \cdot c^2 \cdot y_S \cdot y_R + 2 \cdot a^2 \cdot b^2 \cdot z_S \cdot z_R) + \\
&b^2 \cdot c^2 \cdot x_S^2 + a^2 \cdot c^2 \cdot y_S^2 + a^2 \cdot b^2 \cdot z_S^2 - a^2 \cdot b^2 \cdot c^2 = 0
\end{aligned} \qquad (2.37)$$

$$A = (b^2 \cdot c^2 \cdot x_R^2 + a^2 \cdot c^2 \cdot y_R^2 + a^2 \cdot b^2 \cdot z_R^2) \qquad (2.38)$$

$$B = (2 \cdot c^2 \cdot b^2 \cdot x_S \cdot x_R + 2 \cdot a^2 \cdot c^2 \cdot y_S \cdot y_R + 2 \cdot a^2 \cdot b^2 \cdot z_S \cdot z_R) \qquad (2.39)$$

$$C = b^2 \cdot c^2 \cdot x_S^2 + a^2 \cdot c^2 \cdot y_S^2 + a^2 \cdot b^2 \cdot z_S^2 - a^2 \cdot b^2 \cdot c^2. \qquad (2.40)$$

Equation 2.37 is a quadratic equation and can be solved with the well known solution approach for quadratic equations and the relations 2.38, 2.39 and 2.40 to obtain k.

$$k_{1,2} = \frac{-B \pm \sqrt{B^2 - 4 \cdot A \cdot C}}{2 \cdot A} \qquad (2.41)$$

Together with equation 2.36 this results in

$$I_{1,2} = \vec{S} + k_{1,2} \cdot \vec{r} \qquad (2.42)$$

As can be seen in Figure 2.6, equation 2.42 leads to two intersection points. If the results of equation 2.42 have imaginary parts, the straight line does not intersect with the ellipsoid.

2.3. Earth models

The Earth is neither a sphere or an ellipsoid nor a rigid body. Flattened by the rotation and deformed by the attraction forces of the sun, the moon and the other planets of the solar system, it is more like a compressed sphere, distorted in all directions. However, depending on the application, adapted models are used for calculations that include the Earth. This section describes the characteristics and inaccuracies of the earth models used in this thesis.
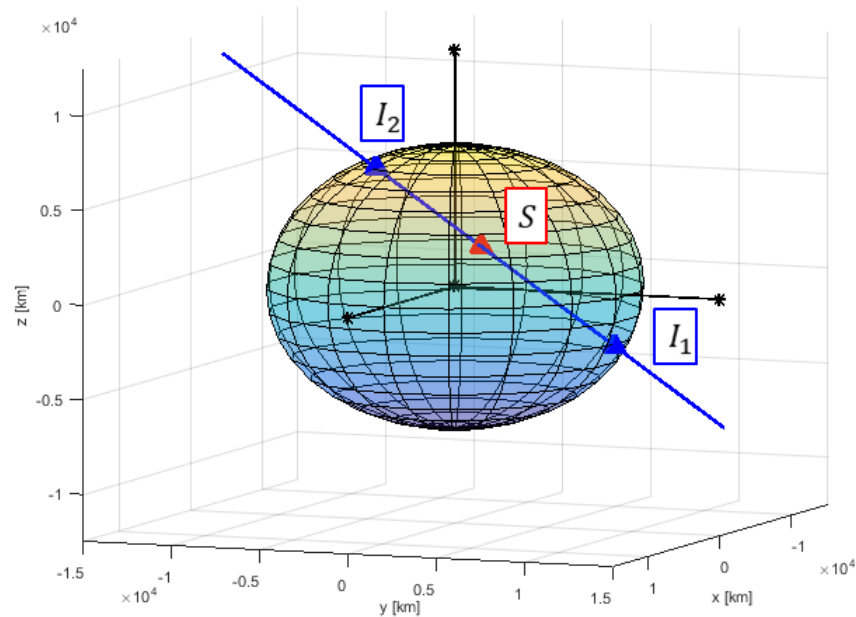
Figure 2.6.: Intersection of a straight line and an ellipsoid

2.3.1. Sphere

The simplest model of the Earth is a sphere. Where the radius of the sphere is the average earth radius r_0. The average earth radius is derived from the WGS 84 model of the Earth for a sphere with the same volume as the ellipsoid.

$$r_0 = 6,371,008.8\,\text{m} \tag{2.43}$$

The comparison of the the average earth radius and the semiminor axis of the WGS 84 reveals a serious inaccuracy of the sphere model. The difference between r_0 and b is about 15 km and therefore could cause serious inexactness. For comparison see Figure 2.7.

2.3.2. WGS 84

One of the most commonly used reference systems is the World Geodetic System 1984 (WGS 84). According to Hofmann-Wellenhof, Lichtenegger, and Wasle (2008, chapter 9.2.1) coordinates of about 1500 terrestrial sites

have been used to realize the WGS 84 reference system. A geocentric ellipsoid of revolution, also called spheroid, is associated to this reference frame. Originally, the spheroid was defined by the semimajor axis (a), the normalized second degree zonal gravitational coefficient $\bar{C}_{2,0}$, the truncated angular velocity of the Earth ω_E and the Earth's gravitational constant μ. Where $\bar{C}_{2,0}$ can be expressed by the flattening of the ellipsoid f. In 1996 a revised version of the reference system, realized by monitor stations with refined coordinates, was implemented. The related geocentric ellipsoid of revolution is defined by the following parameters.

$$a = 6,378,137.0 \, \text{m} \tag{2.44}$$

$$f = \frac{1}{298.257223563} = 0.003352811 \tag{2.45}$$

$$\omega_E = 7,292,115 \times 10^{-11} \, \text{rad/s} \tag{2.46}$$

$$\mu = 3,986,004.418 \times 10^{8} \, \text{m}^3/\text{s}^2 \tag{2.47}$$

Out of equation 2.17 and the equations 2.15 and 2.16 as stated in section 2.2.1 the semiminor axis and the numeric eccentricity of the spheroid can be calculated.

$$b = a - f \cdot a = 6,356,752.3 \, \text{m} \tag{2.48}$$

$$\epsilon = \frac{\sqrt{a^2 - b^2}}{a} = 0.081819191 \tag{2.49}$$

Figure 2.7 shows a scheme of the ellipse related to the WGS 84 spheroid. Hofmann-Wellenhof, Lichtenegger, and Wasle (2008, chapter 9.2.1) describes the inaccuracy of the WGS 84 earth model as systematic difference of about 1 cm compared to the International Terrestrial Reference Frame 2005 (ITRF2005, see International Terrestrial Reference Frame (2005)) and therefore as insignificant.

2.3.3. Transformation of geodetic coordinates on the surface of the WGS 84 into ECEF Cartesian coordinates

Positions on the WGS 84 spheroid are normally given in geodetic coordinates (longitude λ and latitude φ). To transform the geodetic coordinates into ECEF (Earth centred Earth fixed) Cartesian coordinates it is not possible
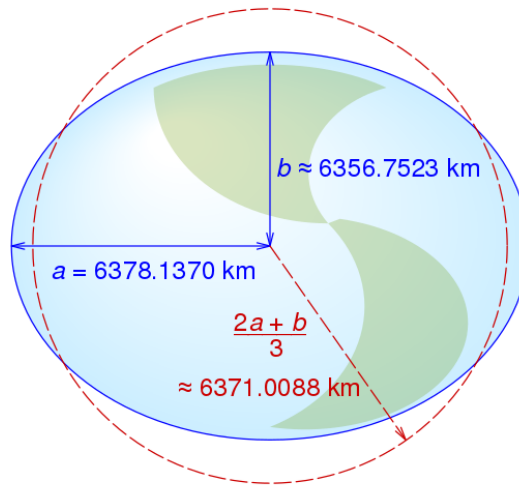
Figure 2.7.: Scheme of the WGS 84 ellipse(blue) and the average earth radius(red) (Wikimedia Commons, 2004, File: WGS84 mean Earth radius.svg)

to use the equations 2.30 to 2.32, since ϕ and λ are geocentric coordinates. Instead the transformation given by the equations 2.50 to 2.52 as stated in Leick (1990, chapter 6.2) has to be used.

$$x = (a \cdot C_1 + h) \cdot \cos\varphi \cdot \cos\lambda \qquad (2.50)$$
$$y = (a \cdot C_1 + h) \cdot \cos\varphi \cdot \sin\lambda \qquad (2.51)$$
$$z = (a \cdot C_2 + h) \cdot \sin\varphi \qquad (2.52)$$

With:

$$C_1 = \frac{1}{\sqrt{1 - \epsilon^2 \cdot \sin^2\varphi}}$$
$$C_2 = C_1 \cdot (1 - \epsilon^2)$$
$$-\frac{\pi}{2} \leq \varphi \leq \frac{\pi}{2}$$
$$-\pi \leq \lambda \leq +\pi$$

Where:
h is the height difference to the WGS 84 surface
φ and λ are the angles that are used to perform a coordinate transformation from geodetic coordinates toe ECEF Cartesian coordinates

For better understanding, Figure 2.8 shows a scheme of the relation between
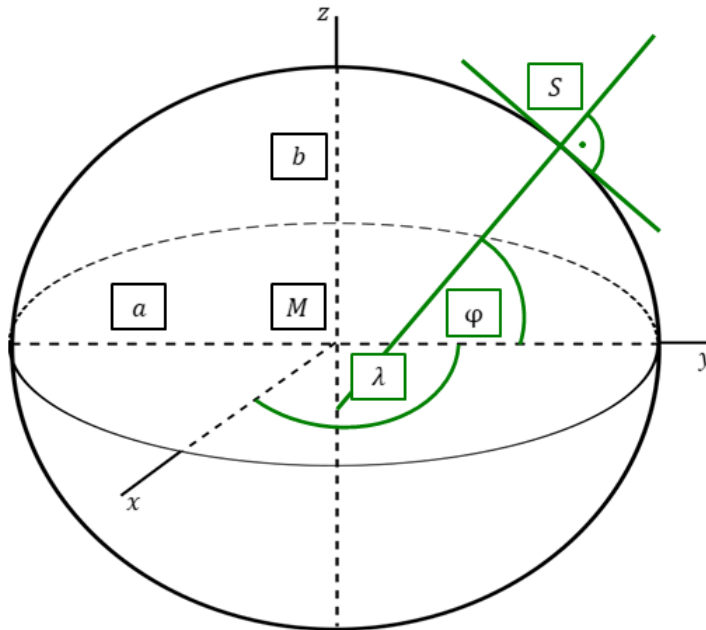
Figure 2.8.: Scheme of geodetic and Cartesian coordinates

the geodetic and the Cartesian coordinates. h can be set to zero for a coordinate transformation of a point on the WGS 84 surface.

2.4. Reflection point calculation

This section describes the physical basics and the basic algorithms used to calculate the reflection point. The implementation of the algorithms is described in detail in chapter 5.

2.4.1. Law of reflection

For an electromagnetic wave reflected on a surface the angle of incidence and the angle of reflection must be equal. This is called the Law of Reflection with the equation:

$$\sin(\theta_{in}) = \sin(\theta_{ref}) \Rightarrow \theta_{in} = \theta_{ref} \tag{2.53}$$
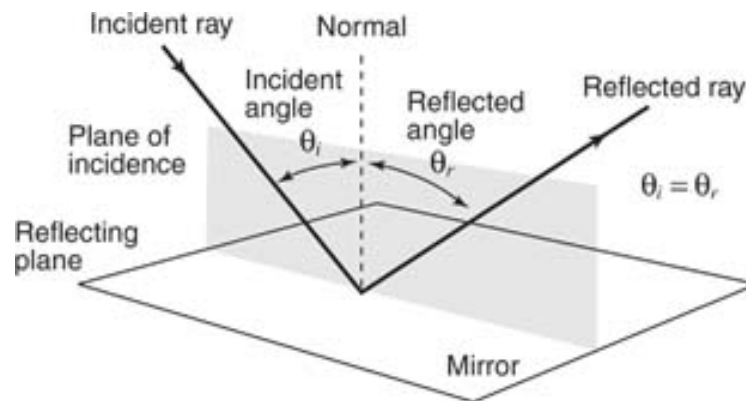
Figure 2.9.: Scheme of Law of Reflection with $\theta_i = \theta_{in}$ and $\theta_r = \theta_{ref}$ (CliffsNotes, 2016)

Where:

θ_{in} is the angle of incidence at the reflection point

θ_{ref} is the reflected angle at the reflection point (This angle can also be called emergent angle.)

Furthermore, the incident and the reflected beam as well as the surface normal must be in the same plane (see Figure 2.9). The plane in which the incident and the reflected ray as well as the surface normal must lie is called plane of incidence or calculation plane.

2.4.2. Binary Search

As stated in Knuth (1998, chapter 6.2.1) the binary search algorithm is a search algorithm used to find a target element within a sorted array of elements. The algorithm starts at the middle element of the array and compares it to the target element. This comparison can yield three results. Result one, the values of both elements are equal and consequently the target element has been found. Result two, the value of the target element is higher than the value of the compared element. In this case the search must be continued in the half containing the larger elements. Result three, the value of the target element is lower than the value of the compared element. In this case the search must be continued in the half containing the smaller elements. In case of result two and three the search continuous with half the list of elements left, following the same procedure as described above, until the target element is found. Hence, Binary Search shows a binary
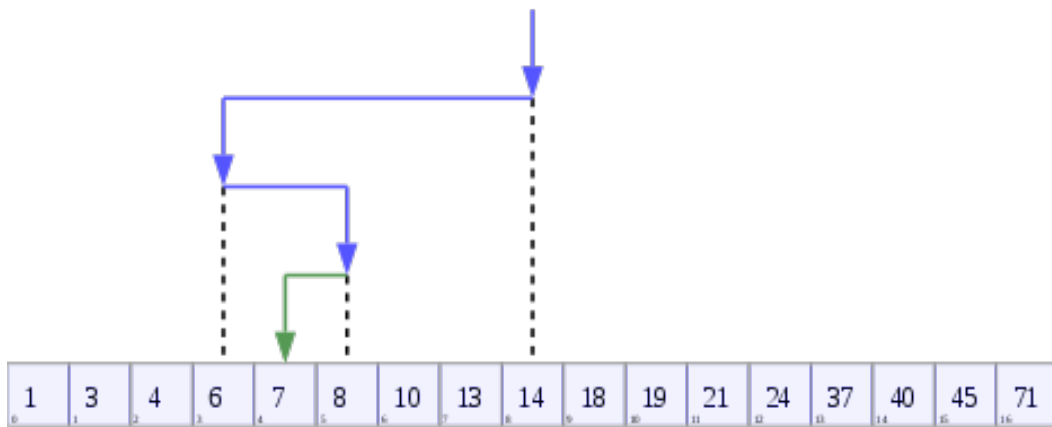
Figure 2.10.: Depiction of binary search (Wikimedia Commons, 2004, File: Binary Search Depiction.svg)

logarithmic time behaviour.

$$N = \log_2(n) \tag{2.54}$$

Where:

N is the maximum number of iterations the search needs

n is the number of elements the array consist of

Figure 2.10 shows an example for binary search where the number seven is looked for in an sorted array consisting of 17 elements. According to equation 2.54 the maximum number of iterations for the example is

$$\log_2(17) = 4.09 \rightarrow 5 \,\text{iterations.}$$

E.g. the search for number 13 needs five iterations.

2.4.3. Monte Carlo methods

As reported by Theis and Kernbichler (2002) the Monte Carlo methods are not particular algorithms,they are a group of numerical solution methods. Monte Carlo methods use random numbers to generate approximate solutions or perform simulations of various processes respectively problems. Though, the original problem does not have to be related to random numbers. The field of application for Monte Carlo methods knows almost no limit. Some applications for example are the direct solution of stochastic

problems, random walks (diffusion processes), statistical physics (calculation of properties of orderless media) or the solution of high-dimensional integrals or particular differential equations with complex boundary conditions (Poisson equation). Monte Carlo methods normally have the following characteristics.

- It is often the only method to provide suitable results within acceptable calculation time.
- The results can be improved by the use of more calculation time.

In case of the evaluation of the reflection point calculation algorithms, it is wiser to use randomly distributed true reflection points instead of evaluating every possible reflection point.

Since Monte Carlo methods depend on random numbers, it is inevitable to mention an inaccurateness of these methods. It is not possible to generate real random numbers with a computer. Therefore several methods to generate random numbers with a computer have been invented. Although, strictly speaking, these random numbers are no real random numbers, since the sequence of the generated numbers repeats itself after a certain time. For more information about the methods to generate random numbers refer to appropriate literature like Theis and Kernbichler (2002).

3. Influence of the atmosphere on the refraction of an electromagnetic signal and its associated effects on the reflection point calculation

Before the thesis deals with the reflection point calculation, this chapter investigates the refraction of an electromagnetic signal caused by the atmosphere and its associated effects on the reflection point calculation. This is done in order to clarify, if this influence has to be taken into account for the calculation of the reflection point.

As already stated in section 2.1, the refraction of an electromagnetic signal is caused by changes of its propagation velocity (v). This changes are caused by height dependent parameters of the atmosphere. Therefore, section 3.1 takes a closer look on the height dependency of the refraction index of the atmosphere. To examine how the atmospheric influence on the refraction effects the reflection point calculation the following parameters are of interest.

- the path length (PL)

- the signal emission angle at the transmitter satellite (θ_T)

- the location of the reflection point (S)

- the location of the receiver satellite (R)

The examination is done by calculation and comparison of these parameters for the non refracted and refracted path. For a simple access to the problem the calculation is done for two cases. Case one is the easy one which assumes

a flat earth model with parallel layers of atmosphere (see section 3.2). For this case Snell's law and basic geometry is required . The second case is the more realistic one which assumes a spherical earth model with radially bent layers of atmosphere (see section 3.3). For this case Snell's law and more advanced geometry is required. Both cases deal with the problem in 2D and were simulated for several different signal emission angles.

Similar parameters for both methods

Some given parameters and conditions apply for both the flat and the spherical earth model. For a better overview these parameters and conditions are summarized here.

- Horizontal distance of the transmitter satellite, $x_T = hd_T = 0\,\text{km}$.
- Height of the transmitter satellite, $h_T = 20000\,\text{km}$
- Height of the receiver satellite, $h_R = 600\,\text{km}$
- Between the earth surface and the height of the ionosphere the height step size (h_{step}) between the boundaries of the layers of the atmosphere can be arbitrarily chosen between 500 m and 10 km.
- Above the ionosphere is only one step to the height of the transmitter satellite.
- Frequency of the electromagnetic signal, $\nu = 1,575.42\,\text{MHz}$
- For the refraction index of the atmosphere n_{atmos} applies equation 3.1
- n_{atmos} is only height dependent.
- N_e is given at $47\,°4'$ N and $15\,°26'$ O on 1 January 2000

In addition here is some input on the selected parameters. Since the transmitter satellite is the position where the signal is emitted, there is no horizontal distance to its position. The height of the transmitter satellite is given with 20000 km because GNSS systems like GPS or GLONASS operate at orbits with about 20000 km of altitude. The PRETTY Cubesat will be operated in a LEO and therefore the height of the receiver satellite is given with 600 km. Between the earth surface and the height of the ionosphere the step size of the atmospheric height can be arbitrarily chosen. Although step sizes under 500 m and above 10 km does not make any sense. Under 500 m there is no considerable change of the refraction index and it simply increases the calculation time. Above 10 km it is not accurate enough anymore and doesn't decrease the calculation time noticeable. From the height of the ionosphere until the height of the transmitter satellite there is only one step

because above the ionosphere is the exosphere without any considerable pressure or amount of charged particles and therefore its refraction index is equal to one (see section 3.1). As signal frequency for the simulation the L1-frequency of the GPS system was selected.

To receive the total refraction index of the atmosphere n_{atmos}, equation 2.2 and equation 2.8 are combined to

$$n_{atoms}(h) = 1 + \frac{7.76 \times 10^{-6}}{T_{atmos}(h)} \cdot \left(p(h) + 4810 \frac{p_w(h)}{T_{atmos}(h)} \right) + K \cdot \frac{N_e(h)}{v^2} \quad (3.1)$$

With:

$$K = \frac{C_x}{2} = 40.3 \, \text{m}^3/\text{s}^2$$

Where $T(h)$, $p(h)$ and $p_w(h)$ are calculated with equation 2.4, 2.5 and 2.6 and the values for $N_e(h)$ are from the International Reference Ionosphere from NASA, 2012. This combination is possible because, as stated in section 2.1, the neutral atmosphere ends where the ionosphere starts. In other words, the refraction index of the neutral atmosphere is one within the ionosphere and the refraction index of the ionosphere is one within the neutral atmosphere (see section 3.1).

As already mentioned in the theory chapter the refraction index of the neutral atmosphere and the one of the ionosphere depend on several parameters like location on Earth, time of the day, height and several known and unknown parameters more. To simplify the calculation the neutral atmosphere and the ionosphere are assumed only height dependent. Another step to ease the calculation is to take a closer look at these height dependencies. The investigation of the height dependencies is stated below.

3.1. Height dependency of the refraction index

As stated in section 2.1.1 and 2.1.2 the refraction index of the neutral atmosphere (n_{natmos}) and the group refraction index of the ionosphere (n_{Gion}) depend on the height above the earth surface (h). As can be seen in equation 3.1 the refraction index of the neutral atmosphere depends on the height dependency of the temperature of the atmosphere ($T_{atmos}(h)$), the atmospheric pressure ($p(h)$) and the water vapour pressure ($p_w(h)$). Whereas the refraction index of the ionosphere depends on the height
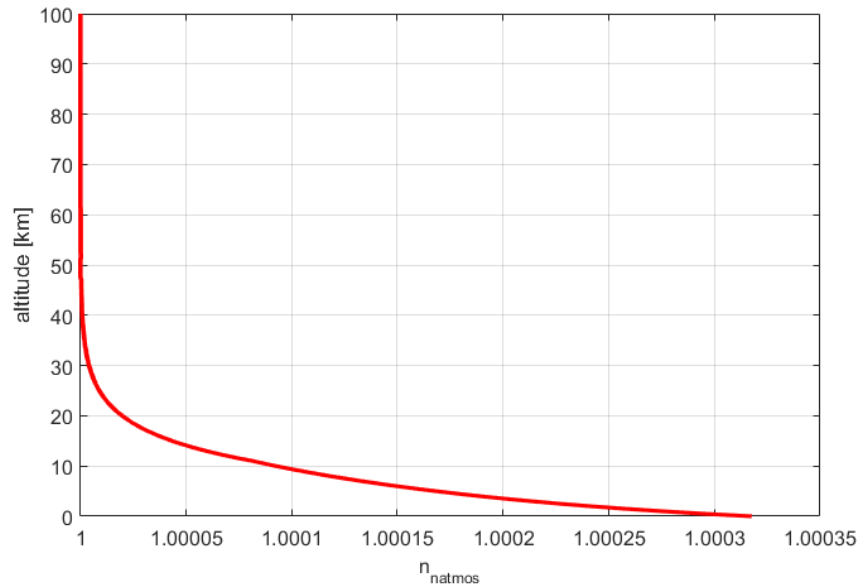
Figure 3.1.: Refraction index for the neutral atmosphere

dependency of the electron content of the atmosphere ($N_e(h)$). Therefore both refraction indices show different height dependencies. Following, the height dependency of the refraction index of the neutral atmosphere and of the ionosphere are investigated. Additionally their impact on the height dependency of the refraction index of the atmosphere is examined.

According to ITU-R P.835 (2017, chapter 1.1) the neutral atmosphere reaches from the earth surface up to about 100 km. Hence, n_{natmos} should be negligible for heights above 100 km. Figure 3.1 shows a simulated height distribution of the refraction index of the neutral atmosphere using the equations from section 2.1.1. Since it shows n_{natmos} going against one already at altitudes of about 40 km, it confirms that the refraction index of the neutral atmosphere can be neglected for altitudes above 100 km. E.g. $n_{natmos}(82 \text{ km}) = 1.000000004112$ and it is rapidly decreasing with increasing altitude because of the decreasing pressure.

As mentioned above, the refraction index of the ionosphere depends on the electron density distribution. The electron density distribution is from NASA (2012) for the location of Graz (latitude: $47°4'$, longitude: $15°26'$) on the 1st of January 2000. At NASA (2012) only N_e distributions between 60 km and 2000 km can be downloaded. As can be seen in Figure 3.2, n_{Gion} is going
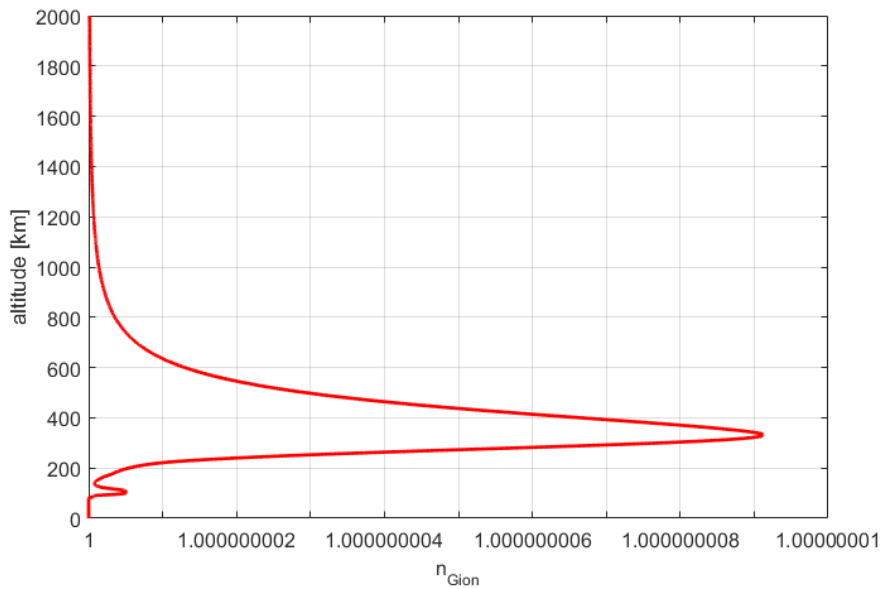
Figure 3.2.: Refraction index for the ionosphere

against one for altitudes above $1400\,\text{km}$. Therefore, the maximum height of $2000\,\text{km}$ for the electron density distribution is completely sufficient. By comparison of Figure 3.1 and 3.2, it is noticeable that the refraction index of the ionosphere is about 10^5 times smaller than the one of the neutral atmosphere. Hence, the refraction index of the ionosphere has no measurable impact on the refraction index of the atmosphere. This can also be noticed by looking at Figure 3.3. Only the bulge of the refraction index of the neutral atmosphere is noticeable.

The refraction indices in Figure 3.1, 3.2 and 3.3 were calculated with the function *Calculation of refraction indices* (see appendix A.1.1) with a step size of $h_{step} = 0.5\,\text{km}$. The function uses equation 3.1 and the equations 2.2 and 2.8 to calculate the refraction indices.

3.2. Flat Earth

This section describes the calculation for the non refracted and the refracted path as well as it states the simulation results for the flat earth model. The flat earth model, as can be seen in Figure 3.4, assumes a flat Earth
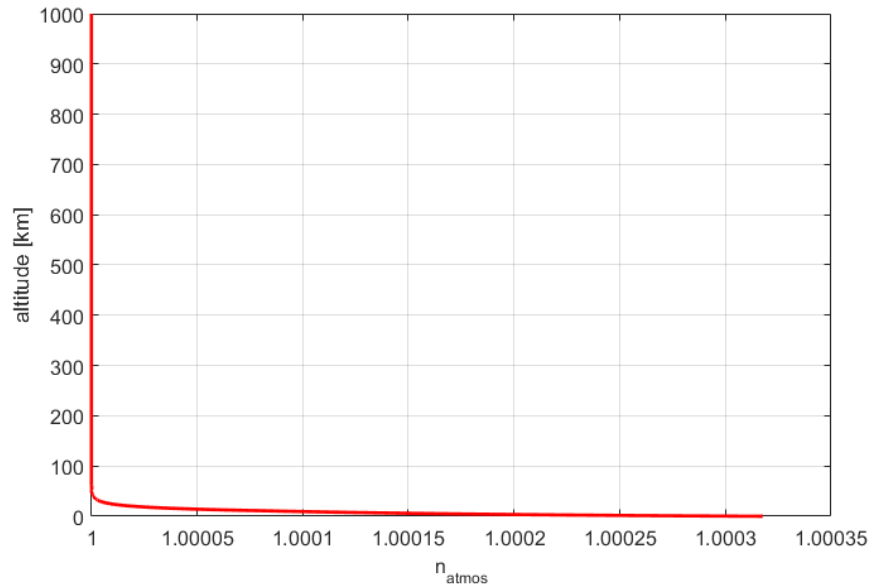
Figure 3.3.: Refraction index for the atmosphere

with parallel layers of atmosphere above the earth surface. The height step sizes for the boundaries between the layers is determined by the data file including the electron density distribution from NASA (2012). For each layer of atmosphere the refraction index is calculated according to equation 3.1 for the height of the lower boundary of the layer. Within a single layer the refraction index stays constant.

The matlab code for the flat earth model is given in the appendix A.1. To allow a comparison of the non refracted and the refracted signal, both signals have to leave the transmitter satellite at the same location and hit the receiver satellite within a determined accuracy at the same location. To achieve this, the signal emission angle of the refracted signal ($\theta_1(1)$) is varied until the condition $x_2(end) = x_R \pm accuracy$ is fulfilled. The initial value of $\theta_1(1)$ is set to the signal emission angle of the non refracted signal (θ_T). It can be expected that the signal emission angle for the refracted signal satisfying the condition is greater than the signal emission angle of the non refracted signal. The equations for the calculation of the non refracted and the refracted path are stated and described below.

The calculations for the flat earth model are performed for the following
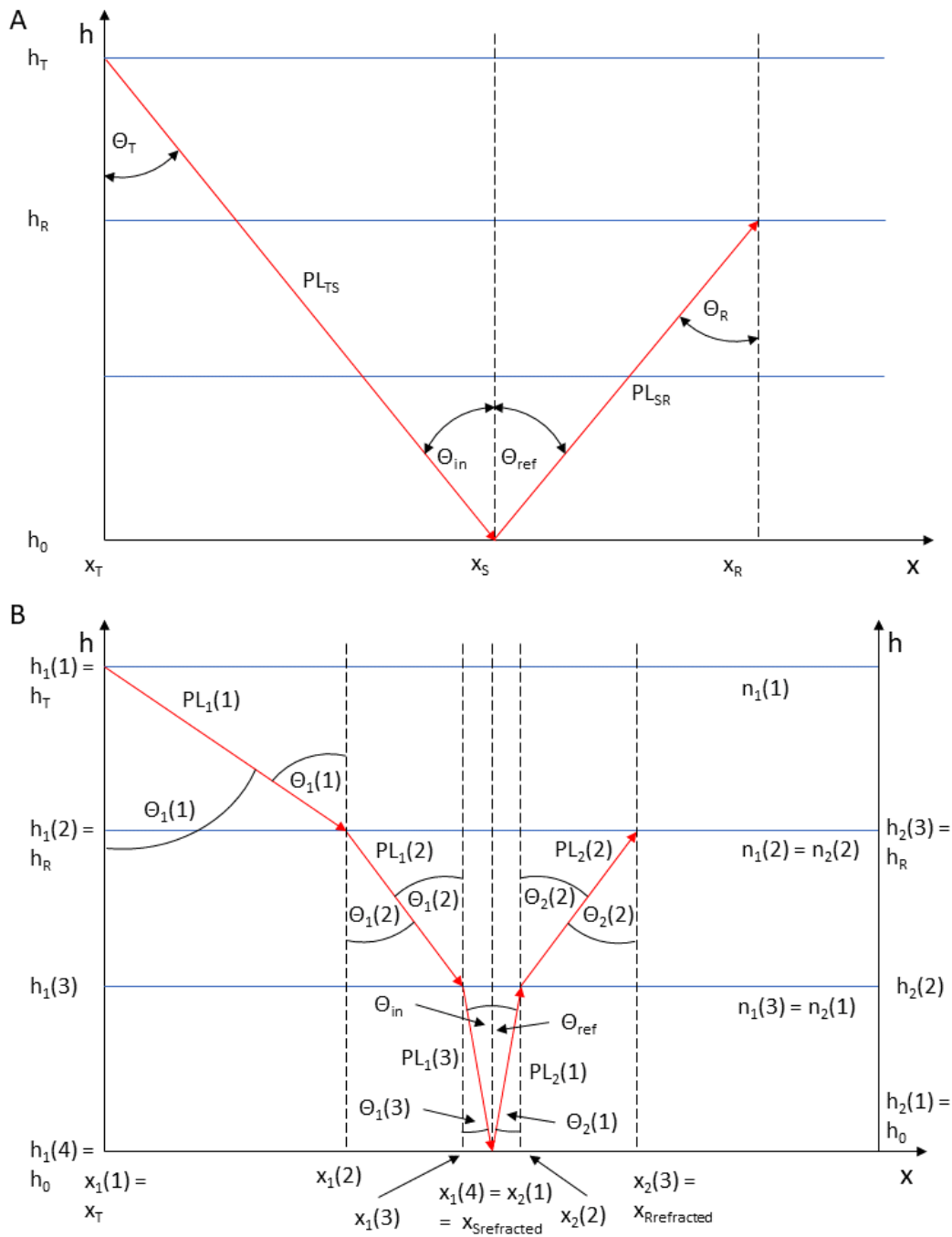
Figure 3.4.: Non refracted signal (A) and refracted signal (B) for the flat earth model with parallel layers of atmosphere

signal emission angles for the non refracted signal.

$$\theta_T = (1, 20, 40, 60, 85)^\circ \tag{3.2}$$

3.2.1. Calculation of the non refracted path

The upper picture in Figure 3.4 shows a scheme of the non refracted path of the signal from the transmitter satellite to the receiver satellite reflected by the earth surface for the flat earth model. The equations to calculate the postulated results for the non refracted path are given below.

Horizontal distances:

$$x_S = \tan(\theta_T) \cdot (h_T - h_0) + x_T \tag{3.3}$$
$$x_R = \tan(\theta_T) \cdot (h_R - h_0) + x_S \tag{3.4}$$

To calculate the horizontal distances for the non refracted signal the characteristics of the tangent function are used.

Angle of incidence:

$$\theta_{in} = \theta_T \tag{3.5}$$
$$\theta_R = \theta_T \tag{3.6}$$

Because there is no refraction the angle of incidence at the reflection point and at the receiver satellite is equal to the signal emission angle of the transmitter satellite.

Path lengths:

$$PL_{TS} = \frac{h_T - h_0}{\cos(\theta_T)} \tag{3.7}$$

$$PL_{SR} = \frac{h_R - h_0}{\cos(\theta_T)} \tag{3.8}$$

$$PL = PL_{TR} + PL_{SR} \tag{3.9}$$

To calculate the path length of the non refracted signal the characteristics of the cosine function are used.

3.2.2. Calculation of the refracted path

The lower picture of Figure 3.4 shows the scheme for the refracted path of the signal from the transmitter satellite to the receiver satellite reflected by the Earth. The refracted path is calculated with the function *Calculation of refracted signal for flat Earth* (appendix A.1.2). To calculate the whole refracted path the following calculation has to be done for every layer of atmosphere. For better comparison the path is split up into a path 1 from the transmitter satellite to the reflection point and a path 2 from the reflection point to the receiver satellite. The initial horizontal distance for the refracted path is set to $x_1(1) = x_T$. The equations to calculate the postulated results for the refracted path are given below. Note that the calculation has to be repeated until the condition $x_2(end) = x_R \pm accuracy$ is fulfilled.

Horizontal distances:

$$x_1(l+1) = \tan(\theta_1(l)) \cdot (h_1(l) - h_1(l+1)) + x_1(l) \tag{3.10}$$

$$x_2(l+1) = \tan(\theta_2(l)) \cdot (h_2(l+1) - h_2(l)) + x_2(l) \tag{3.11}$$

$$x_{Srefracted} = x_1(end) \tag{3.12}$$

$$x_{Rrefracted} = x_2(end) \tag{3.13}$$

To calculate the horizontal distances for the refracted signal again the characteristics of the tangent function are used. The index l corresponds to the numbers in Figure 3.4 and to the counter variable used in MATLAB.

Angles of refraction:

$$\theta_1(l+1) = \arcsin\left(\frac{n_1(l) \cdot \sin(\theta_1(l))}{n_1(l+1)}\right) \tag{3.14}$$

$$\theta_2(l+1) = \arcsin\left(\frac{n_2(l) \cdot \sin(\theta_2(l))}{n_2(l+1)}\right) \tag{3.15}$$

$$\theta_{Trefracted} = \theta_1(1) \tag{3.16}$$

With:

$$\theta_2(1) = \theta_1(end)$$

To calculate the angles of refraction for the refracted signal equation 2.9 (Snell's law) is used.

Path lengths:

$$PL_1(l) = \frac{h_1(l) - h_1(l+1)}{\cos(\theta_1(l))} \qquad (3.17)$$

$$PL_2(l) = \frac{h_2(l+1) - h_2(l)}{\cos(\theta_2(l))} \qquad (3.18)$$

To calculate the path length of the refracted signal again the characteristics of the cosine function are used. The path length from the transmitter satellite to the reflection point for the refracted signal is received by summing up all elements of PL_1 and the path length from the reflection point to the receiver satellite for the refracted signal is received by summing up all elements of PL_2.

$$PL_{TSrefracted} = \sum PL_1 \qquad (3.19)$$

$$PL_{SRrefracted} = \sum PL_2 \qquad (3.20)$$

The sum of $PL_{TSrefracted}$ and $PL_{SRrefracted}$ results the total path length of the refracted signal.

$$PL_{refracted} = PL_{TSrefracted} + PL_{SRrefracted} \qquad (3.21)$$

3.2.3. Results flat Earth

In this section the results for the non refracted and the refracted path for the flat earth model for the determined θ_T are shown.

The *accuracy* to fulfil the condition $x_2(end) = x_R \pm accuracy$ and the variation step size (θ_{1step}) of the signal emission angle for the simulation of the refracted signal path are:

$$accuracy = \pm 1\,\text{m}$$

$$\theta_{1step} = 0.005\,^\circ$$

Description of the abbreviations used below:

$theta_T$	is the signal emission angle for the non refracted signal related to nadir
$theta_{Trefracted}$	is the signal emission angle for the refracted signal related to nadir
x_{Rdiff}	is the difference between the refracted and the non refracted horizontal distance from the transmitter satellite to the receiver satellite
x_{Sdiff}	is the difference between the refracted and the non refracted horizontal distance from the transmitter satellite to the reflection point
PL_{diff}	is the difference between the refracted and the non refracted total path length

Where x_{Sdiff}, x_{Rdiff} and PL_{diff} are received through the following equations.

$$x_{Sdiff} = |x_S - x_{Srefracted}| \tag{3.22}$$
$$x_{Rdiff} = |x_R - x_{Rrefracted}| \tag{3.23}$$
$$PL_{diff} = |PL - PL_{refracted}| \tag{3.24}$$

Height step size $h_{step} = 500\,\text{m}$

θ_T [°]	$\theta_{Trefracted}$ [°]	x_{Rdiff} [m]	x_{Sdiff} [m]	PL_{diff} [m]
1.0	1.000 000	0.09	0.04	0.0
20.0	20.000 005	0.06	0.91	0.0
40.0	40.000 012	0.38	3.71	0.2
60.0	60.000 024	0.75	16.91	0.6
85.0	85.000 153	0.99	3408.00	1.6

Table 3.1.: Results for flat earth model, $h_{step} = 500\,\text{m}$

Table 3.1 shows the results of the signal path simulation for the flat earth model with a selected height step size of 500 m. x_{Rdiff} is smaller than 1 m for all five signal emission angles and therefore the accuracy condition is fulfilled for each signal emission angle. The superelevation of the signal emission angle for the refracted signal increases with the increase of the signal emission angle for the non refracted signal. This is because, the higher the signal emission angle is, the longer is the horizontal distance to

the receiver satellite. Therefore $\theta_{Trefracted}$ has to be more superelevated for higher θ_T to fulfil the accuracy condition. Although, a difference between the reflection points of $x_{Sdiff} \approx 3.4\,\text{km}$ for $\theta_T = 85\,^\circ$ seems rather high, it is not. A signal emission angle of $85\,^\circ$ means, it is nearly parallel to the surface of the flat Earth ($\theta_T = 90\,^\circ$ would be parallel). And, a parallel signal would not have a reflection point at all. Hence, 3.4 km difference between the non refracted and the refracted reflection point are realistic ($x_S(\theta_T = 85\,^\circ) \approx 228,601\,\text{km}$). The path length difference for all signal emission angles except $85\,^\circ$ is lower than 1 m. The reason for the comparatively large $PL_{diff}(\theta_T = 85\,^\circ) = 1.6\,\text{m}$ is the accuracy criterion, that has just been fulfilled ($x_{Rdiff} = 0.99\,\text{m}$).

Height step size $h_{step} = 5\,\text{km}$

θ_T [°]	$\theta_{Trefracted}$ [°]	x_{Rdiff} [m]	x_{Sdiff} [m]	PL_{diff} [m]
1.0	1.000 000	0.11	0.06	0.0
20.0	20.000 005	0.72	0.57	0.2
40.0	40.000 015	0.44	4.00	0.3
60.0	60.000 032	0.07	21.53	0.1
85.0	85.000 201	0.06	4481.34	0.9

Table 3.2.: Results for flat earth model, $h_{step} = 5\,\text{km}$

Table 3.2 shows the results of the signal path simulation for the flat earth model with a selected height step size of 5 km. The results show nearly the same behaviour as for a step size of 500 m and also satisfies the required accuracy ($x_{Rdiff} < 1\,\text{m}$). There is only one small differences. With an increasing θ_T, x_{Sdiff} becomes larger compared to the results for a height step size of 500 m. The reason for this is a smoother curve (more elements) for calculations with small step sizes. This results in a more precise calculation of the reflection point for the refracted signal for calculations with smaller height step sizes. Due to the more precise calculation the horizontal distances are smaller for smaller height step sizes.

3.3. Spherical Earth

This section describes the calculation for the non refracted and the refracted path as well as it states the simulation results for the spherical earth model. The spherical earth model, as can be seen in Figure 3.5, assumes a spherical Earth (see section 2.3.1) and radially bent layers of atmosphere above the earth surface. The satellite orbits are assumed to be circular orbits. Just as in the flat earth model the height step sizes for the boundaries between the layers is determined by the data file including the electron density distribution from NASA (2012) and the refraction index for each layer of atmosphere is calculated according to equation 3.1 for the height of the lower boundary of the layer. Again, within a single layer the refraction index stays constant.

The MATLAB code for the calculation is given in the appendix A.2. For the spherical earth model the same accuracy condition as for the flat earth model applies. The horizontal distance to the receiver satellite for the refracted signal has to be equal to the horizontal distance to receiver for the non refracted signal ($hd_2(end) = hd_R \pm accuracy$). Note, that the horizontal distances for the spherical earth model are denoted as hd and that they are measured on the earth surface (r_0) (see Figure 3.5). Again, a superelevation of the signal emission angle for the refracted signal compared to the signal emission angle of the non refracted signal can be expected. The equations for the calculation of the non refracted and the refracted path are stated and described below.

The calculations for the spherical earth model are performed for the following signal emission angles for the non refracted signal.

$$\theta_T = (1, 2, 3, 4, 5, 6, 7, 8, 9, 10, 11, 12, 13, 13.5, 13, 9, 13.95, 13.97)^\circ \qquad (3.25)$$

3.3.1. Maximum signal emission angle for spherical earth model

Before the calculation of the signal paths is described, one characteristic of the spherical earth model has to be investigated. For the spherical earth model a maximum signal emission angle (θ_T) exists. If θ_T would exceed this maximum angle the electromagnetic signal would miss the Earth. This is

3. Influence of the atmosphere on the refraction of an electromagnetic signal and its associated effects on the reflection point calculation

Figure 3.5.: Non refracted signal (A) and refracted signal (B) for the spherical earth model with radially bent layers of atmosphere

also true for the Earth modelled as an ellipsoid or as geoid. Therefore the first step for the spherical earth model is to determine the maximum signal emission angle θ_{Tmax} by the use of the following equation.

$$\theta_{Tmax} = \arcsin\left(\frac{r_0}{h_T}\right) = 13,9805\,° \tag{3.26}$$

The maximum signal emission angle occurs whenever the electromagnetic wave is a tangent to the earth surface. In this case the electromagnetic wave is normal on the earth radius and equation 3.26 applies.

3.3.2. Calculation of the non refracted path

The upper picture in Figure 3.5 shows a scheme of the non refracted path of the signal from the transmitter satellite to the receiver satellite reflected by the earth surface for the spherical earth model. The equations to calculate the postulated results for the non refracted path are given below.

Angles of incidence:

$$\theta_{in} = \arcsin\left(\frac{\sin(\theta_T)\cdot r_T}{r_0}\right) \tag{3.27}$$

$$\theta_R = \arcsin\left(\frac{\sin(\theta_{in})\cdot r_0}{r_R}\right) \tag{3.28}$$

With:

$$r_T = r_0 + h_T$$
$$r_R = r_0 + h_R$$

Where:
  r_T is the radius of circular transmitter satellite orbit
  r_R is the radius of circular receiver satellite orbit

θ_{in} and θ_{ref} are calculated according to equation 2.13 as described in section 2.1.3). The calculation uses the fact that for a non refractive atmosphere θ_T can be mirrored at the tangent to r_T where the signal ray crosses r_T and θ_{in} can be mirrored at the tangent to r_0 where the signal ray crosses r_0.

Angles between horizontal distances

$$\varphi_S = \theta_{in} - \theta_T \tag{3.29}$$
$$\varphi_R = \theta_{ref} - \theta_R + \varphi_S \tag{3.30}$$

To calculate the angles between the horizontal distance the fact that the sum of all angles within a triangle has to be π rad is used. E.g. $\varphi_S = \pi - \theta_T - (\pi - \theta_{in})$

Note that both angles φ_S and φ_R are related to the r-axis.

Horizontal distances:

$$hd_S = r_0 \cdot \varphi_S \tag{3.31}$$
$$hd_R = r_0 \cdot \varphi_R \tag{3.32}$$

To calculate the horizontal distances, the formula to calculate a circular arc is used. Note, the horizontal distances for the spherical earth model are measured on the earth surface (r_0).

Path lengths:

$$PL_{TS} = \sqrt{r_T^2 + r_0^2 - 2 \cdot r_T \cdot r_0 \cdot \cos(\varphi_S)} \tag{3.33}$$
$$PL_{SR} = \sqrt{r_R^2 + r_0^2 - 2 \cdot r_R \cdot r_0 \cdot \cos(\varphi_R - \varphi_S)} \tag{3.34}$$
$$PL = PL_{TS} + PL_{SR} \tag{3.35}$$

To calculate the path length for the non refracted signal the characteristics of the cosine function are used.

3.3.3. Calculation of the refracted path

The lower picture of Figure 3.5 shows the scheme for the refracted path of the signal from the transmitter satellite to the receiver satellite reflected by the Earth. The refracted path is calculated with the function *Calculation of refracted signal for spherical Earth* (appendix A.2.1). To calculate the whole refracted path, similar to the flat earth model the following calculations have to be done for every layer of atmosphere. Again, the path is split up into a path 1 from the transmitter satellite to the reflection point and a path 2 from the reflection point to the receiver satellite. The initial value for horizontal distance for the refracted path is set to $hd_1(1) = hd_T$ and the initial value for the refraction angle is set to $\beta_1(1) = \theta_T$. Note that the calculation has to be repeated until the condition $hd_2(end) = hd_R \pm accuracy$ is fulfilled.

Refraction angles: with equation 2.13

$$\beta_1(l+1) = \arcsin\left(\frac{\sin(\beta_1(l)) \cdot n_1(l) \cdot r_1(l)}{n_1(l+1) \cdot r_1(l+1)}\right) \tag{3.36}$$

$$\beta_2(l+1) = \arcsin\left(\frac{\sin(\beta_2(l)) \cdot n_2(l) \cdot r_2(l)}{n_2(l+1) \cdot r_2(l+1)}\right) \tag{3.37}$$

Equation 3.36 and 3.37 are calculated by the use of equation 2.13. The fact that the atmosphere layer above r_T and the first layer underneath have the same refraction index is used to calculate equation 3.36. Therefore $\theta_1(1)$ can be mirrored at the tangent to r_T where the signal ray crosses r_T so $\beta_1(1) = theta_1(1)$. This is not necessary for equation 3.37 because $beta_2(1) = \beta_1(end)$ and equation 2.13 applies without any mirroring. Similar to the flat earth model the index l corresponds to the numbers in Figure 3.5 and to the counter variable used in MATLAB.

Angles after refraction:

$$\theta_1(l) = \arcsin\left(\frac{sin(\beta_1(l)) \cdot n_1(l)}{n_1(l+1)}\right) \tag{3.38}$$

$$\theta_2(l) = \arcsin\left(\frac{sin(\beta_2(l+1) \cdot n_2(l+1)}{n_2(l)}\right) \tag{3.39}$$

$$\theta_{Trefracted} = \theta_1(1) \tag{3.40}$$

Where:
$\theta_{Trefracted}$ is the superelevated signal emission angle at transmitter satellite for the refracted signal

To calculate the angles of refraction for the refracted signal equation 2.9 (Snell's law) is used.

Angles between horizontal distances:

$$\varphi_1(l+1) = \beta_1(l+1) - \theta_1(l) + \varphi_1(l) \tag{3.41}$$
$$\varphi_2(l+1) = \beta_2(l) - \theta_2(l) + \varphi_2(l) \tag{3.42}$$

With:

$$\varphi_1(1) = 0^\circ$$
$$\varphi_2(1) = \varphi_1(end)$$

To calculate the angles between the horizontal distance the fact that the sum of all angles within a triangle has to be π rad is used. E.g. $\varphi_1(2) =$

$\pi - \theta_1(1) - (\pi - \beta_1(2)) + \varphi_1(1)$

Note that the angles $\varphi_1(l)$ and $\varphi_2(l)$ are related to the r-axis.

Horizontal distances:

$$hd_1(l+1) = r_0 \cdot \varphi_1(l+1) \tag{3.43}$$
$$hd_2(l+1) = r_0 \cdot \varphi_2(l+1) \tag{3.44}$$
$$hd_{Srefracted} = hd_1(end) \tag{3.45}$$
$$hd_{Rrefracted} = hd_2(end) \tag{3.46}$$

With:

$$hd_2(1) = hd_1(end)$$

To calculate the horizontal distances, the formula to calculate a circular arc is used. Note, the horizontal distances for the spherical earth model are measured on the earth surface (r_0).

Path lengths:

$$PL_1(l) = \sqrt{r_1(l)^2 + r_1(l+1)^2 - 2 \cdot r_1(l) \cdot r_1(l+1) \cdot \cos(\varphi_1(l+1) - \varphi_1(l))} \tag{3.47}$$

$$PL_2(l) = \sqrt{r_2(l)^2 + r_2(l+1)^2 - 2 \cdot r_2(l) \cdot r_2(l+1) \cdot \cos(\varphi_2(l+1) - \varphi_2(l))} \tag{3.48}$$

To calculate the path length of the refracted signal again the characteristics of the cosine function are used. The path length from the transmitter satellite to the reflection point for the refracted signal is received by summing up all elements of PL_1 and the path length from the reflection point to the receiver satellite for the refracted signal is received by summing up all elements of PL_2.

$$PL_{Srefracted} = \sum PL_1 \tag{3.49}$$
$$PL_{Rrefracted} = \sum PL_2 \tag{3.50}$$

The sum of $PL_{Srefracted}$ and $PL_{Rrefracted}$ results the total path length of the refracted signal.

$$PL_{refracted} = PL_{Srefracted} + PL_{Rrefracted} \tag{3.51}$$

3.3.4. Results spherical Earth

In this section the results for the non refracted and the refracted path for the spherical earth model for the determined θ_T are shown.

The *accuracy* to fulfil the condition $x_2(end) = x_R \pm accuracy$ and the variation step size (θ_{1step}) of the signal emission angle for the simulation of the refracted signal path are:

$$accuracy = \pm 1\,\text{m}$$
$$\theta_{1step} = 0.005\,°$$

For the spherical earth model the same abbreviations as for the flat earth model, with slight changes and additions, apply.

Description of the changed and added abbreviations used below:

hd_{Rdiff} is the difference between the refracted and the non refracted horizontal distance from the transmitter satellite to the receiver satellite, hd_R and $hd_{Rrefracted}$

hd_S is the horizontal distance from the transmitter satellite to the reflection point for the non refracted signal

$hd_{Srefracted}$ is the horizontal distance from the transmitter satellite to the reflection point for the refracted signal

hd_{Sdiff} is the difference between hd_S and $hd_{Srefracted}$

Where hd_{Rdiff} and hd_{Sdiff} are received through the following equations.

$$hd_{Rdiff} = |hd_R - hd_{Rrefracted}| \tag{3.52}$$
$$hd_{Sdiff} = |hd_S - hd_{Srefracted}| \tag{3.53}$$

Height step size $h_{step} = 500\,\text{m}$

Table 3.3 shows the results of the signal path simulation for the spherical earth model with a selected height step size of 500 m. Similar to the flat earth simulations it is easy to see that hd_{Rdiff} is smaller than 1 m for all signal emission angles and therefore the accuracy condition is fulfilled for each signal emission angle. The superelevation of the signal emission angle for the refracted signal increases with increasing signal emission angle for the non refracted signal. This has the same reason as for the flat earth model.

θ_T [°]	$\theta_{Trefracted}$ [°]	hd_{Rdiff} [m]	hd_S [km]	$hd_{Srefracted}$ [km]	hd_{Sdiff} [m]	PL_{diff} [m]
1.0	1.000 000	0.36	349.4437	349.4435	0.2	0.0
2.0	2.000 000	0.74	701.1761	701.1757	0.4	0.1
3.0	3.000 005	0.81	1057.5960	1057.5972	1.2	0.2
4.0	4.000 005	0.39	1421.3380	1421.3390	1.0	0.1
5.0	5.000 005	0.11	1795.4317	1795.4325	0.8	0.0
6.0	6.000 005	0.73	2183.5259	2183.5264	0.5	0.3
7.0	7.000 010	0.78	2590.2291	2590.2312	2.1	0.4
8.0	8.000 010	0.19	3021.6677	3021.6694	1.8	0.1
9.0	9.000 012	0.31	3486.4818	3486.4841	2.3	0.2
10.0	10.000 017	0.44	3997.7828	3997.7868	4.0	0.3
11.0	11.000 022	0.03	4577.5555	4577.5608	5.3	0.0
12.0	12.000 032	0.50	5268.7772	5268.7857	8.6	0.4
13.0	13.000 060	0.90	6183.6102	6183.6307	20.5	0.8
13.5	13.500 107	0.85	6847.2978	6847.3390	41.3	0.8
13.9	13.900 438	0.50	7784.8379	7785.0282	190.3	0.7
13.95	13.950 838	0.34	8039.8710	8040.2416	370.6	1.1
13.97	13.971 453	0.92	8210.0357	8210.6828	647.0	0.9

Table 3.3.: Results for spherical earth model, $h_{step} = 500\,\mathrm{m}$

For clarification, the horizontal distances can be greater than the radius of the Earth because the horizontal distances are measured on the earth surface. The path length difference for all signal emission angles is about 1 m and therefore has an acceptable value compared to the allowed signal path difference for the reflection point calculation.

Height step size $h_{step} = 5\,\mathrm{km}$

Table 3.4 shows the results of the signal path simulation for the spherical earth model with a selected height step size of 5 km. Obviously the results show nearly the same behaviour as for a step size of 500 m and also satisfies the accuracy condition. They only difference is, that the signal emission angle for the refracted signal, the horizontal distance to the receiver satellite and the horizontal distance to the reflection point show slightly higher values. This is because of the bigger height step size. Similar to the results of the flat earth model, a higher height step size results a less precise

θ_T [°]	$\theta_{Trefracted}$ [°]	hd_{Rdiff} [m]	hd_S [km]	$hd_{Srefracted}$ [km]	hd_{Sdiff} [m]	PL_{diff} [m]
1.0	1.000 000	0.48	349.4437	349.4435	0.2	0.0
2.0	2.000 000	1.00	701.1761	701.1756	0.5	0.1
3.0	3.000 005	0.43	1057.5960	1057.5970	1.0	0.1
4.0	4.000 005	0.14	1421.3380	1421.3387	0.7	0.0
5.0	5.000 005	0.83	1795.4317	1795.4321	0.4	0.3
6.0	6.000 010	0.51	2183.5259	2183.5279	2.0	0.2
7.0	7.000 010	0.49	2590.2290	2590.2306	1.6	0.2
8.0	8.000 015	0.62	3021.6677	3021.6707	3.0	0.4
9.0	9.000 017	0.10	3486.4818	3486.4853	3.5	0.1
10.0	10.000 022	0.15	3997.7828	3997.7877	4.9	0.1
11.0	11.000 030	0.09	4577.5555	4577.5642	8.7	0.1
12.0	12.000 043	0.00	5268.7772	5268.7890	11.8	0.1
13.0	13.000 078	0.52	6183.6102	6183.6361	25.9	0.5
13.5	13.500 142	0.03	6847.2978	6847.3516	53.8	0.1
13.9	13.900 572	0.93	7784.8379	7785.0856	247.7	0.5
13.95	13.951 078	0.76	8039.8710	8040.3480	477.0	1.9
13.97	13.971 824	0.62	8210.0357	8210.8486	812.9	3.3

Table 3.4.: Results for spherical earth model, $h_{step} = 5\,\text{km}$

calculation. Therefore, the results of the calculation performed with the smaller height step size are significant.

3.4. Discussion of the results

The objective of this chapter was to investigate how the atmosphere influences the refraction of an electromagnetic signal propagating through it and to clarify, if this influence has to be taken into account for the reflection point calculation. For this purpose, the path length difference (PL_{diff}) between the refracted and the non refracted signal is the determining factor. For all four calculations the path length difference is below 2 m. Except for the spherical earth model with $h_{step} = 5\,\text{km}$. Since a higher height step size results less precise calculations, the results of the calculation with $h_{step} = 500\,\text{m}$ are significant. The maximum allowed signal path difference for the reflection point calculation is 10 m (stated in section 1.4). Since 1.19 m is a tenth of

the signal path difference allowed, the impact of the influence of the atmosphere on the refraction of an electromagnetic signal on the reflection point calculation can only be clarified in relation to the signal path difference of the results of the reflection point calculation.

Since the spherical earth model is the more realistic one, we will take a closer look at it below. As stated in section 1.4, the satellite elevation angle above the horizontal plane has to be within $0°$ to $15°$. A satellite elevation angle of $15°$ corresponds to $13.5°$ of signal emission angle and a satellite elevation angle of $0°$ corresponds to the maximum signal emission angle for the spherical earth model of $13.9805°$. This means, all signal emission angles of the spherical earth model equal or higher than $13.5°$ are significant for the reflection point calculation. For a height step size of $500\,m$ the highest path length difference for these angles is $1.1\,m$. Again, this is a tenth of the signal path difference allowed. Therefore, the influence on the reflection point calculation has to be clarified in relation to the signal path difference of the results of the reflection point calculation. If the influence of the atmosphere has to be taken into account for the reflection point calculation, a height step size of $500\,m$ for the atmosphere model is recommended.

Additionally it can be seen that neither for the flat earth nor the spherical earth simulations, the superelevation of the signal emission angle for the refracted signal has an significant impact on the satellite alignment. Because in both simulation cases, the effect on $\theta_{Trefracted}$ is visible first in the fourth decimal place, if at all.

4. Methods for the reflection point calculation

Chapter 4 deals with the calculation of the reflection point. More precisely, different methods and approaches for the reflection point calculation are presented and explained here. In addition, their advantages, disadvantages and possible problems concerning the implementation are elaborated.

The chapter starts with sketches and a description of the problem to give a better understanding of the reflection point calculation and the abbreviations used. It continuous with a brief description of four methods presented by Jales (2012, chapter 4). Since he describes four possible methods with increasing complexity, this serves as a good access to the topic. The second section explains how the *Binary Search* algorithm can be used for the calculation of the reflection point. In the third section the idea of calculating the reflection point by the use of *Ray Tracing* is elucidated. Both *Binary Search* and *Ray Tracing* are based on ideas of Dipl. Ing. Andreas Dielacher (RUAG Space). Section four outlines how the reflection characteristic of an ellipse could be used for the calculation and section five avows how a calculation method by the use of *Finite Elements* could work. An inaccuracy that affects many of the calculation methods is explained as penultimate point. The chapter ends with a calculation addition that could cancel out this inaccuracy.

4.1. Problem description and used abbreviations

In order to better understand the problem of the reflection point calculation and to get an overview of the abbreviations used later on, the Figures 4.1 to 4.4 show sketches of the problem. These sketches do not use the WGS 84 earth model. Instead a spheroid with a semimajor axis of $a = 10000\,\text{km}$ and a much higher flattening of $f = 0.25$ is used. For comparison, the

WGS 84 has a flattening of $f = 0.0034$. The altitudes of the satellites are $h_T = 10000\,\text{km}$ and $h_R = 7500\,\text{km}$ above the "earth surface". This is done to point out the positions and distances necessary for the calculation. Because, with the WGS 84 as earth model and the real satellite altitudes the sketches would be narrow and unclear.

As stated in section 1.4, one of the objectives of this thesis is to find a method which calculates the reflection point (S_{calc}) nearest to the true reflection point (S). Which is the point on the earth surface, where an electromagnetic signal leaving the transmitter satellite (T) is reflected in such a way to hit the receiver satellite (R). Therefore at S the Law of Reflection (see section 2.4.1) has to prevail. Although, Figures 4.1 to 4.4 do not show the WGS 84 earth model, later on the model of the Earth shall be the WGS 84 (see section 1.4 and 2.3.2) with the centre of the Earth (M) located at $(0,0,0)$ in Earth Centered Earth Fixed (ECEF) coordinates. The absolute value of the vector between the transmitter and the receiver satellite ($\overrightarrow{TR}$) is denoted as the direct signal path between transmitter and receiver satellite or as the signal path of the non reflected signal ($SP_d = |\overrightarrow{TR}|$). The sum of the absolute value of the vector between the transmitter satellite and the true reflection point ($\overrightarrow{TS}$) and the absolute value of the vector between the true reflection point and the receiver satellite ($\overrightarrow{SR}$) is the true earth-reflected signal path from the transmitter to the receiver satellite ($SP_r = |\overrightarrow{TS}| + |\overrightarrow{SR}|$). The position of the calculated reflection point is denoted as S_{calc}. With $\overrightarrow{TS_{calc}}$ is the vector between the transmitter satellite and the calculated reflection point and $\overrightarrow{S_{calc}R}$ is the vector between the calculated reflection point and the receiver satellite. The sum of $\overrightarrow{TS_{calc}}$ and $\overrightarrow{S_{calc}R}$ is SP_{rcalc}, the calculated earth-reflected signal path from the transmitter to the receiver satellite. SP_{diff} is the difference between the true reflected signal path (SP_r) and the calculated reflected signal path (SP_{rcalc}). For both, the true and the calculated reflection point a surface normal exists. The surface normal of the true reflection point is denoted as N_S and the surface normal of the calculated reflection point as N_{Scalc}. The vectors between the centre of the Earth (M) and either the true or the calculated reflection point (S and S_{calc}) are $\overrightarrow{MS}$ and $\overrightarrow{MS_{calc}}$. SS_{calc} is denoted as the distance between the true and the calculated reflection point. SS_{calc} is the absolute value of the vector between the true and the calculated reflection point ($\overrightarrow{SS_{calc}}$).

Note, all positions such as R, T or S_{calc} are points in ECEF coordinates.

Differences between two positions / points such as $\overrightarrow{SS_{calc}} = S - S_{calc}$ or $\overrightarrow{TR} = T - R$ are nominal vectors and therefore marked with an overhead right arrow. To every vector exists an associated scalar which is the distance between the two positions (e.g. $SP_d = |\overrightarrow{TR}|$ or $SS_{calc} = |\overrightarrow{SS_{calc}}|$). An exception are the surface normals (N_S and N_{Scalc}). They are neither a position nor a vector. They are a direction of a straight line and need a point like S or S_{calc} to be well-defined (see section 2.2.1).
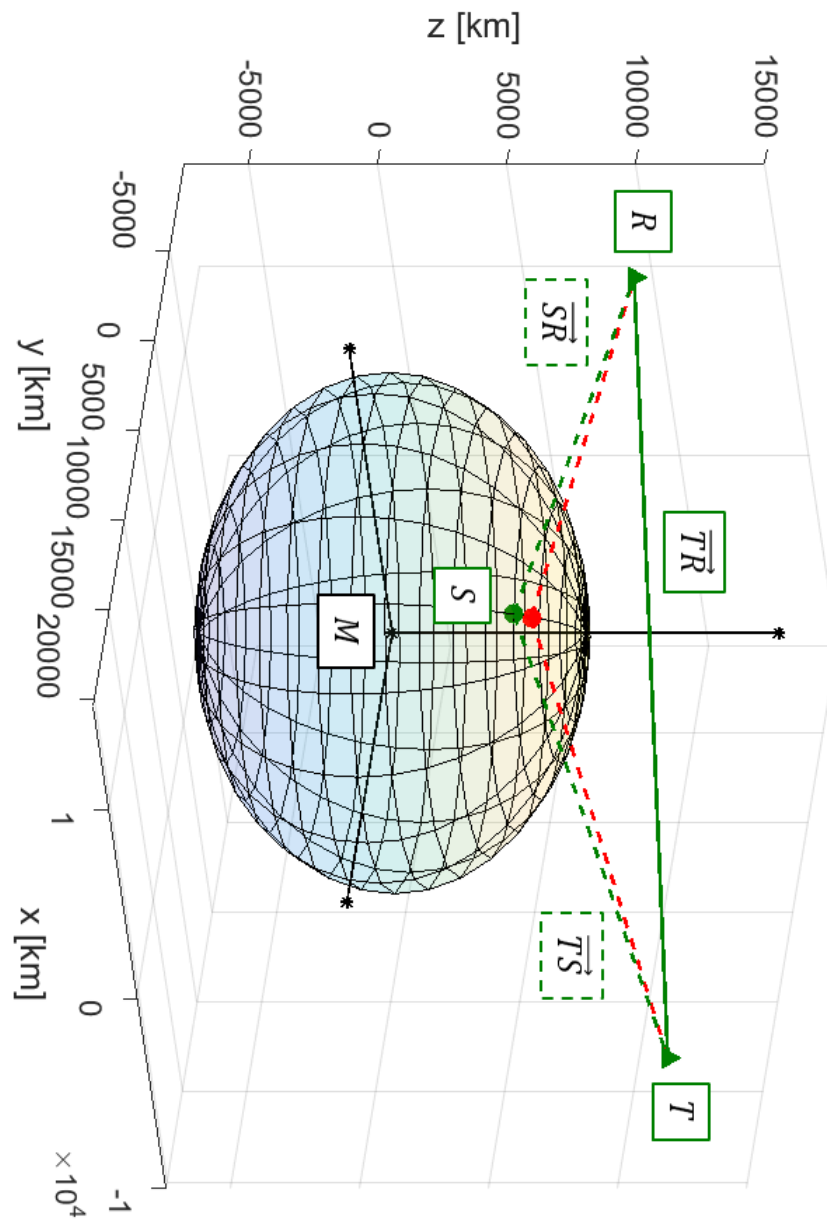
Figure 4.1.: Outline sketch 1 of the reflection point calculation
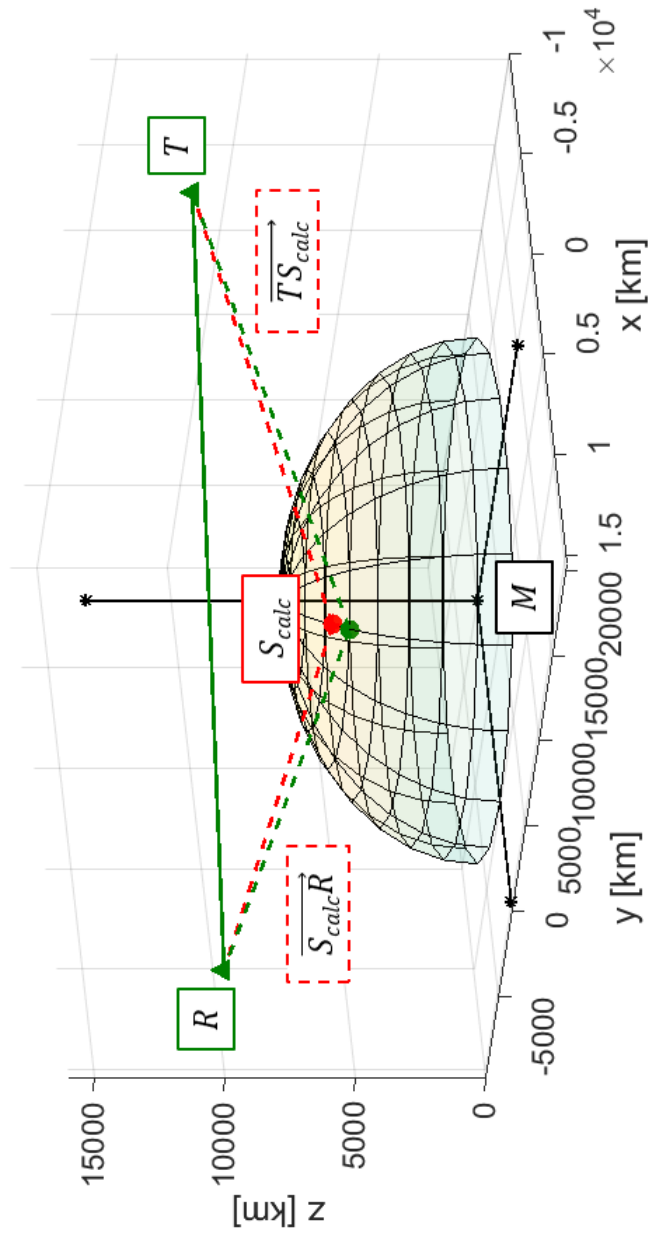
Figure 4.2.: Outline sketch 2 of the reflection point calculation
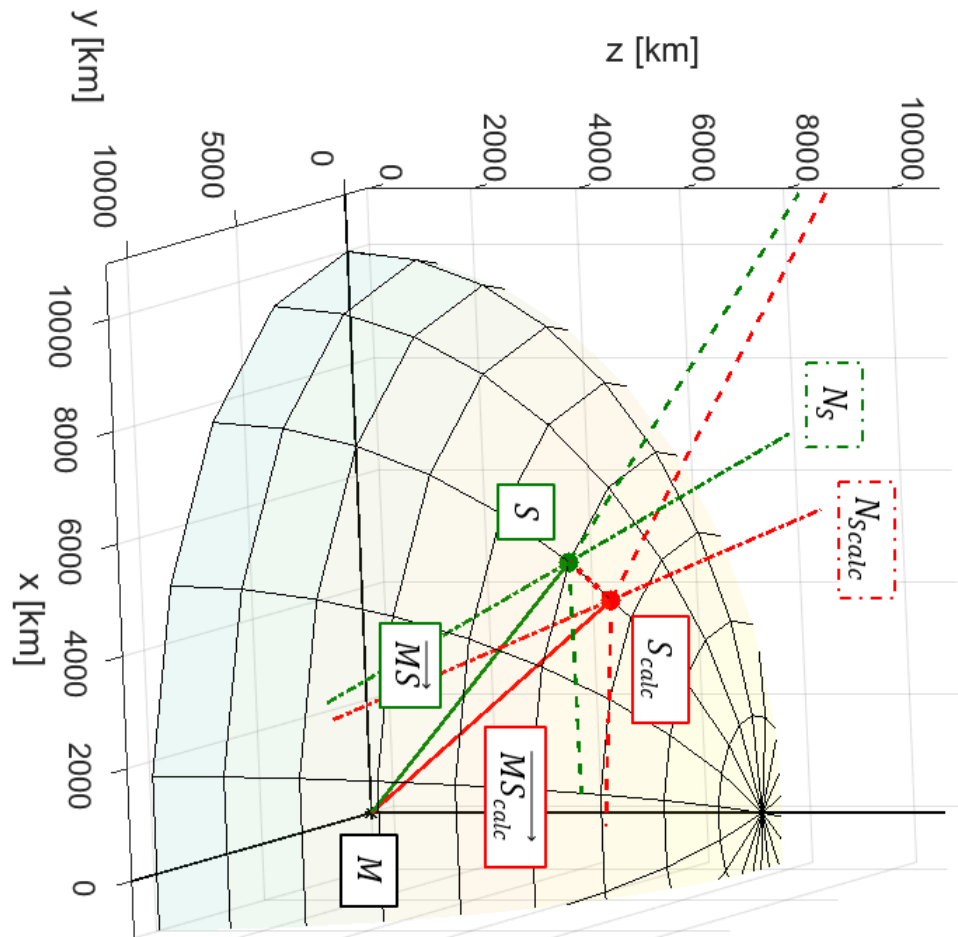
Figure 4.3.: Outline sketch 3 of the reflection point calculation

Figure 4.4.: Outline sketch 4 of the reflection point calculation

4.2. Methods from Philip Jales

Jales (2012, chapter 4.4) describes four different methods to calculate the reflection point for a GNSS-R mission. The description starts with an approximation using the spherical earth model. It continuous with a quasi spherical earth approach followed by a description of the calculation for the ellipsoidal earth model (WGS 84). Finally, an optimisation of the ellipsoidal earth model by the use of polar coordinates is described.

Jales uses the ellipsoidal earth model (see section 4.2.3) as reference solution to allow comparison with the spherical and the quasi-spherical earth model. Therefore, he performed Monte-Carlo simulations with a random receiver location (R) at an alltitude of 700 km and a random transmitter location (T) at an alltitude of 20200 km. The results of the Monte-Carlo simulations are not stated in the following description.

4.2.1. Spherical Earth

For the description of the spherical earth approach Jales refers to Martin-Neira (1993, chapter 2). The description of Martin-Neira is not explicitly stated here. In short, the spherical earth model can transform the reflection point calculation into a 2D problem that has to fulfil the Law of Reflection (see section 2.4.1). To calculate the reflection point S_{calc} a quartic polynomial has to be solved.

According to [Jales, 2012, chapter 4.4.1] the maximum deviation between the real and the calculated reflection point is $SS_{calc} < 25$ km and the maximum signal path difference is $SP_{diff} < 4$ km. Obviously, this model does not achieve the required accuracy of $SP_{diff} < 10$ m. Therefore a more accurate model than the spherical earth model will be needed.

4.2.2. Quasi-Spherical Earth

In Jales (2012, chapter 4.4.2) a more accurate model named the quasi-spherical earth approach is described. For the quasi-spherical earth approach the WGS 84 model of the Earth (see 2.3.2) is used. Figure 4.5 shows how the quasi-spherical earth approach works. In the left picture the coordinates of the transmitter (T) and the receiver (R) are given in correct relation to the
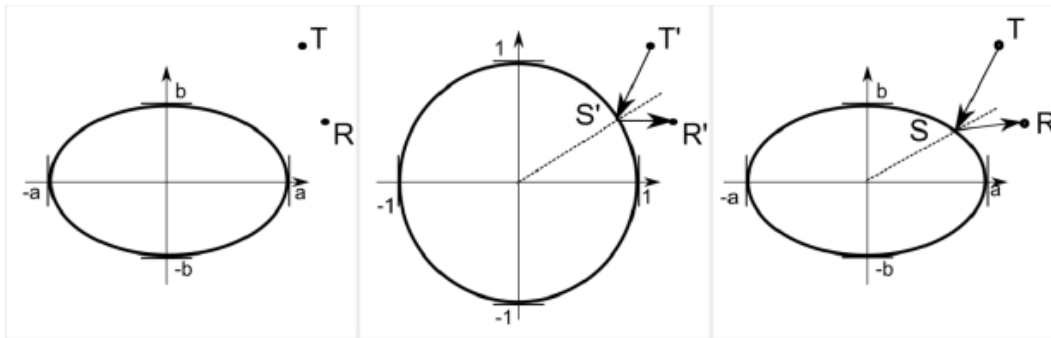
Figure 4.5.: Quasi-spherical earth approach, Jales, 2012

WGS 84 model of the Earth. In the first step a coordinate transformation to scale down the WGS 84 ellipsoid to a unit sphere is applied (see Figure 4.5 transformation from the left to the middle picture). The transformation is done independently for the polar and the equatorial axes. Due to the transformation the coordinates of the transmitter and the receiver are scaled into new (primed) coordinates equivalently to the model of the Earth. As second step the calculation of the reflection point is performed similar to the spherical earth approach described in Martin-Neira (1993, chapter 2) (4.5 middle picture). Finally the inverse of the previously performed coordinate transformation is applied (see Figure 4.5 transformation form the middle to the right picture). Thus the unit sphere and the positions of the satellites are scaled back to the WGS 84 model and the related coordinates of the satellites.

According to Jales (2012, chapter 4.4.2) the maximum deviation between the real and the calculated reflection point is $SS_{calc} < 4\,\text{km}$ and the maximum signal path difference is $SP_{diff} < 15\,\text{m}$. Therefore, the quasi-spherical earth approach does not achieve the required accuracy of $SP_{diff} < 10\,\text{m}$.

4.2.3. Ellipsoidal Earth

As stated in Jales (2012, chapter 4.4.3), for the ellipsoidal Earth the calculation of the reflection point is a minimization problem of SP_{rcalc} which is subjected to the surface of the WGS 84. Philip Jales describes the solution of this

problem as follows.

$$\text{minimise: } f(S_{calc}) = |S_{calc} - T| + |R - S_{calc}| = SP_{rcalc} \qquad (4.1)$$

$$\text{subjected to: } g(S_{calc}) = \frac{S_{xcalc}^2}{a^2} + \frac{S_{ycalc}^2}{a^2} + \frac{S_{zcalc}^2}{b^2} \qquad (4.2)$$

Where:
S_{xcalc} x coordinate of S_{calc}
S_{ycalc} y coordinate of S_{calc}
S_{zcalc} z coordinate of S_{calc}

According to Jales (2012, chapter 4.4.3), there is no analytical way to solve this non linear optimisation problem with non linear constraints, although convex optimization methods are able to solve this problem. Gleason and Gebre-Egziabher (2009, appendix 16A on the enclosed DVD, includes MAT-LAB code) show a method, based on the method of steepest descent, to solve the problem. Jales refers to this method, although he mentions serious short comings.

The method of Gleason and Gebre-Egziabher (2009, appendix 16A on the enclosed DVD) starts with an initial estimate of the reflection point S_n. Based on S_n, the true reflection point is iteratively calculated. Every improved reflection point S' for every iteration step is found along the direction of the 3D gradient of the path length function $f(S)$ and has to be constraint to the earth surface. The iteration procedure is as follows. For better understanding, see Figure 4.6.

1. Partial derivation of $f(S)$:

$$\nabla f(S_n) = \frac{(S_n - T)}{|S_n - T|} - \frac{(R - S_n)}{|R - S_n|} \qquad (4.3)$$

2. Calculation of new unconstrained estimate S' in direction of the deviation:

$$S' = S_n - K * \nabla f(S_n) \qquad (4.4)$$

3. Constrain S' to the earth surface by use of the radius $R(S')$:

$$S_{n+1} = \frac{S'}{|S'|} * R(S') \qquad (4.5)$$

Where:
K is the update gain
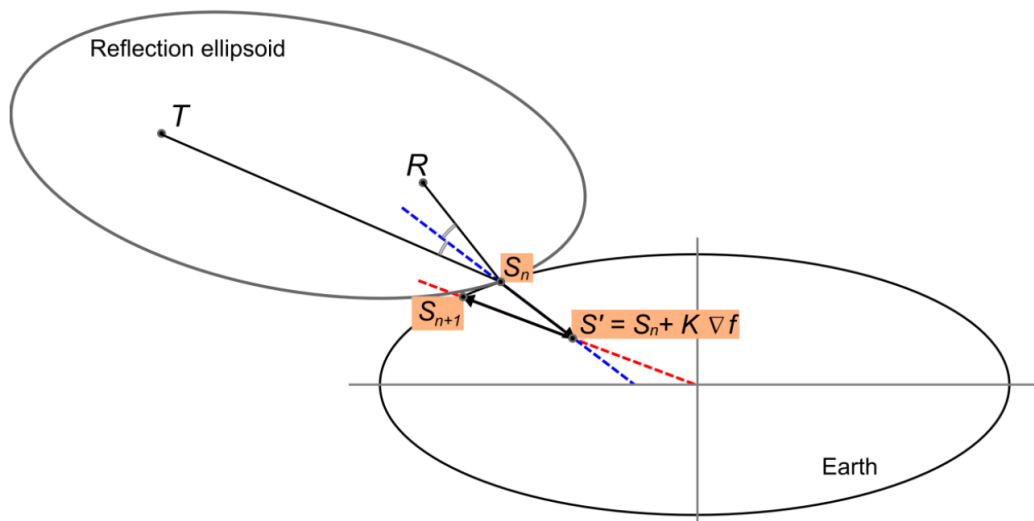
Figure 4.6.: Ellipsoidal earth approach with exaggerated earth flattening, Jales, 2012

The calculation is continued until the difference between S and $S(n+1)$ is within a defined accuracy. The last S_{n+1} is the calculated reflection point S_{calc}

Jales (2012, chapter 4.4.3) describes two major problems with this method. The first concerns the gain K and is already mentioned in Gleason and Gebre-Egziabher (2009, appendix 16A on the enclosed DVD). The optimum of K varies with the position of the satellites and the distance between the true and the estimated reflection point. Therefore the gain should be adjusted for every iteration step to achieve short calculation times. The second problem arises because of the difference between the direction of the earth radius and the surface normal for an spheroid. The problems are not further examined here. For more information refer to Jales (2012, chapter 4.4.3).

The accuracy of the method is given with $SP_{diff} < 10\,\text{m}$.

4.2.4. Optimisation in Polar Coordinates

According to Jales (see 2012, chapter 4.4.4) the method *Ellipsoidal Earth* can be improved by the use of polar coordinates instead of ECEF coordinates. He describes the advantage of the use of polar coordinates as a complexity
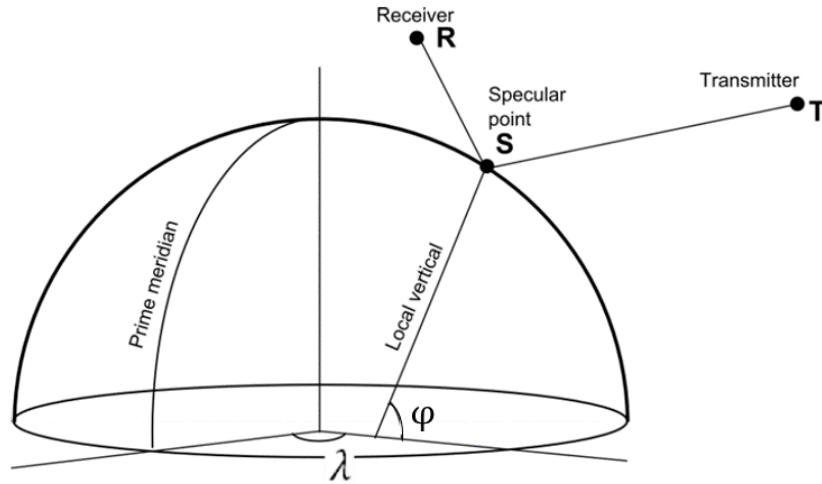
Figure 4.7.: Ellipsoidal earth approach with polar coordinates, Jales, 2012

reduction. By the use of polar coordinates (see Figure 4.7) the problem becomes an unconstrained minimisation problem. For the calculation of the path length the coordinates of S are converted back to the Cartesian system similar to section 2.3.3.

$$S(\varphi, \lambda) = \frac{1}{\sqrt{a^2 * \cos^2(\varphi) + b^2 * \sin^2(\varphi)}} * \begin{pmatrix} a^2 * \cos(\varphi) * \cos(\lambda) \\ a^2 * \cos(\varphi) * \sin(\lambda) \\ b^2 * \sin(\lambda) \end{pmatrix} \quad (4.6)$$

Thereby the problem has been changed into an unconstrained minimisation problem.

$$\text{minimise } f(S(\varphi, \lambda)) = |S(\varphi, \lambda) - T| + |R - S(\varphi, \lambda)| \quad (4.7)$$

What is an easier problem to solve.

4.2.5. Feasibility

The method *Spherical Earth* described in section 4.2.1 is an rather easy to implement method but does not fulfil the accuracy required. The same applies for the method *Quasi-Spherical Earth* described in section 4.2.2.

The *Ellipsoidal Earth* method and its optimisation in polar coordinates described in section 4.2.3 and 4.2.4 seem to deliver satisfying results. Since Gleason and Gebre-Egziabher (2009, appendix 16A on the enclosed DVD) deliver a working MATLAB code for the *Ellipsoidal Earth* method (see section 4.2.3), this method is recommended for further investigation.

4.3. Binary Search for reflection point calculation

The method Binary Search for reflection point calculation (from now on called BS) is based on the basic Binary Search algorithm as described in section 2.4.2. In case of the reflection point calculation the sorted array of elements consists of all points along the distance $\overrightarrow{TR}$. According to the Law of Reflection (section 2.4.1), at the reflection point the angle of incidence θ_{in} has to be equal to the emergent angle θ_{ref} (e.g. see Figure 4.8). For this reason, BS searches along $\overrightarrow{TR}$ for the point P_{BS} whose satellite sub-point (S_{calc}) fulfils the Law of Reflection (see Figure 4.8). Note, although P_{BS} is no satellite, the point on the surface of the Earth which surface normal hits P_{BS} is called the satellite sub-point of P_{BS}. This means, the Law of Reflection is the stopping criteria for BS. Since there is no easy way to deduce a suitable resolution for $\overrightarrow{TR}$ out of the stopping criteria, the maximum number of iterations BS could require is calculated for an extreme case. Assumed, $h_T = 20,000\,\text{km}$ and $h_R = 600\,\text{km}$, $|\overrightarrow{TR}| = SP_d = 26,000\,\text{km}$. For an assumed resolution of 1 mm, according to equation 2.54 the maximum number of iterations BS requires to find the target element is

$$\log_2(26 \times 10^9) = 34.6 \rightarrow 35\,\text{iterations}.$$

The problem to solve is the calculation of the satellite sub-point (S_{calc}). Therefore the point of intersection of the vector $\overrightarrow{MP_{BS}}$ and the earth surface has to be calculated. The intersection point is calculated according to section 2.2.4. Figure 4.8 shows a scheme for the method BS for a spherical Earth and Figure 4.9 shows a scheme for the method BS for a spheroid. As can be seen in Figure 4.8, for the spherical Earth the vector $\overrightarrow{MP_{BS}}$ is equal to the surface normal N_{Scalc}. Hence, the Law of Reflection is completely fulfilled. For the spheroid on the other hand, the vector $\overrightarrow{MP_{BS}}$ is not equal to the surface normal N_{Scalc}. This means, the calculated reflection point

does not completely fulfil the Law of Reflection. Although, equation 2.53 is fulfilled, the incident beam, the reflected beam and the surface normal are no longer in the same plane and therefore S_{calc} is no true reflection point in the mathematical sense. To obtain a more precise calculation with BS for a spheroid, it will be extended with a more precise calculation of the satellite sub-point as described in section 4.8.

The idea to use Binary Search to calculate the reflection point is from Dipl. Ing. Andreas Dielacher (RUAG Space).

4.3.1. Feasibility

The method BS as described above is an easy to implement reflection point calculation method. According to the rough calculation, BS will require only a small number of iterations to perform the reflection point calculation. For the spherical earth model this method should be able to deliver the true reflection point, within a small tolerance necessary as stopping criteria for the numerical calculation. BS for a spheroid as described above, is not able to calculate the reflection point in the sense of its mathematical definition (see section 4.7). Therefore the calculated reflection point could be inaccurate. However, this inaccuracy will strongly depend on the model of the Earth selected for the calculation. Since the WGS 84 is used as earth model, the method BS is recommended for further investigation.

4.4. Ray tracing

To calculate the reflection point S_{calc} a signal ray leaving the transmitter satellite T under a defined signal emission angle θ_T is assumed. The point of intersection of the signal ray and the earth surface is assumed to be the reflection point S_{calc}. If the emitted signal ray does not intersect with the earth surface, a new signal ray has to be assumed. According to the Law of Reflection (section 2.4.1) the angle θ_{in} of the incoming ray $\overrightarrow{TS_{calc}}$ and the angle θ_{ref} of the reflected ray $\overrightarrow{S_{calc}R}$ have to be equal. If $\overrightarrow{S_{calc}R}$ with $\theta_{ref} = \theta_{in}$ hits the receiver satellite, the reflection point has been found. If the reflected ray doesn't hit the receiver satellite, a new signal emission angle has to be selected and the calculation has to be repeated. The idea to use Ray tracing
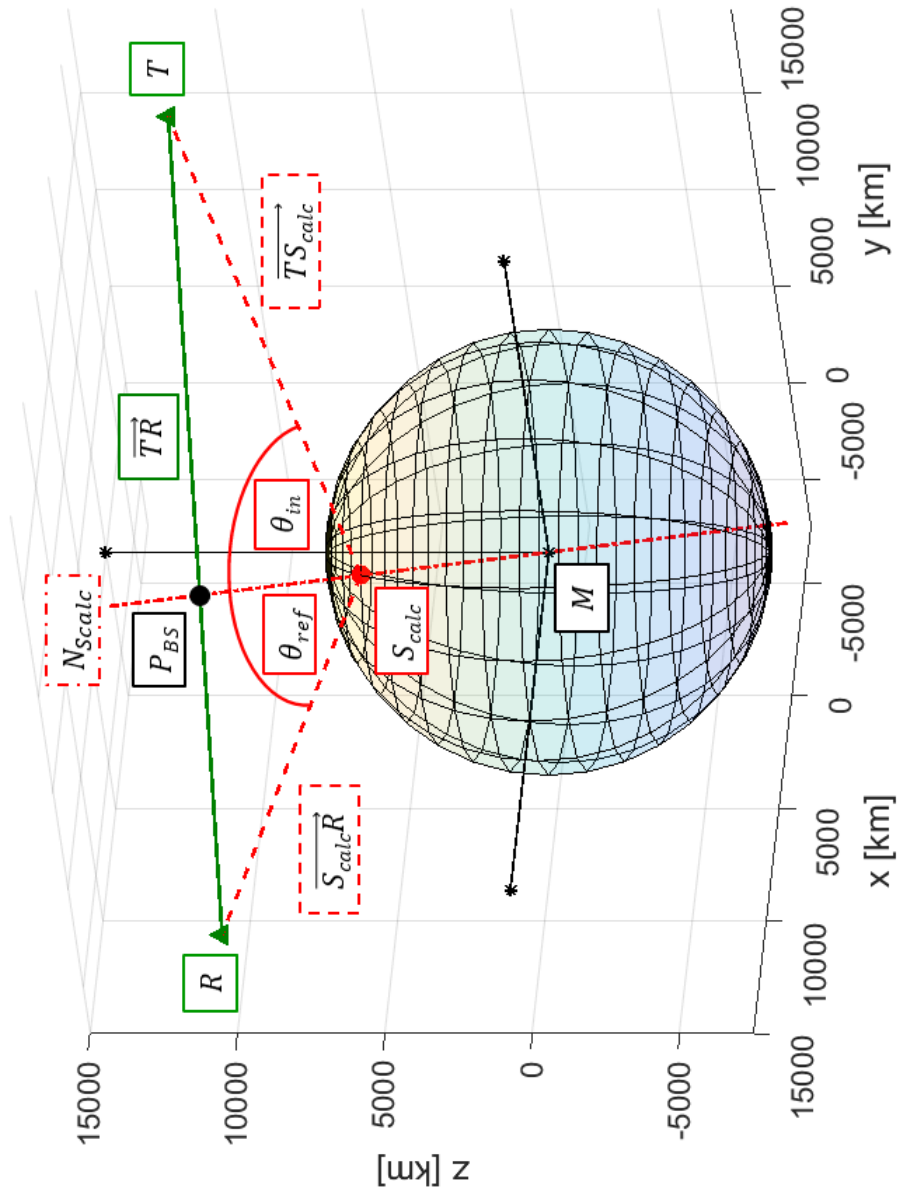
Figure 4.8.: Sketch of BS for a spherical Earth
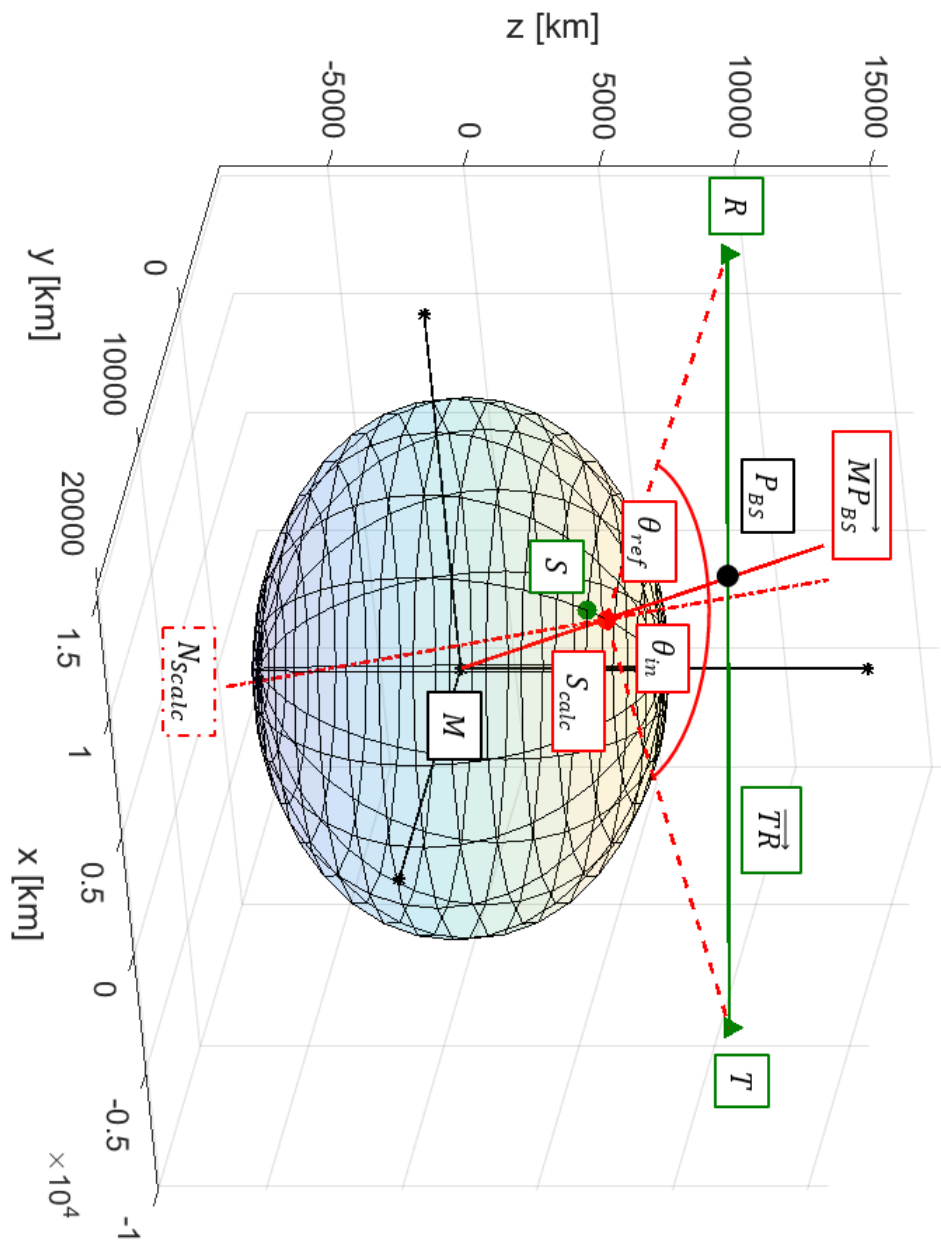
Figure 4.9.: Sketch of BS for a spheroid with the same parameters as figure 4.1

to calculate the reflection point is from Dipl. Ing. Andreas Dielacher (RUAG Space).

4.4.1. Feasibility

Although the ray tracing method sounds simple, the determination of the directioni of the signal ray is challenging. Theoretically the ray leaving the transmitter satellite can point in any direction around the satellite. The optimal direction of the emitted signal ray is in the plane defined by the Law of Reflection. Therefore, the true reflection point (S) has to be known. Since the reflection point is the thing to be looked for this is not possible and other methods have to be used. One method would be to point the ray at the centre of the Earth. This method leads to a similar calculation method as BS (described in section 4.3) with the difference that the signal emission angle is changed and not P_{BS}. Therefore, this method is not further investigated.

Another and probably more precise method to obtain the direction is to pre calculate the satellite sub-point as described in section 4.8 and vary the signal emission angle within the plane defined by T, R and one of the two satellite sub-points.

4.5. Reflection ellipse method

This method uses the property of an ellipse that each beam which leaves at one focus T of the ellipse is reflected from the circumference of the ellipse to the other focus R. As can be seen in Figure 4.10 the angle of incidence θ_{in} at the point of reflection S is equal to the emergent angle θ_{ref} at the point of reflection. Therefore, S is a reflection point. The idea is based on Olivik et al. (2005).

This property of an ellipse can be used to calculate the reflection point. Assumed that one focus of the ellipse is the transmitter and the other is the receiver, a spheroid can be generated. In Figure 4.11 it is clear to see that the reflection point is the point where the generated spheroid touches the earth model spheroid. To calculate the parameters necessary to construct the spheroid out of the satellite positions equations 2.15 to 2.19 are used. The equations shows that either the path length of the reflected signal SP_r

or the semimajor or the semiminor axis has to be known to calculate the satellite spheroid. Since these parameters are not given, the problem has to be solved numerically. The set of equations to be solved is received out of equation 2.29 to 2.32 and is given below.

$$a_S \cdot \cos(\phi_S) \cdot \cos(\lambda_S) = a_E \cdot \cos(\phi_E) \cdot \cos(\lambda_E) \tag{4.8}$$
$$a_S \cdot \cos(\phi_S) \cdot \sin(\lambda_S) = a_E \cdot \cos(\phi_E) \cdot \sin(\lambda_E) \tag{4.9}$$
$$b_S \cdot \sin(\phi_S) = b_E \cdot \sin(\phi_E) \tag{4.10}$$

With:

$$b_S = \sqrt{a_S^2 - e_S^2}$$
$$e_S = \frac{T - R}{2}$$
$$a_S = \frac{SP_r}{2}$$

Where the indices of the variable indicate:
  S indicates parameters of the satellite spheroid
  E indicates parameters of the earth spheroid

Equations 4.8 to 4.10 describe a problem consisting of a set of three equations with five unknowns. Such a problem cannot be solved analytically, but only numerically by variation of unknowns. Since the angles of the satellite spheroid and the angles of the earth spheroid are not coherent, a numerical solution has to vary three of the five unknowns (e.g. ϕ_S, ϕ_E and a_S).

4.5.1. Feasibility

The reflection ellipse method would be able to calculate the true reflection point, with only the calculation accuracy as a deviation. This is possible, because there is only one point where the earth spheroid and the satellite spheroid can touch. Solving the set of equations for the reflection ellipse method numerically is possible. However, since all five unknowns have to be varied, it can be predicted that this method will take a lot of calculation time and computing power. Therefore, this method is likely to be unusable on-board a satellite and will therefore not be further investigated. To speed up the method the conversion into a 2D problem would be an interesting approach. However, to transform it into 2D, the plane including the satellite positions and the reflection point has to be known. Of course, this plane can
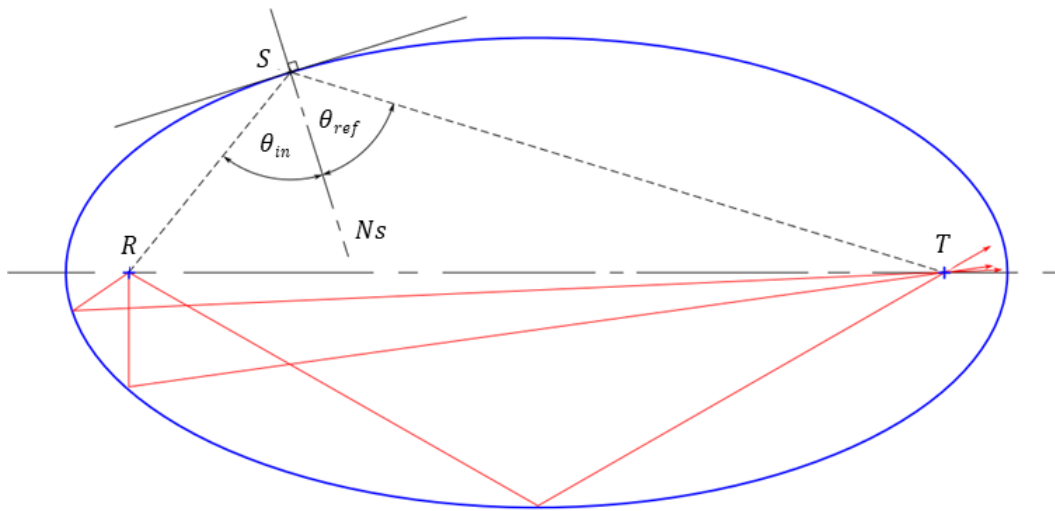
Figure 4.10.: Reflection Ellipse, (Wikimedia Commons, 2004, File: Propriete reflexion ellipse tangente bissectrice.svg)
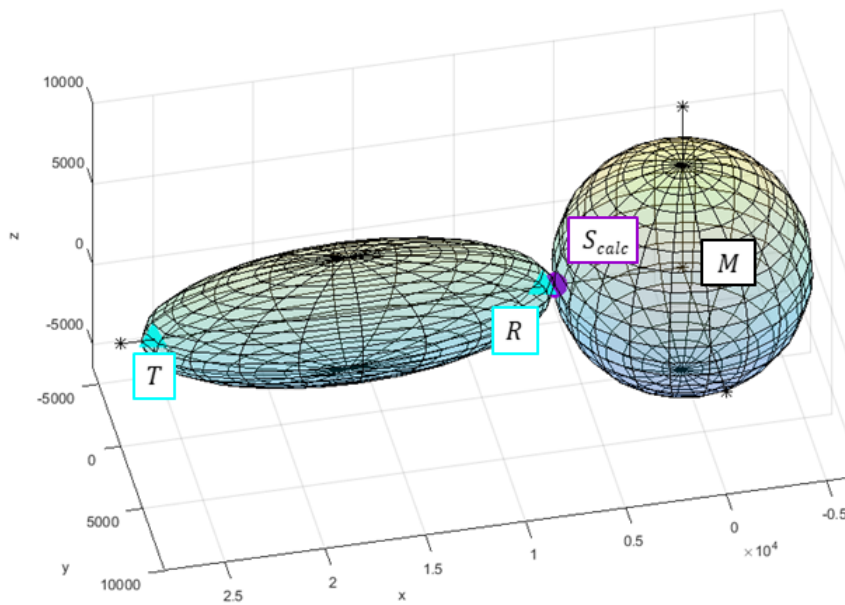
Figure 4.11.: Intersection of spheroid generated by satellite positions and WGS 84 spheroid

not be known. Therefore an approach like a plane including the satellite positions and the centre of the Earth is necessary. In this case again it becomes a similar problem as BS for a spheroid.

Olivik et al. (2005) describe three approaches to solve the reflection ellipse problem without a variation of five variables. Since their approaches requires SP_r as known parameter and SP_r can only be known when S_{true} is known, their approaches seem not useful for a satellite mission.

4.6. Finite elements method

The idea of the finite elements (FE) method is to model the WGS 84 model of the Earth out of finite number of single square surface elements of a defined size (see Figure 4.12) and calculate the surface normal (see section 2.2.3) for each of these elements. Only the elements at the equator have the defined size and the elements become smaller towards the poles. The goal is to find the element which reflects the ray from the transmitter satellite to the receiver satellite within a certain deviation. This element is called the reflecting element. There are several different methods to determine the reflecting element by the use of this model. One method called "FE Ray tracing" is described below.

4.6.1. FE Ray tracing

First a straight line between the transmitter and the receiver satellite is drawn. Any element whose surface normal intersects the link line within a defined deviation can be the reflecting element. Figure 4.13 shows a scheme of the square elements, their surface normals, the two satellites and the link line. The surface elements which could be the reflecting element are marked with a red surface normal. To determine the reflecting element check for which element θ_{in} is equal to θ_{ref} within a certain deviation.

4.6.2. Feasibility

Although the FE method described in this section looks promising and easy to calculate it has a big disadvantage. To guarantee a sufficient accuracy for

Figure 4.12.: FE model of the Earth
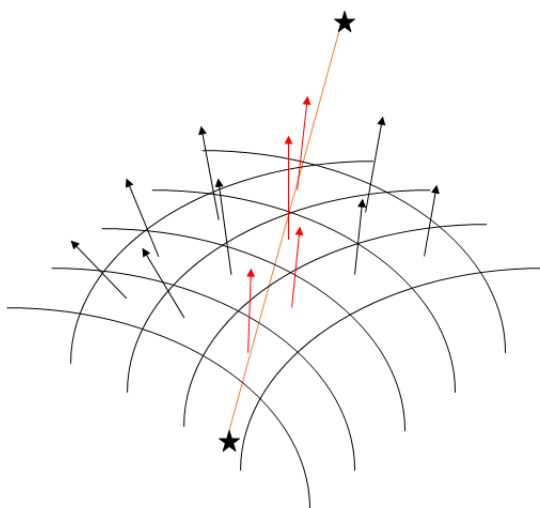
Figure 4.13.: Scheme of ray tracing for FE modelled Earth

the reflection point calculation the square elements have to be rather small. For example, if the elements are $100\,\text{m} \times 100\,\text{m}$, the model would consist of $1{,}6 * 10^{11}$ elements. To save all the node coordinates of a model with this element size would require more than $1100\,\text{GB}$ of storage space. Therefore a quite well equipped computer is required to calculate the model of the Earth. That is why it is better to begin with only a view big elements and check which one of them includes the reflection point. Than model the big element including the reflection point out of smaller elements and check again which one of these elements does include the reflection point. This is done until the model size gets small enough to include the reflection point within a sufficient deviation.

4.7. The uncertainty of performing the reflection point calculation in the plane defined by T, R and M

Although it has been mentioned in several sections above (e.g. section 4.3), once more the uncertainty of performing the reflection point calculation in the plane including the satellite positions and the centre of the Earth is pointed out in this section.

According to the Law of Reflection (see section 2.4.1), the incident ray $\overrightarrow{TS}$, the reflected ray $\overrightarrow{SR}$ and the surface normal at the point of reflection N_S have to lie in the same plane. Therefore, the position of the receiver satellite and the position of the transmitter satellite have to lie in the same plane as the surface normal of the reflection point does. For all methods, where the surface normal of the reflection point is not included in the calculation plane (spanned by T, R and S), the calculated reflection point (S_{calc}) is not a reflection point in the mathematical sense. Figure 4.14 and 4.15 show a scheme including the satellite positions, the calculated and the true reflection point and the calculation plane. Especially Figure 4.15 shows that the calculation plane does not include the surface normal N_{Scalc}. The reflection point calculation in these figures was done with the BS method.

Figure 4.14.: Scheme 1 of the calculation plane

Figure 4.15.: Scheme 2 of the calculation plane

4.7.1. Influence on calculation

Although, the calculated reflection point is no reflection point in the technical sense, it has to be said, that the inaccuracy between S and S_{calc} strongly depends on the deviation of the spheroid from the sphere. More precisely on the flattening (see equation 2.17) of the spheroid. The bigger the value of the flattening is, the bigger is the inaccuracy of the calculated reflection point. Therefore, it is necessary to examine for each problem whether and to what extent the calculation is influenced by the selected calculation plane.

4.8. Method enhancement with the calculation of the satellite sub-point

As mentioned in section 4.7, some of the methods described in this chapter have an inaccuracy due to the selected calculation plane. This inaccuracy can be minimised or even eliminated by using the satellite sub-point to define the calculation plane. The satellite sub-point, is the point on the surface of the Earth (or the earth model) whose surface normal hits the satellite orbiting the Earth (or an imaginary point above the earth surface).

According to Kelso (2014) the calculation of a satellite sub-point is given below as example for R_{SP}. First the longitude λ of the satellite is calculated with equation 4.11.

$$\lambda = \arctan\left(\frac{y_R}{x_R}\right) \tag{4.11}$$

Secondly the geocentric latitude ϕ of the satellite is calculated with equation 4.12.

$$\phi = \arctan\left(\frac{z_R}{\sqrt{x_R^2 + y_R^2}}\right) \tag{4.12}$$

Starting with $\varphi_i = \phi$ the geodetic latitude φ of the satellite sub-point is calculated iteratively by the use of the following equations.

$$C = \frac{1}{\sqrt{1 - \epsilon^2 \cdot \sin^2 \varphi_i}} \tag{4.13}$$

$$\varphi = \arctan\left(\frac{z_R + a \cdot C \cdot \epsilon^2 \cdot \sin \varphi_i}{R}\right) \tag{4.14}$$

With:

$$R = \sqrt{x_R^2 + y_R^2}$$

Equation 4.13 and 4.14 are repeated until $|\varphi - \varphi_i|$ is within a predefined accuracy. Before each repetition φ_i is set to the previously calculated φ. If $|\varphi - \varphi_i|$ is within the predefined accuracy, λ and φ are the geodetic longitude and the latitude of the satellite sub-point and can be transformed into Cartesian coordinates a stated in section 2.3.3.

The method from Kelso (2014) as described above calculates the true satellite sub-point within the calculation accuracy. The question is, how much the satellite sub-point calculation can improve the methods described above. Figure 4.16 shows an example, where the satellite sub-points for T and R are calculated. As can be seen, a calculation plane defined by the two satellite positions R and T and the satellite sub-point R_{SP} is closer to the true reflection point than the calculated reflection point S_{calc}. For reference, S_{calc} was calculated with BS within the less precise calculation plane shown in the Figure 4.15. As a result, the method BS, for example, can be improved simply by defining a more precise calculation plane by using the satellite sub-point calculation. Therefore, the enhancement of BS with the satellite sub-point calculation is recommended for further investigation.
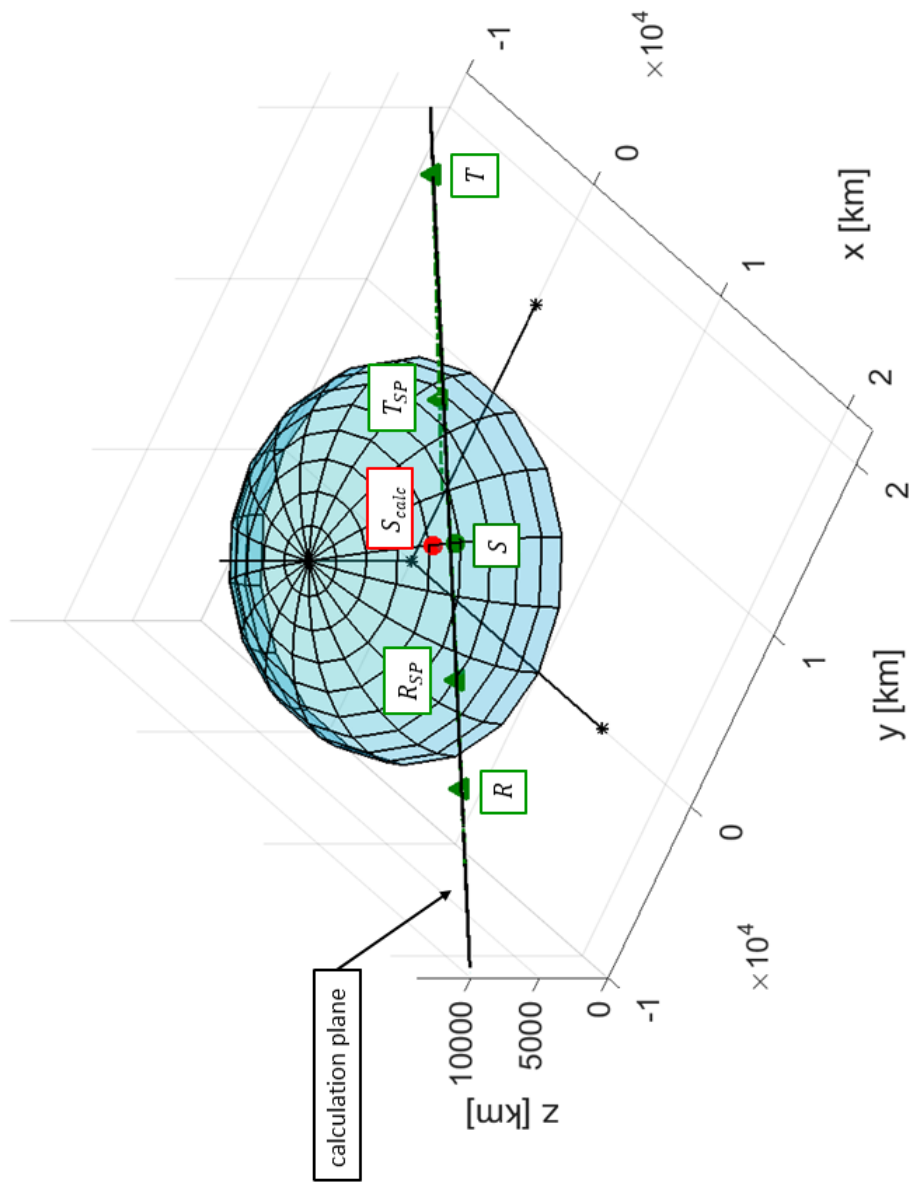
Figure 4.16.: satellite sub-point and calculation plane

5. Evaluation, results and discussion for three reflection point calculation methods

Chapter 4 introduced several, partly very different methods to calculate the reflection point. The following methods are evaluated in this chapter.

- *Ellipsoidal Earth* (henceforward: SG), described in section 4.2.3, MAT-LAB code from Gleason and Gebre-Egziabher (2009)
- *Binary Search for an ellipsoid* (henceforward: BS), described in section 4.3
- *Binary Search for a spheroid enhanced with satellite sub-point calculation* (henceforward: BSSSP), described in section 4.3 and 4.8

The method SG was selected because Gleason and Gebre-Egziabher (2009) already deliver a verified MATLAB code. Therefore, the evaluation consists of at least one correctly working implementation. Which is a good reference for the other implemented methods. The implementation of the method BS was recommended by Dipl. Ing. Andreas Dielacher. It is his idea and has already been fundamentally tested by him. Hence, it should deliver satisfactory results and was selected as second method. The method BSSSP is an enhancement of the method BS and was implemented to evaluate the benefit of an accuracy enhancement compared to an possible increase of calculation time due to an additional iterative calculation.

The method BS and BSSSP calculate the reflection point according to the method *Binary Search* (see section 4.3). SG calculates the reflection point according to the method *Ellipsoidal Earth* (see section 4.2.3). Because of the two different methods, there is a serious difference in the accuracy/stopping criteria. SG is a minimization problem that stops when the difference between two reflection points calculated in successive iterations is less than the given accuracy. BS and BSSSP search for the point for which the Law of Reflection is fulfilled with the given accuracy. Therefore, the accuracy criteria of SG

and BS/BSSSP cannot be compared. For this reason, section 5.2.1 and 5.2.2 attempt to bring SG, BS and BSSSP to a comparable accuracy.

In the list above, BS is described as method working for an ellipsoid. Its enhancement BSSSP is described as method working for a spheroid. An ellipsoid has three semi axes. If all three semi axes are different, it is called ellipsoid. If two of the three semi axes are equal it is called ellipsoid of revolution or spheroid. And, if all three semi axes are equal it is a sphere. Therefore, the WGS 84 is a spheroid (see section 2.2.1 and 2.3.2). The method BS works for both an ellipsoid and a spheroid, whereas the method BSSSP only works for a spheroid. This is because, for an ellipsoid the satellite sub-point calculation can not be performed.

Chapter 5 is divided into three main sections. Section 5.1 describes how the evaluation is carried out. Section 5.2 states and describes the results of the evaluation and section 5.3 discusses the stated results.

5.1. Evaluation

This section describes how the evaluation of the three methods listed above happens. The evaluation is done with regard to the following parameters

- SS_{calc}, distance between the true and the calculated reflection point
- SP_{diff}, difference between the signal path of the signal reflected at the true reflection point and the signal path of the signal reflected at the calculated reflection point ($SP_r - SP_{rcalc}$)
- Number of iterations necessary to find the reflection point
- Calculation time

and bound to the requirements stated in section 1.4. For a better overview, the requirements are listed once more below.

Requirements:

- snapshot of the measurement constellation with the WGS 84 as earth model
- altitude of the transmitter satellite, $h_T = 20,000\,\text{km}$
- altitude of the receiver satellite, $h_R = 600\,\text{km}$.
- satellite elevation angle, $0° < ele < 15°$.
- maximum signal path difference, $SP_{diff} < 10\,\text{m}$.

- as little calculation time as possible

To receive all the parameters listed above the knowledge of the true reflection point (S) is necessary. Therefore, Monte Carlo simulations (see section 2.4.3) with true reflection points randomly distributed over the northern hemisphere have been performed. The MATLAB code for the Monte Carlo simulation is given in appendix A.3. Since the WGS 84 is symmetrical at the equator plane, it is enough to perform the evaluation only on one hemisphere. As symmetrical satellite constellations would appear on the northern and the southern hemisphere. This allows the simulation of a larger number of reflection points with the same validity as for the whole Earth, but with less computing time. Figure 5.1 shows the distribution of 1,000 true reflection points over the northern hemisphere. The well distributed coverage of the northern hemisphere is good to see. Out of the position of the true reflection point a measurement constellation for the transmitter satellite (T) and the receiver satellite (R) is calculated. The satellite positions for the measurement constellation are random for each reflection point. Although the constellation is random, it has to fulfil the requirements mentioned above and the Law of Reflection (see section 2.4.1). The MATLAB code to calculate the measurement constellation is given in appendix A.3.4. To calculate the measurement constellation the following mathematical basics are required.

- a coordinate transformation form geodetic to ECEF coordinates. described in section 2.3.3, MATLAB code in appendix A.3.8

- the calculation of the surface normal on a point on the WGS 84, described in section 2.2.3, MATLAB code in appendix A.3.7

- the calculation of the intersection of a straight line and an ellipsoid, described in section 2.2.4, MATLAB code in A.3.6

For all measurement constellations the calculated reflection point (S_{calc}) is calculated with SG, BS and BSSSP. For how the methods work, refer to chapter 4. The MATLAB code for SG is from Gleason and Gebre-Egziabher (2009, appendix 16A on the enclosed DVD). The reference also includes a more detailed description. Since the code has been modified slightly, it is also given in appendix A.3.1. The changes affect mainly the transfer parameters of the function. So, that all required parameters are passed to the main function. The MATLAB code for BS is given in appendix A.3.2 and the MATLAB code for BSSSP is given in appendix A.3.3. BS require the
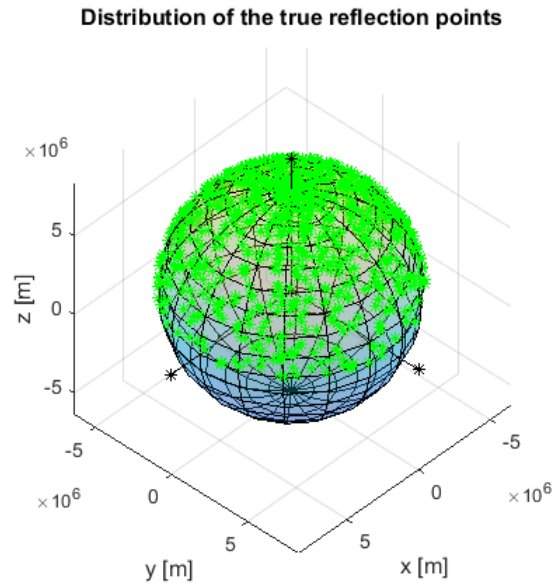
Figure 5.1.: Distribution of the true reflection points S over the northern hemisphere

mathematics to calculate the intersection of a straight line and an ellipsoid and BSSSP require the mathematics to calculate the precise satellite sub-point (see section 4.7.1). Unlike the example given in section 4.7.1, the satellite sub-point is not calculated for one of the two satellites (T or R). Instead, the satellite sub-point of P_{BS} is calculated. Since, despite the calculation accuracy, the satellite sub-point calculation will calculate the true satellite sub-point for P_{BS}, the Law of Reflection (see section 2.4.1) will be completely fulfilled for the reflection point calculated with BSSSP. This means, $\theta_{in} = \theta_{ref}$ and the incident beam, the reflected beam and the surface normal of the calculated reflection point will be in the same plane. Therefore, BSSSP can be expected to approach the true reflection point down to the calculation accuracy.

5.2. Results

In this section the results of the Monte Carlo simulations for different numbers of simulated reflection points and different accuracies are presented and described.

The parameters that can be varied for the different simulations are:

n_{points}	the number of calculated reflection points
$maxit$	the maximal number of iterations a method is allowed to need for the reflection point calculation
$accuracy_{SG}$	the accuracy / stopping criteria for the method SG
$accuracy_{BS}$	the accuracy / stopping criteria for the method BS
$accuracy_{BSSSP}$	the accuracy / stopping criteria for the method BSSSP

Note that with latitude and longitude always the geodetic latitude and longitude is meant.

5.2.1. Overview of performance

The first simulation is intended to provide an overview of the performance of the three methods. This is done to compare the influence of $accuracy_{SG}$ to $accuracy_{BS}$ and $accuracy_{BSSSP}$ on the particular calculation method. Since, as stated at the beginning of this chapter, it is not possible to compare them. Therefore only a small number of reflection points is calculated. This, however, with a large number of maximal iterations and an assumed high accuracy.

Parameters:

n_{points}	$= 100$
$maxit$	$= 1 \times 10^5$ iterations
$accuracy_{SG}$	$= 0.05\,\text{m}$
$accuracy_{BS}$	$= 1 \times 10^{-4}\,\text{rd}$
$accuracy_{BSSSP}$	$= 1 \times 10^{-4}\,\text{rd}$

Distance between the true and the calculated reflection point, SS_{calc}

The Figures 5.2, 5.3 and 5.4 show the distance between the true and the calculated reflection point related to either the longitude or the latitude of the true reflection point or the elevation of the satellites. It is easy to see, that SG has the weakest performance and that BSSSP is better than BS. Figure 5.4 shows that for elevations above $\approx 4°$ SG is able to deliver the same accurateness as BS. As can be seen in Figure 5.2, no method has any longitude dependency. Figure 5.3 shows that BS has a small latitude dependency. SS_{calc} is shortest at the poles and the equator. In Figure 5.4 the poor performance of SG for small elevations can be seen.
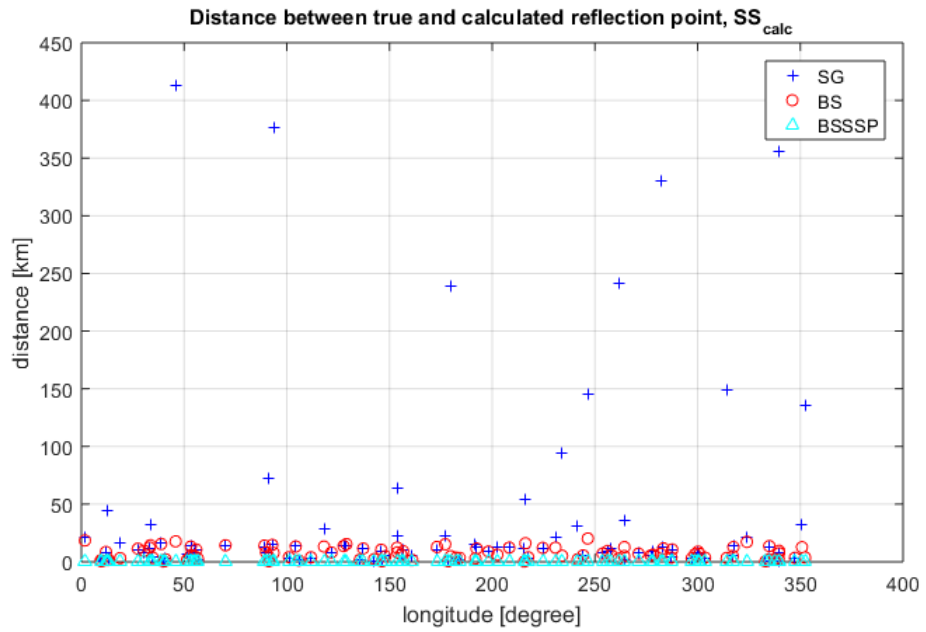
Figure 5.2.: SS_{calc} vs. longitude, $n_{points} = 100$, $maxit = 1 \times 10^5$ iterations, $accuracy_{SG} = 0.05\,\text{m}$, $accuracy_{BS} = accuracy_{BSSSP} = 1 \times 10^{-4}\,\text{rd}$
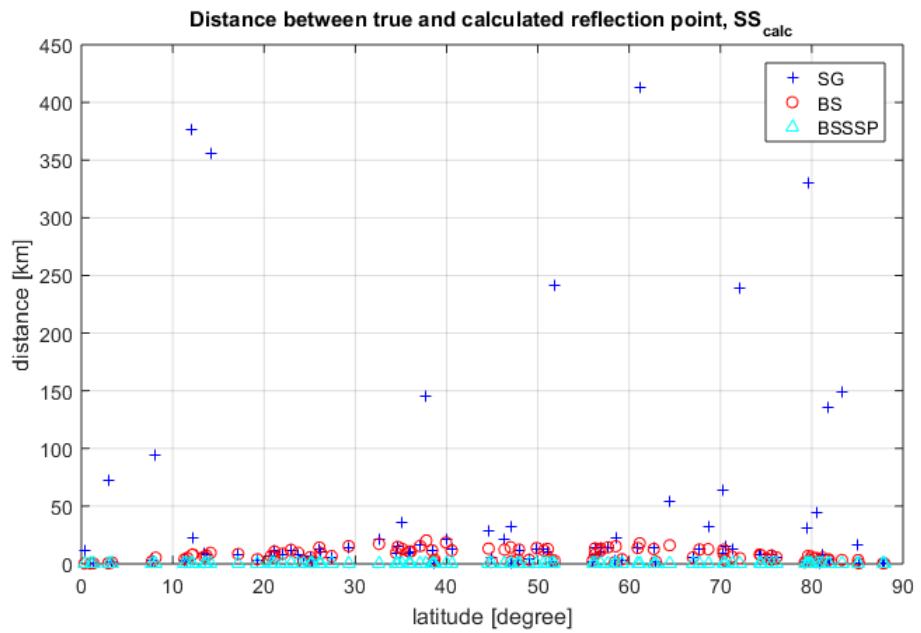
Figure 5.3.: SS_{calc} vs. latitude, $n_{points} = 100$, $maxit = 1 \times 10^5$ iterations, $accuracy_{SG} = 0.05\,\text{m}$, $accuracy_{BS} = 1 \times 10^{-4}\,\text{rd}$
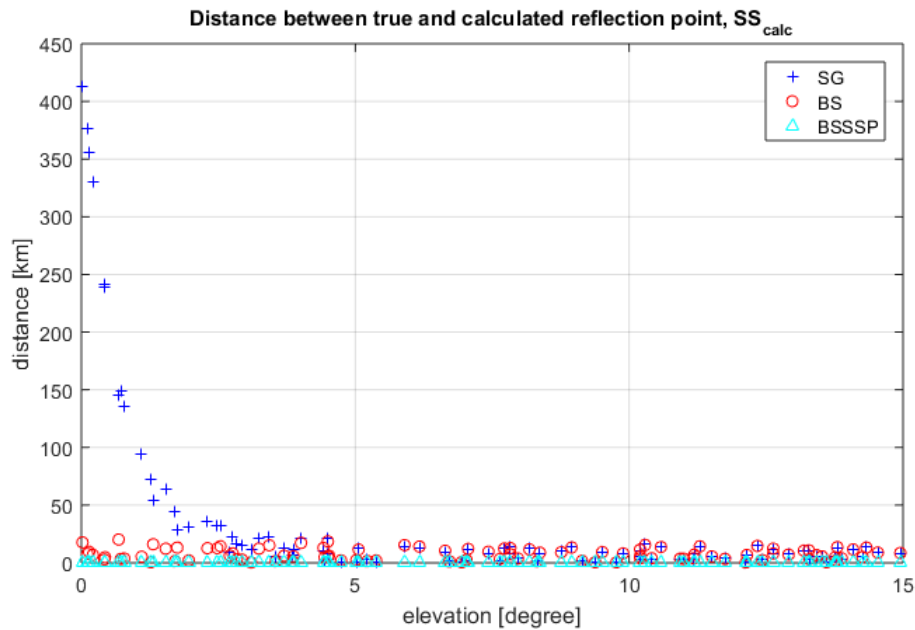
Figure 5.4.: SS_{calc} vs. elevation, $n_{points} = 100$, $maxit = 1 \times 10^5$ iterations, $accuracy_{SG} = 0.05\,\text{m}$, $accuracy_{BS} = 1 \times 10^{-4}\,\text{rd}$

Signal path difference, SP_{diff}

The Figures 5.5, 5.6 and 5.7 show the signal path difference between SP_{rcalc} and SP_r related to either the longitude or the latitude of the true reflection point or the elevation of the satellites. SP_{diff} shows the same dependencies with the same reason for longitude and latitude as SS_{calc} does. In Figure 5.7 it can be seen, that SG has a much higher signal path difference for low elevations similar to its SS_{calc} shown in Figure 5.4. Both, SG and BS show an increasing signal path difference for increasing elevations. BSSSP shows hardly any signal path difference at all.

Number of iterations

The Figures 5.8, 5.9 and 5.10 show the number of iterations each method required for the calculation of each reflection point related to either the longitude or the latitude of the true reflection point or the elevation of the satellites. It is good to see, that BSSSP has no dependency at all and that BS and BSSSP require much less iterations to calculate the reflection
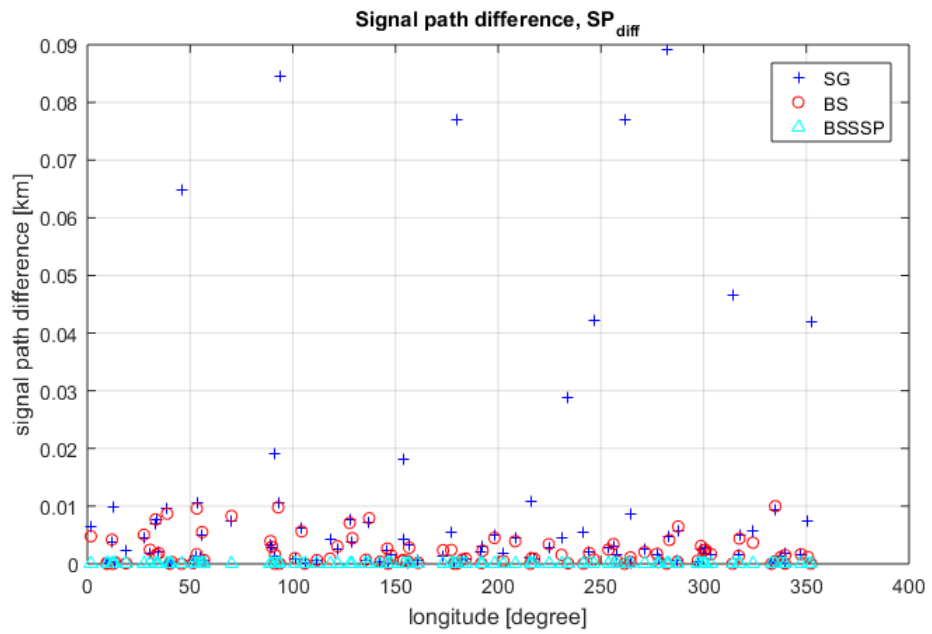
Figure 5.5.: SP_{diff} vs. longitude, $n_{points} = 100$, $maxit = 1 \times 10^5$ iterations, $accuracy_{SG} = 0.05$ m, $accuracy_{BS} = accuracy_{BSSSP} = 1 \times 10^{-4}$ rd
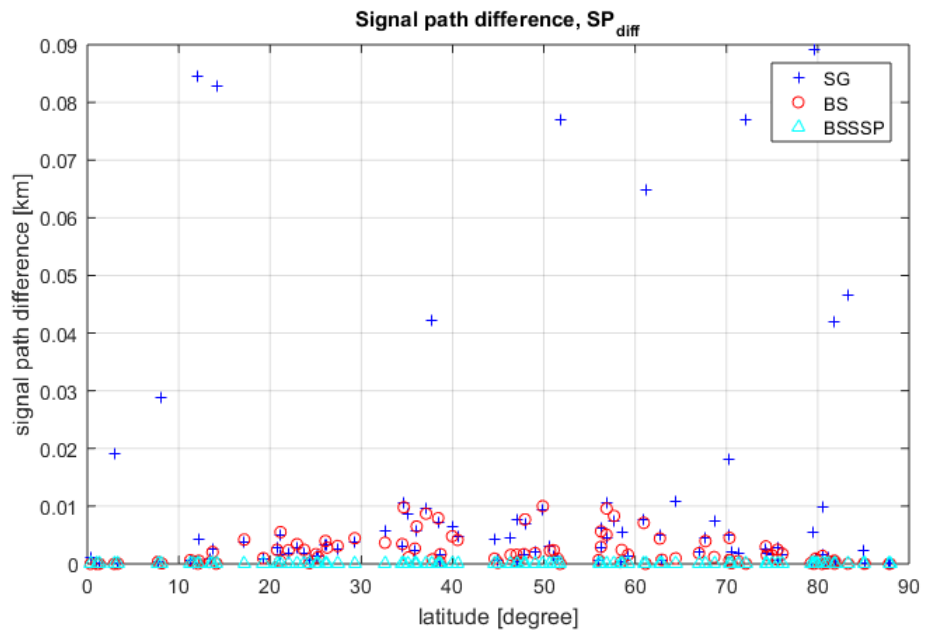
Figure 5.6.: SP_{diff} vs. latitude, $n_{points} = 100$, $maxit = 1 \times 10^5$ iterations, $accuracy_{SG} = 0.05$ m, $accuracy_{BS} = accuracy_{BSSSP} = 1 \times 10^{-4}$ rd
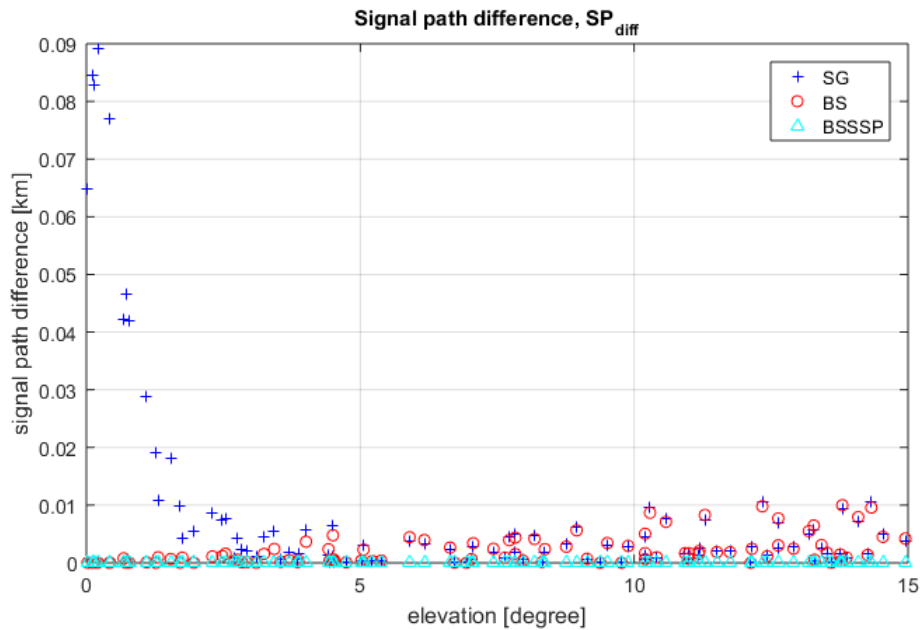
Figure 5.7.: SP_{diff} vs. elevation, $n_{points} = 100$, $maxit = 1 \times 10^5$ iterations, $accuracy_{SG} = 0.05$ m, $accuracy_{BS} = accuracy_{BSSSP} = 1 \times 10^{-4}$ rd

point than SG. Figure 5.10 shows the reason for bad performance of SG for small elevations. For elevations lower than $\approx 5\degree$ SG needs the maximum number of iterations. Therefore the results of the performance overview are no longer evaluated because SG can not be compared reasonably.

5.2.2. Identification of working parameters for SG

Since SG was the only method which did not perform well in the performance overview, this section is used to identify a working combination of *maxit* and $accuracy_{SG}$ for SG. Working means, all reflection points can be calculated without reaching the maximum number of iterations and therefore SG can reach the determined accuracy. To identify the working parameters several simulations with different *maxit* and $accuracy_{SG}$ are performed and evaluated with respect to the number of iterations required. Since BS and BSSSP performed well for the selected parameters and Figure 5.10 shows that for $n_{points} = 100$ the reflection points are well distributed over the elevation angles and SG shows bad performance for low elevations,
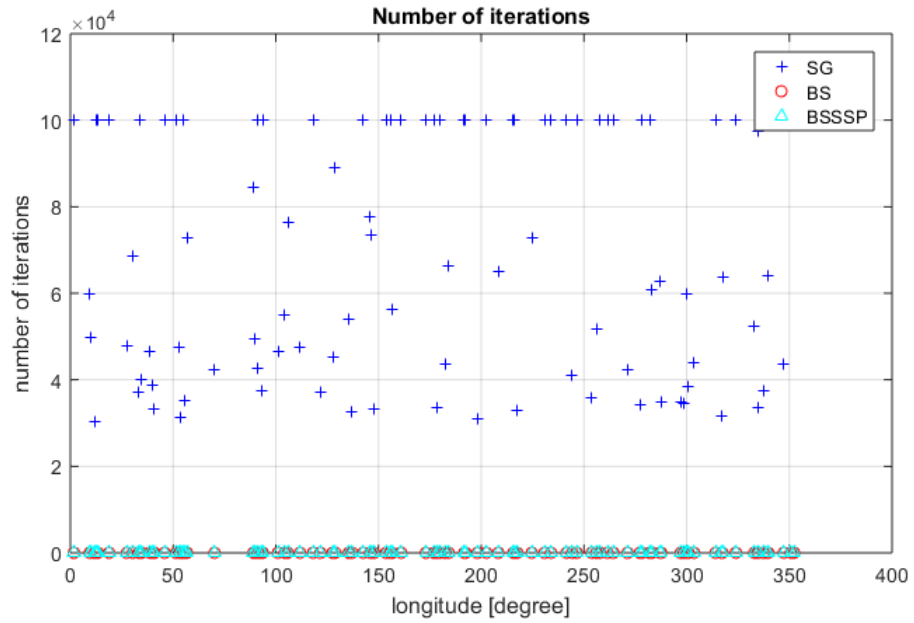
Figure 5.8.: Number of iterations vs. longitude, $n_{points} = 100$, $maxit = 1 \times 10^5$ iterations, $accuracy_{SG} = 0.05\,\text{m}$, $accuracy_{BS} = accuracy_{BSSSP} = 1 \times 10^{-4}\,\text{rd}$
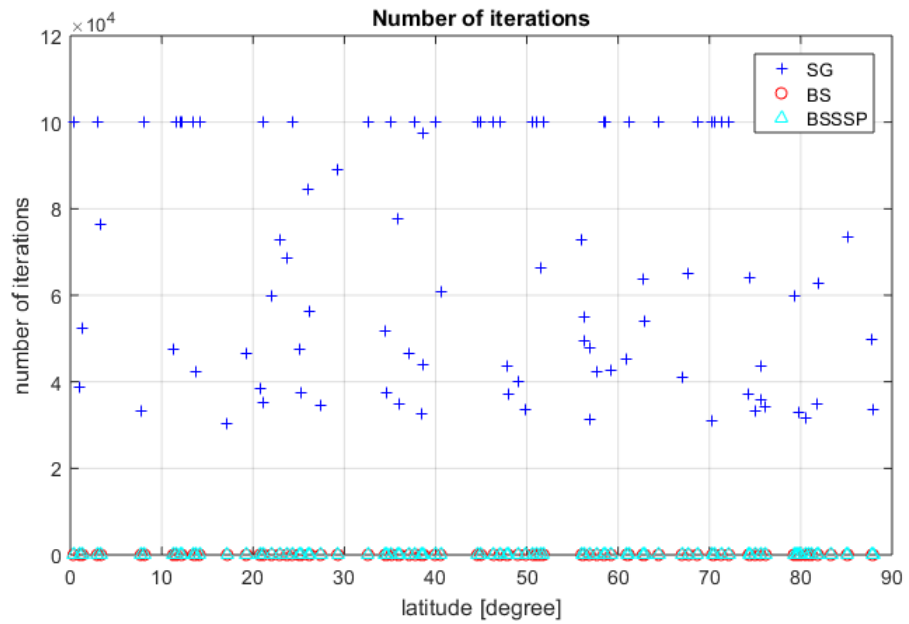
Figure 5.9.: Number of iterations vs. latitude, $n_{points} = 100$, $maxit = 1 \times 10^5$ iterations, $accuracy_{SG} = 0.05\,\text{m}$, $accuracy_{BS} = accuracy_{BSSSP} = 1 \times 10^{-4}\,\text{rd}$
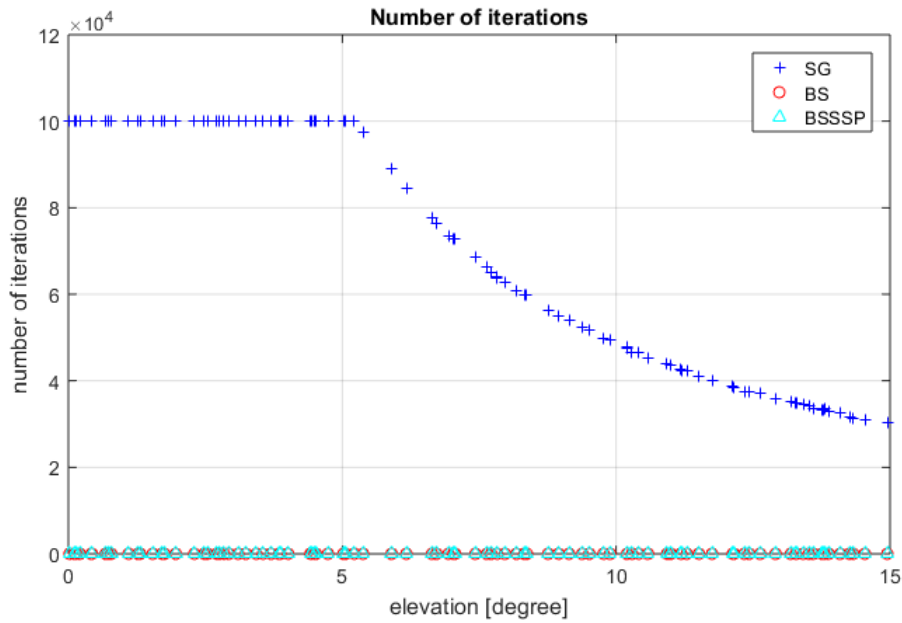
Figure 5.10.: Number of iterations vs. elevation, $n_{points} = 100$, $maxit = 1 \times 10^5$ iterations, $accuracy_{SG} = 0.05\,\text{m}$, $accuracy_{BS} = accuracy_{BSSSP} = 1 \times 10^{-4}\,\text{rd}$

the number of reflection points and the accuracy of BS and BSSSP are kept from section 5.2.1.

Fixed parameters for section 5.2.2:

n_{points}	$= 100$
$accuracy_{BS}$	$= 1 \times 10^{-4}\,\text{rd}$
$accuracy_{BSSSP}$	$= 1 \times 10^{-4}\,\text{rd}$

1st try

For the 1st try the number of iterations has been increased. Since the reflection point calculations of SG which did not require the maximal number of iterations from section 5.2.1 showed an accurateness comparable to that of BS, $accuracy_{SG}$ from section 5.2.1 is used.

Variable parameters for 1st try:

$maxit$	$= 1.5 \times 10^5$ iterations
$accuracy_{SG}$	$= 0.05\,\text{m}$
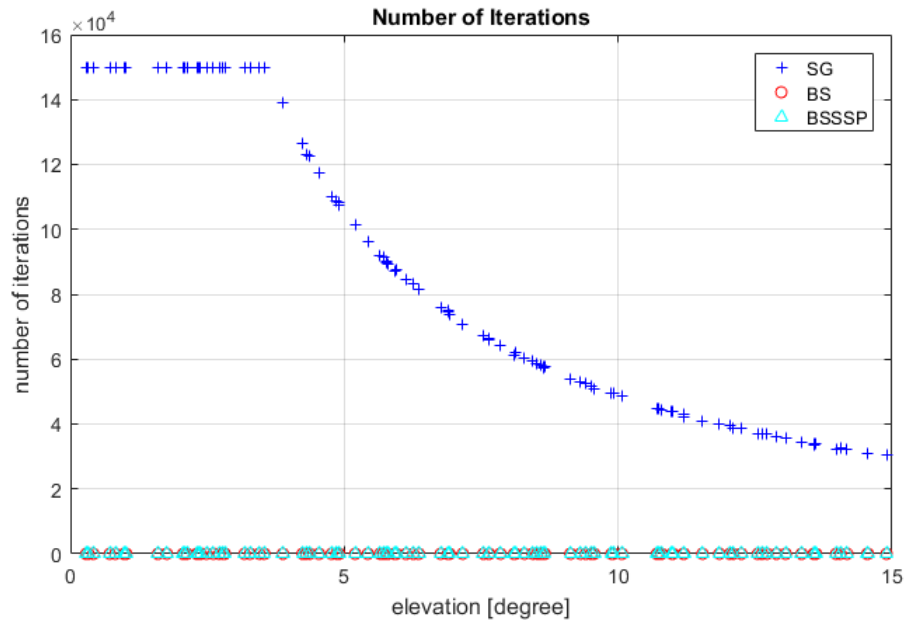
Figure 5.11.: Number of iterations vs. elevation, $n_{points} = 100$, $maxit = 1.5 \times 10^5$ iterations, $accuracy_{SG} = 0.05\,\text{m}$, $accuracy_{BS} = accuracy_{BSSSP} = 1 \times 10^{-4}\,\text{rd}$

Figure 5.11 shows the number of iterations related to the elevation of the satellites for the parameters stated above. It is obvious at first sight, that these parameter are no working combination for SG, since SG reaches the maximum number of iterations for elevations lower than $\approx 4°$. Hence another try with a higher number of iterations or lower accuracy is necessary.

2nd try

Since the 1st try did not lead to a working combination of the parameters for SG, for the 2nd try the accuracy for SG is lowered. A lower accuracy means a higher number for $accuracy_{SG}$. Following are the parameters for SG for the 2nd try.

Variable parameters for 2nd try:

$maxit \qquad = 1.5 \times 10^5 \text{ iterations}$
$accuracy_{SG} \quad = 0.5\,\text{m}$

Figure 5.12 again shows the number of iterations related to the elevation of the satellites. It is good to see, that for an accuracy lowered by the factor of
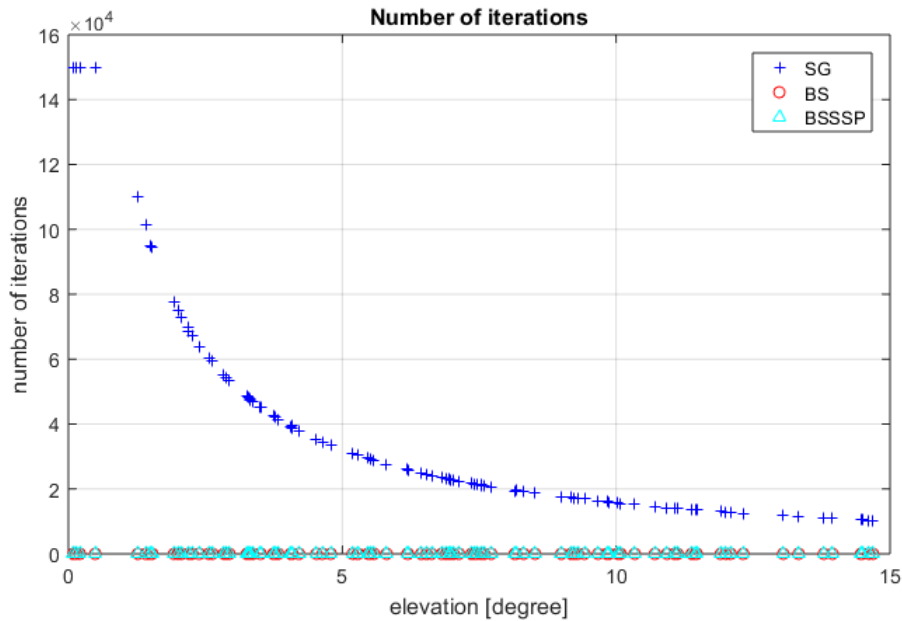
Figure 5.12.: Number of iterations vs. elevation, $n_{points} = 100$, $maxit = 1.5 \times 10^5$ iterations, $accuracy_{SG} = 0.5\,\text{m}$, $accuracy_{BS} = accuracy_{BSSSP} = 1 \times 10^{-4}\,\text{rd}$

10 more reflection point calculations get along with the number of iterations. However, SG needs much more iterations than BS or BSSSP. This can be seen in Figure 5.13 which is already zoomed in and BS and BSSSP are still on the zero line. According to the calculated extreme case in section 4.3, BS and BSSSP will require a maximum of 35 iterations. SG needs at least $\approx 10,000$ iterations with the parameters selected above.

Lets have a look at the signal path difference for these parameters (Figure 5.14) and see if the accurateness of SG with the selected parameters is comparable to BS and BSSSP. Similar to SP_{diff} in section 5.2.1 SG has problems with low elevations. For the lower accuracy though, only with very small ones. The values of SP_{diff} over the whole range of elevation show clearly, that the accurateness of SG is about 10 m worse than the one of BS. SG has an accurateness of $\leq 25\,\text{m}$ and BS has an accurateness of $SP_{diff} < 15\,\text{m}$. Therefore SG and BS do not achieve the required accurateness of $SP_{diff} < 10\,\text{m}$, as stated at the beginning of this chapter. BSSSP on the other hand is easily within the required accurateness.

For the sake of completeness lets have a look at the calculation time. Figure 5.15 shows the calculation time for each reflection point related to the
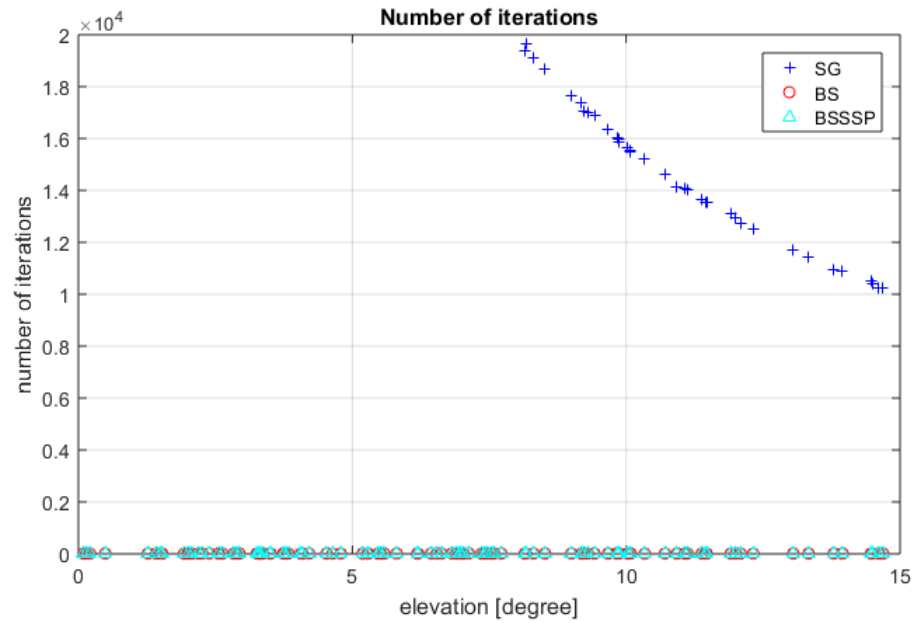
Figure 5.13.: Number of iterations vs. elevation zoomed in, $n_{points} = 100$, $maxit = 1.5 \times 10^5$ iterations, $accuracy_{SG} = 0.5\,\mathrm{m}$, $accuracy_{BS} = accuracy_{BSSSP} = 1 \times 10^{-4}\,\mathrm{rd}$
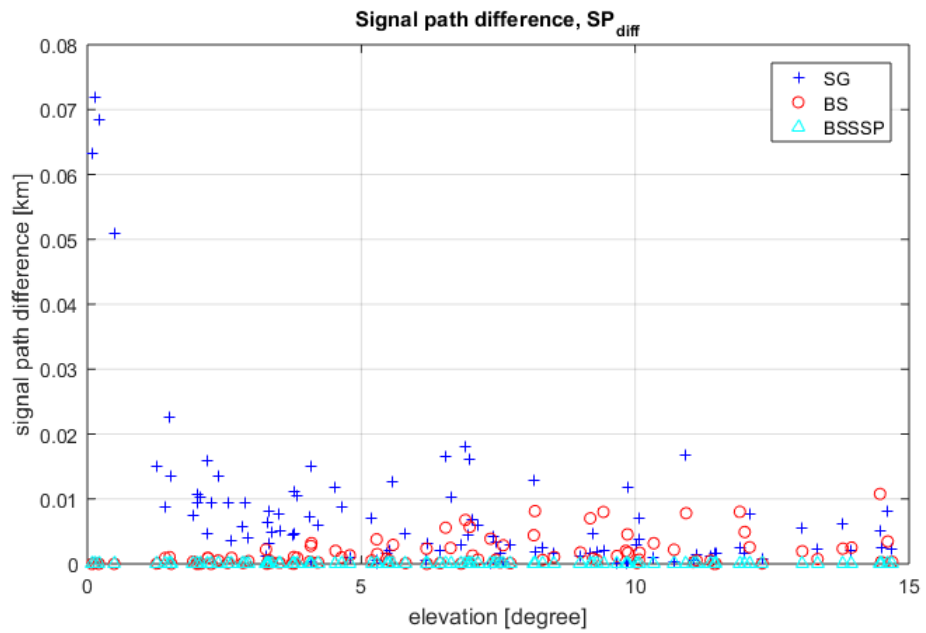
Figure 5.14.: SP_{diff} vs. elevation, $n_{points} = 100$, $maxit = 1.5 \times 10^5$ iterations, $accuracy_{SG} = 0.5\,\mathrm{m}$, $accuracy_{BS} = 1 \times 10^{-4}\,\mathrm{rd}$
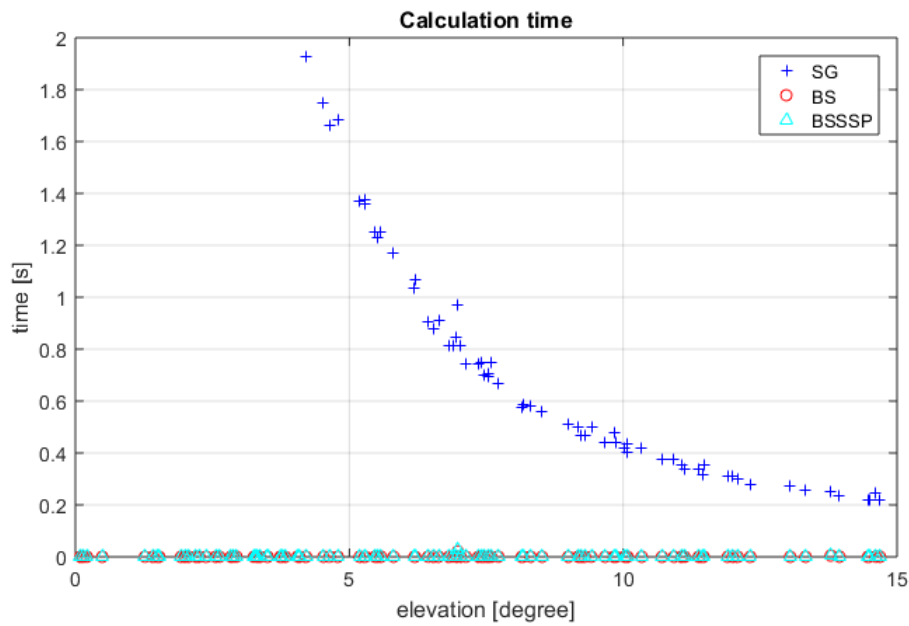
Figure 5.15.: Calculation time vs. elevation, $n_{points} = 100$, $maxit = 1.5 \times 10^5$ iterations, $accuracy_{SG} = 0.5\,\text{m}$, $accuracy_{BS} = 1 \times 10^{-4}\,\text{rd}$

elevation of the satellites. Since the calculation time of SG for small elevations goes up to $\approx 33\,\text{s}$, Figure 5.15 is already zoomed in for better comparison. Thus, no values of SG are displayed for elevations lower than $\approx 4.5\,°$. It is clear at first sight, that SG can not compete with BS or BSSSP concerning the calculation time. Since SG does not achieve the required accurateness and a higher $accuracy_{SG}$ would require more iterations and thus an even longer calculation time, it can be said here that SG performs worse than BS and BSSSP.

5.2.3. BS vs. BSSSP

In section 5.2.2 it turns out that the accurateness of SG cannot compete with BS and BSSSP for small elevations and only with a much high number of iterations and much longer calculation time for large elevations. Therefore, SG is no longer evaluated. This section takes a closer look at the performance of BS and BSSSP. To obtain a statistically more significant statement, the number of calculated reflection points was increased to $1,000$. Since BS and BSSSP should require a maximum of 35 iterations, the maximum number of iterations allowed was decreased to $1,000$. The high number of $1,000$ iterations was selected in order to better investigate any outliers that might occur. The accuracy for BS was kept the same. The accuracy for BSSSP has been reduced because Figure 5.14 shows that BSSSP is much more accurate than BS.

Parameters for the comparison of BS and BSSSP:

$$n_{points} \quad\quad = 1,000$$
$$maxit \quad\quad = 1,000 \, \text{iterations}$$
$$accuracy_{BS} \quad = 1 \times 10^{-4} \, \text{rd}$$
$$accuracy_{BSSSP} \quad = 1 \times 10^{-3} \, \text{rd}$$

Distance between true and calculated reflection point, SS_{calc}

Figures 5.16, 5.17 and 5.18 show the distance between the true and the calculated reflection point related to either the longitude or the latitude of the true reflection point or the elevation of the satellites. The reflection points calculated with BSSSP are much closer to the true reflection points than the ones calculated with BS. Similar to section 5.2.1 the SS_{calc} does not show any longitude dependency. Figure 5.17 shows an significant latitude dependency of BS similar to section 5.2.1. SS_{calc} for BS is shortest at the poles and the equator and largest at $\approx 45°$ latitude. This is because the vector $\overrightarrow{MP_{BS}}$, BS uses for the satellite sub-point calculation of P_{BS}, is equal to the surface normal of the reflection point at the poles and the equator (see section 4.3). Figure 5.18 shows, that SS_{calc} for BS decreases with increasing satellite elevation. The maximum distance between the true and the calculated reflection point for BS is $\approx 22 \, \text{km}$. To be able to read the maximal distance for BSSSP, Figure 5.19 shows SS_{calc} related to the elevation only for BSSSP. The maximum distance between the true and the calculated reflection point for BSSSP is $\approx 2.15 \, \text{km}$ and it is also decreasing for increasing satellite
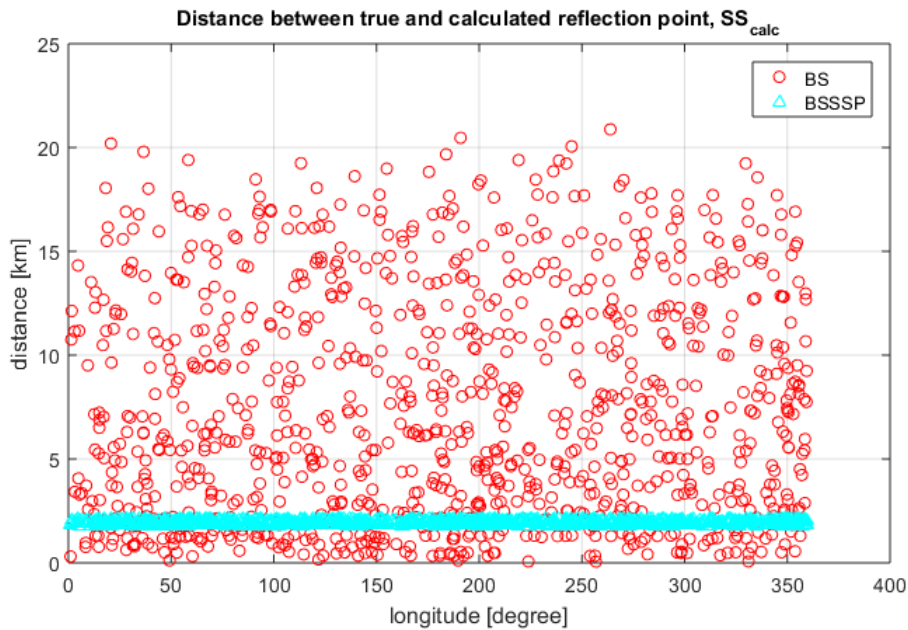
Figure 5.16.: SS_{calc} vs. longitude, $n_{points} = 1000$, $maxit = 1,000$ iterations, $accuracy_{BS} = 1 \times 10^{-4}$ rd, $accuracy_{BSSSP} = 1 \times 10^{-3}$ rd

elevations. The fact that SS_{calc} for BSSSP only varies slightly around 2 km and decreases continuously without variance was not expected. At the moment there is no explanation for this behaviour. It might be an indication of an error in the BSSSP implementation.

Additionally to its latitude and elevation dependency, BS has a dependency on the orientation of the plane defined by T, R and S. Figure 5.20 shows a scheme of this plane. For better visibility, the scheme is not true to scale. T and R are calculated from S and must be in one plane with N_S to fulfil the Law of Reflection. The orientation (rather north-south or east-west) of this plane is generated by a random number. Since BS uses a plane defined by T, R and M to calculate the reflection point, the calculation is more accurate, the more the plane defined by T, R and S is orientated north-south. Because, for a north-south orientation, the plane defined by T, R and S does include M. Therefore, the accuracy of the reflection point calculation of BS will depend not only on the longitude and elevation, but also on the orientation of this plane. This is also the reason that BS can calculate reflection points with a lower SS_{calc} than BSSSP. Since the maximum values are of interest, there is no need to further investigate this dependency. Because, it will not change the maximum values.
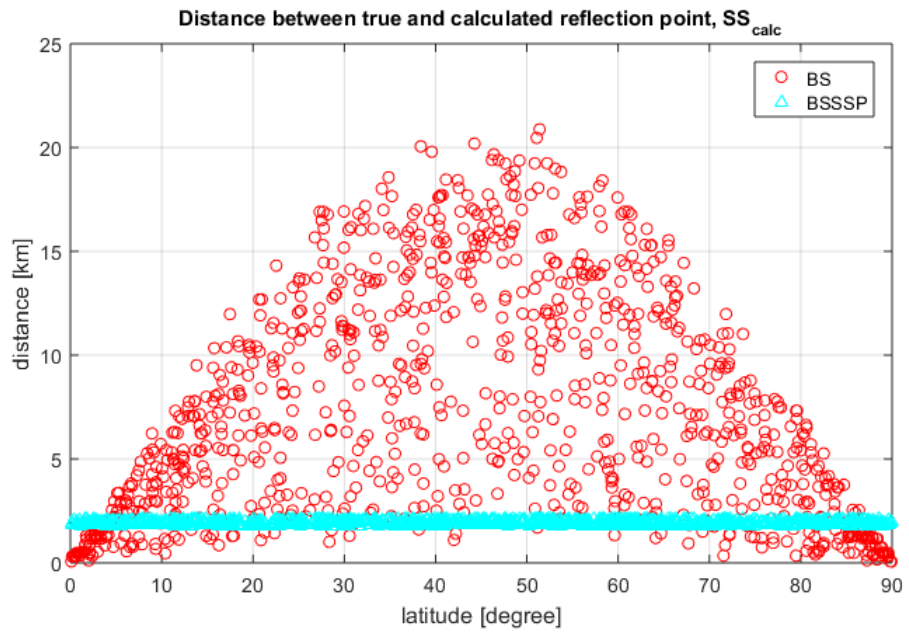
Figure 5.17.: SS_{calc} vs. latitude, $n_{points} = 1000$, $maxit = 1,000$ iterations, $accuracy_{BS} = 1 \times 10^{-4}$ rd, $accuracy_{BSSSP} = 1 \times 10^{-3}$ rd
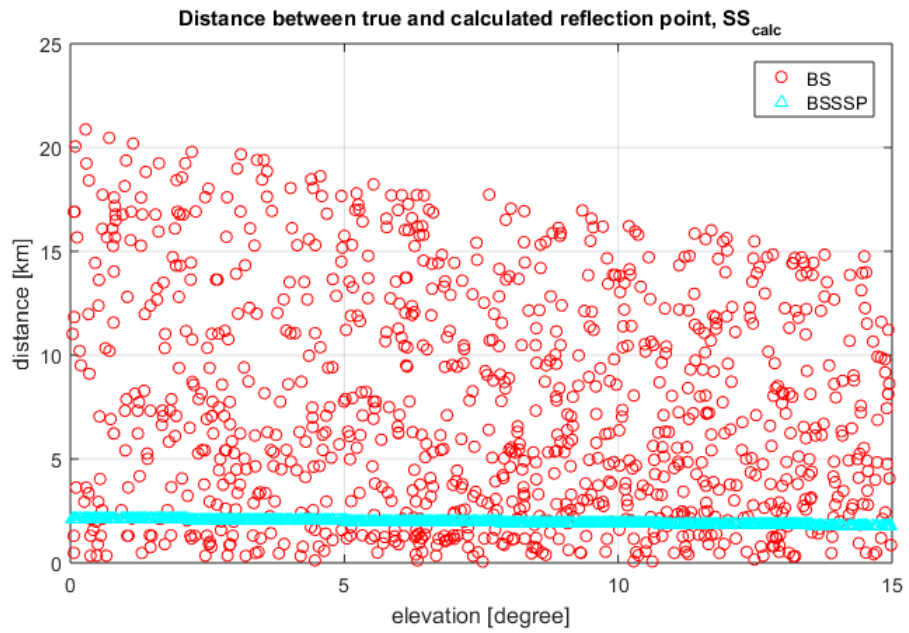
Figure 5.18.: SS_{calc} vs. elevation, $n_{points} = 1000$, $maxit = 1,000$ iterations, $accuracy_{BS} = 1 \times 10^{-4}$ rd, $accuracy_{BSSSP} = 1 \times 10^{-3}$ rd
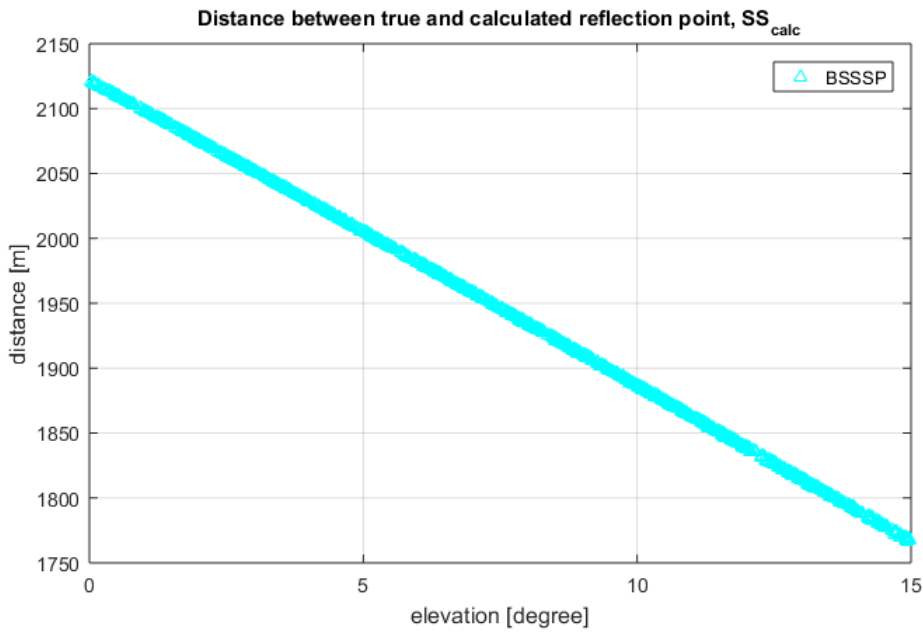
Figure 5.19.: SS_{calc} vs. elevation, $n_{points} = 1000$, $maxit = 1,000$ iterations, $accuracy_{BSSSP} = 1 \times 10^{-3}$ rd

Signal path difference, SP_{diff}

Figures 5.21, 5.22 and 5.23 show the signal path difference between SP_{rcalc} and SP_r related to either the longitude or the latitude of the true reflection point or the elevation of the satellites. It is good to see, that BSSSP has a much lower signal path difference than BS. BS shows the same latitude dependency with the same reason for $SPdiff$ as it does for SS_{calc}. The elevation dependency of BS is reversed. This is logical, because for an elevation of $ele = 0°$ the signal path stays the same. No matter where on the signal path the calculated reflection point is located, since the straight line between T and R already is the direct and the reflected signal path. The maximum signal path difference for BS is ≈ 12 m. Again, to be able to read the maximal signal path difference for BSSSP, Figure 5.24 shows SP_{diff} related to the elevation only for BSSSP. The maximum signal path difference for BSSSP is ≈ 18 cm and it is also increasing for increasing satellite elevations. As for SS_{calc}, BSSSP shows a continuous behaviour without variance for SP_{diff} too. Again, this behaviour was not expected and there is no explanation for this effect, than a possible implementation error.
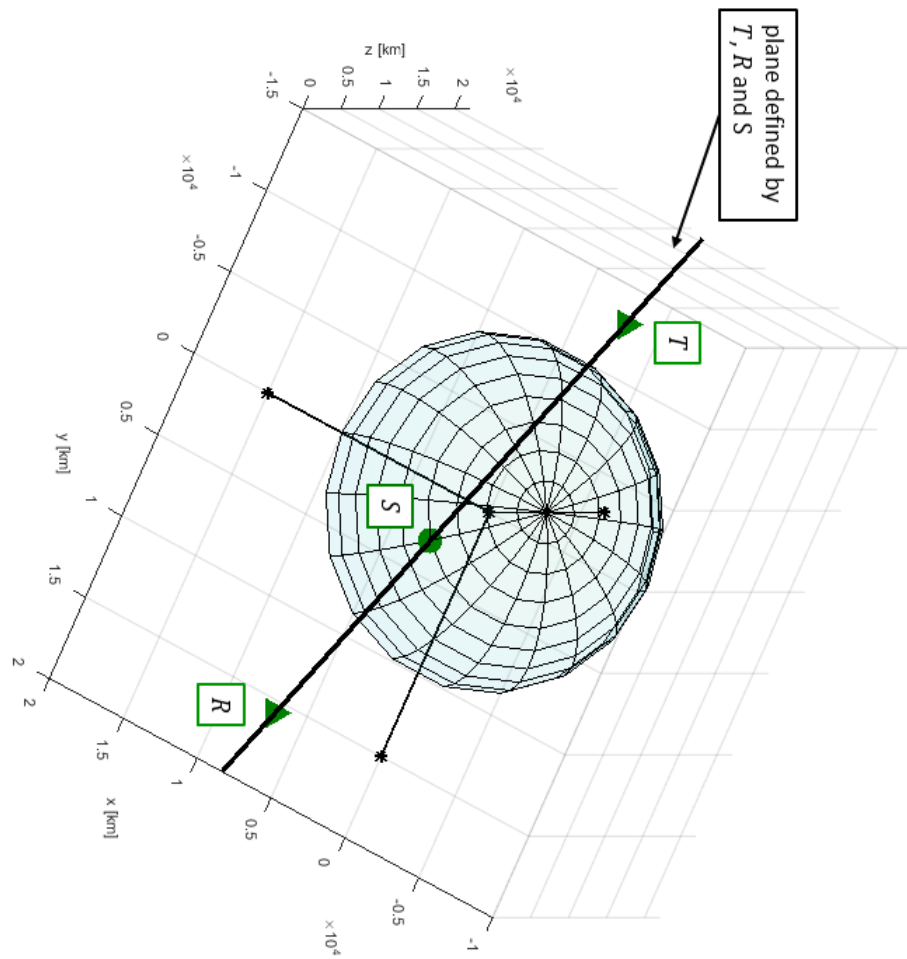
Figure 5.20.: Scheme of a measurement constellation
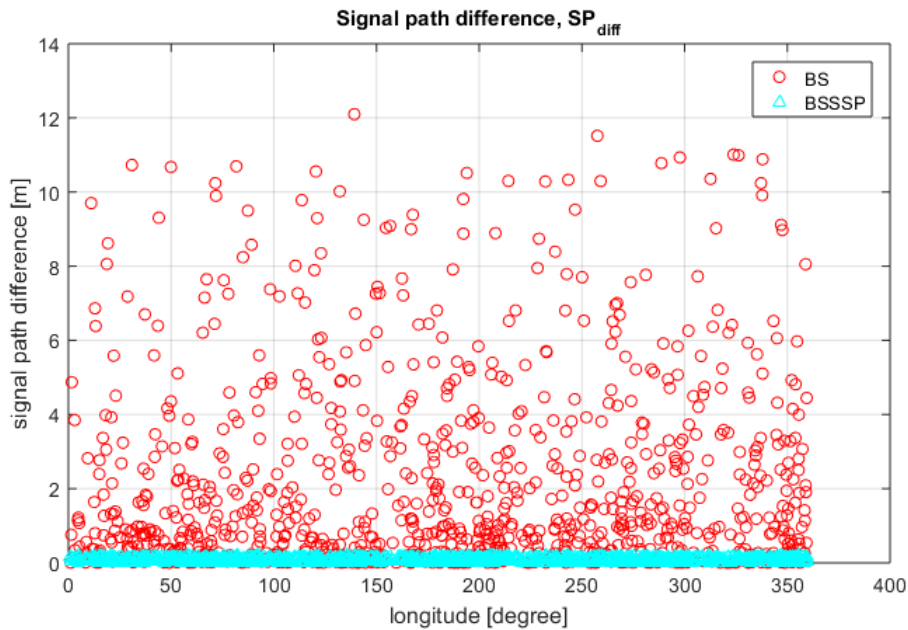
Figure 5.21.: Signal path difference SP_{diff} vs. longitude, $n_{points} = 1000$, $maxit = 1,000$ iterations, $accuracy_{BS} = 1 \times 10^{-4}$ rd, $accuracy_{BSSSP} = 1 \times 10^{-3}$ rd

Since BS has a maximum signal path difference of 12 m, Figure 5.25 shows a simulation with higher accuracy for BS ($accuracy_{BS} = 1 \times 10^{-5}$ rd) but the same for BSSSP ($accuracy_{BSSSP} = 1 \times 10^{-3}$ rd). Although, the simulation was performed with a higher accuracy for BS, BS still has a maximum signal path difference of 12 m. Hence, BS already reached the maximal accurateness possible with $SP_{diff} = 12$ m. This limitation is because of the calculation plane (see section 4.7).

Number of iterations

Figures 5.26, 5.27 and 5.28 show the number of iterations each reflection point calculation needed related to either the longitude or the latitude of the true reflection point or the elevation of the satellites. As can be seen, BSSSP requires less iterations to calculate the reflection point than BS. This is because of the lower accuracy required. An interesting thing is that BSSSP requires the same number of iterations for each reflection point calculation. This is because of the use of the satellite sub-point calculation. By using this calculation, the accurateness of the reflection point calculation performed
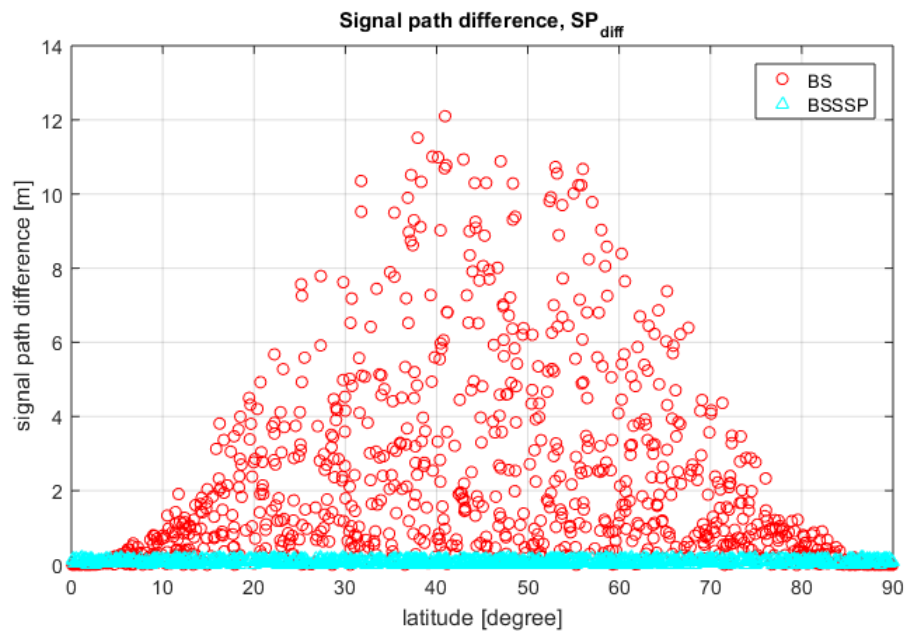
Figure 5.22.: Signal path difference SP_{diff} vs. latitude, n_{points} = 1000, $maxit$ = 1,000 iterations, $accuracy_{BS} = 1 \times 10^{-4}$ rd, $accuracy_{BSSSP} = 1 \times 10^{-3}$ rd
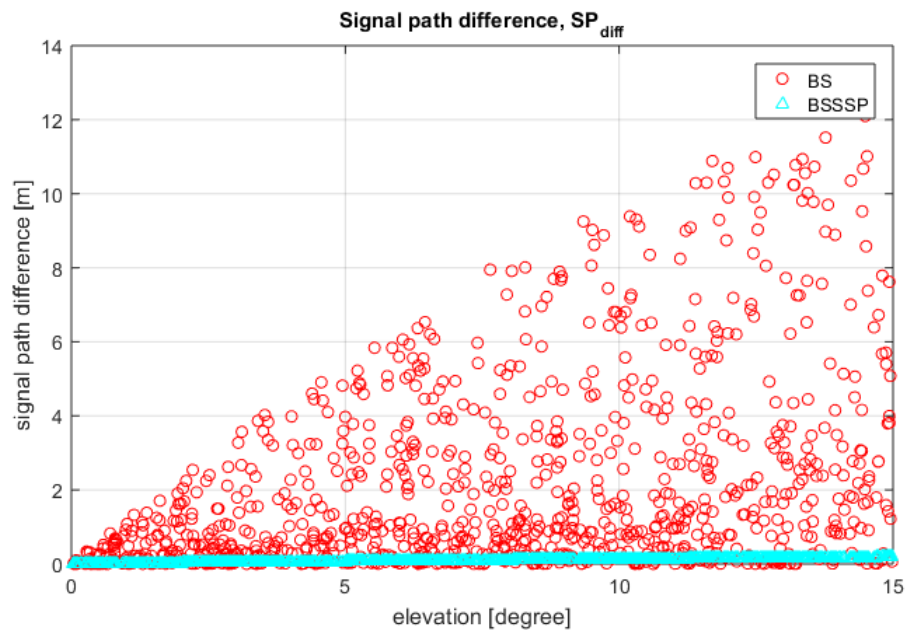
Figure 5.23.: Signal path difference SP_{diff} vs. elevation, n_{points} = 1000, $maxit$ = 1,000 iterations, $accuracy_{BS} = 1 \times 10^{-4}$ rd, $accuracy_{BSSSP} = 1 \times 10^{-3}$ rd
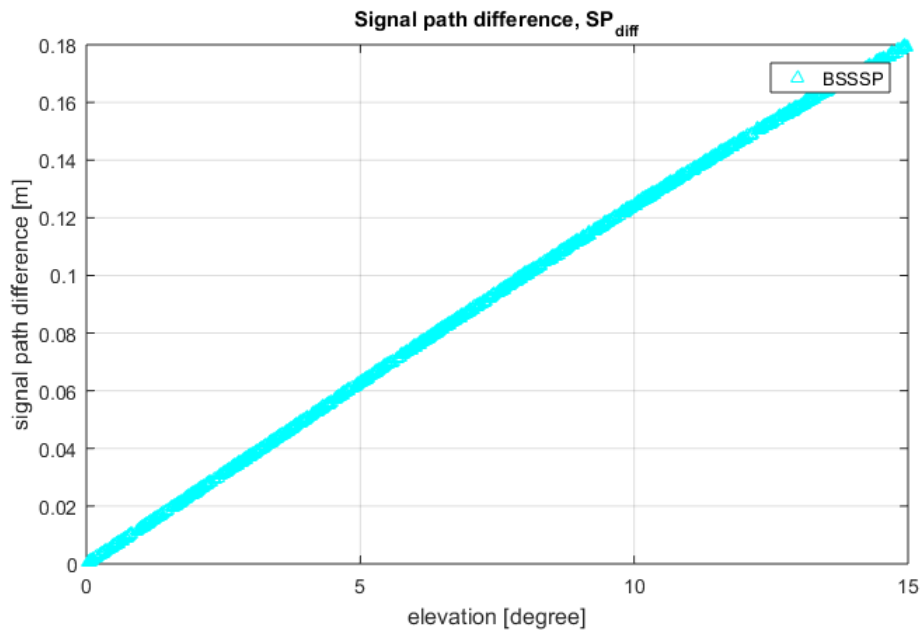
Figure 5.24.: Signal path difference SP_{diff} vs. elevation, $n_{points} = 1000$, $maxit = 1,000$ iterations, $accuracy_{BSSSP} = 1 \times 10^{-3}$ rd
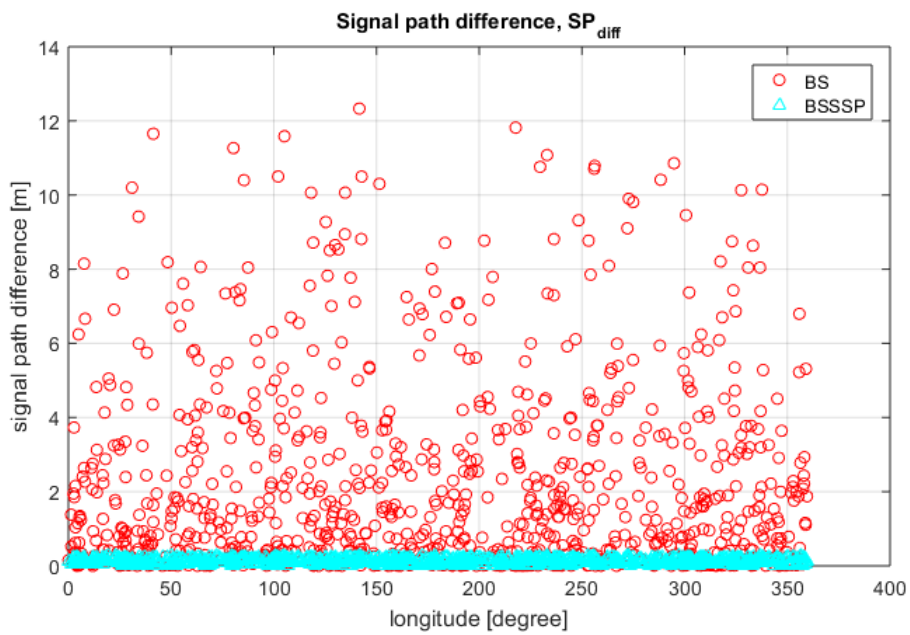
Figure 5.25.: Signal path difference SP_{diff} vs. longitude, Closer Look, $n_{points} = 1000$, $maxit = 1,000$ iterations, $accuracy_{BS} = 1 \times 10^{-5}$ rd, $accuracy_{BSSSP} = 1 \times 10^{-3}$ rd
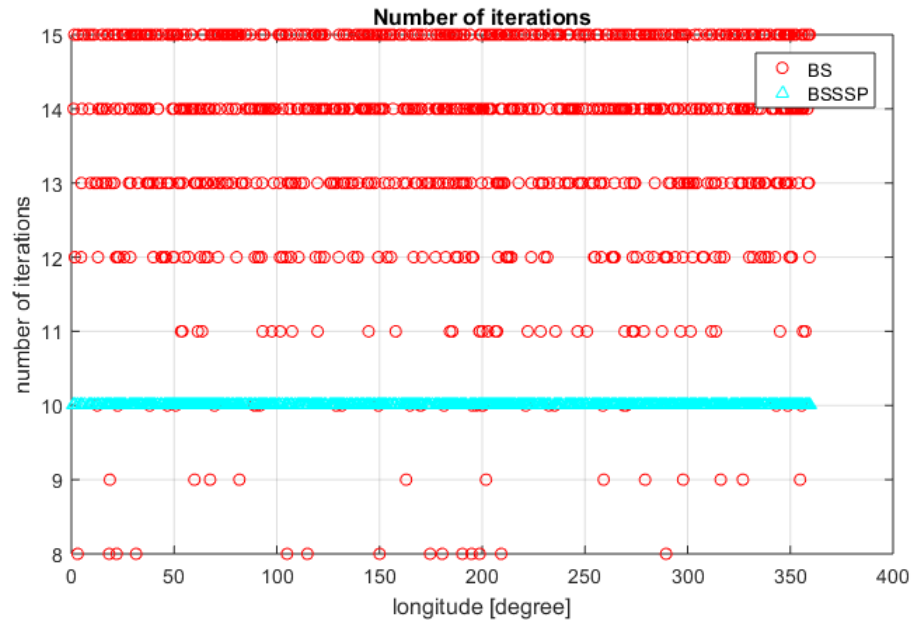
Figure 5.26.: Number of iterations vs. longitude, $n_{points} = 1000$, $maxit = 1,000$ iterations, $accuracy_{BS} = 1 \times 10^{-4}$ rd, $accuracy_{BSSSP} = 1 \times 10^{-3}$ rd

with BSSSP does not depend on the reflection point location (longitude and latitude) or the orientation of the plane defined by T, R and S. The accuracy of the reflection point calculation performed with BS on the other hand does depend on the location of the reflection point or the orientation of the plane defined by T, R and S. BS requires maximum 15 iterations and BSSSP requires 10 iterations.

The calculation of the satellite sub-point BSSSP performs is an iterative process too. Therefore, BSSSP has additional iterations. According to Kelso (2014) the satellite sub-point calculation does require a maximum of three iterations to reach a sufficient accuracy.

Calculation time

Figures 5.29, 5.30 and 5.31 show the calculation time each reflection point calculation requires related to either the longitude or the latitude of the true reflection point or the elevation of the satellites. Since, except of a few outliers, in all three figures the calculation time is somewhat around zero, Figure 5.32 shows the calculation time zoomed in related to the latitude. As
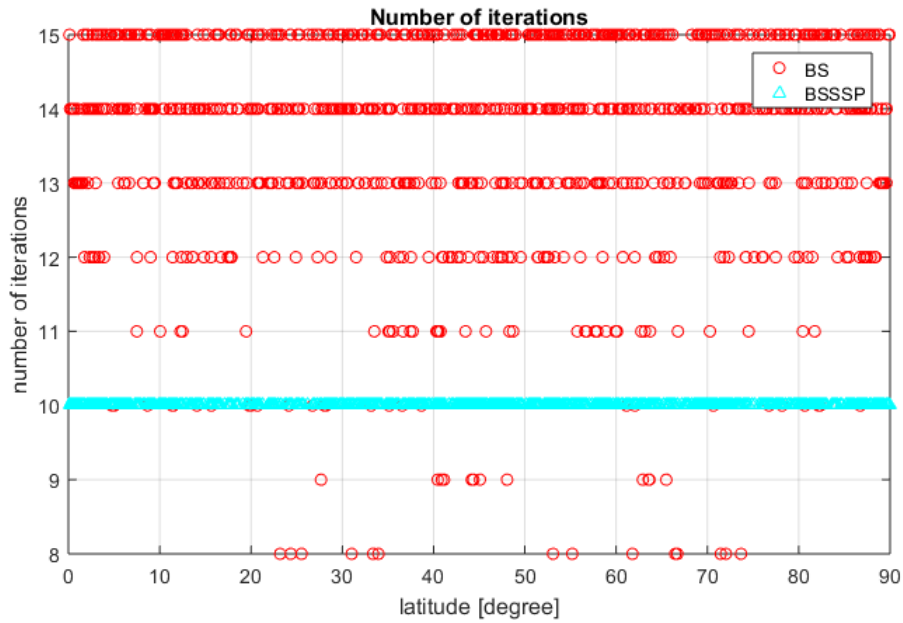
Figure 5.27.: Number of iterations vs. latitude, $n_{points} = 1000$, $maxit = 1,000$ iterations, $accuracy_{BS} = 1 \times 10^{-4}$ rd, $accuracy_{BSSSP} = 1 \times 10^{-3}$ rd
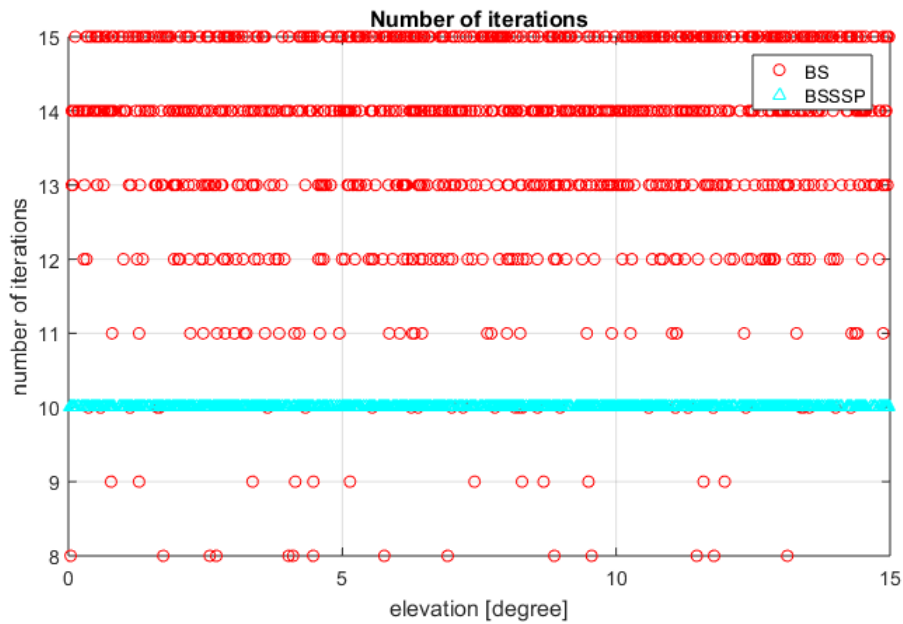
Figure 5.28.: Number of iterations vs. elevation, $n_{points} = 1000$, $maxit = 1,000$ iterations, $accuracy_{BS} = 1 \times 10^{-4}$ rd, $accuracy_{BSSSP} = 1 \times 10^{-3}$ rd
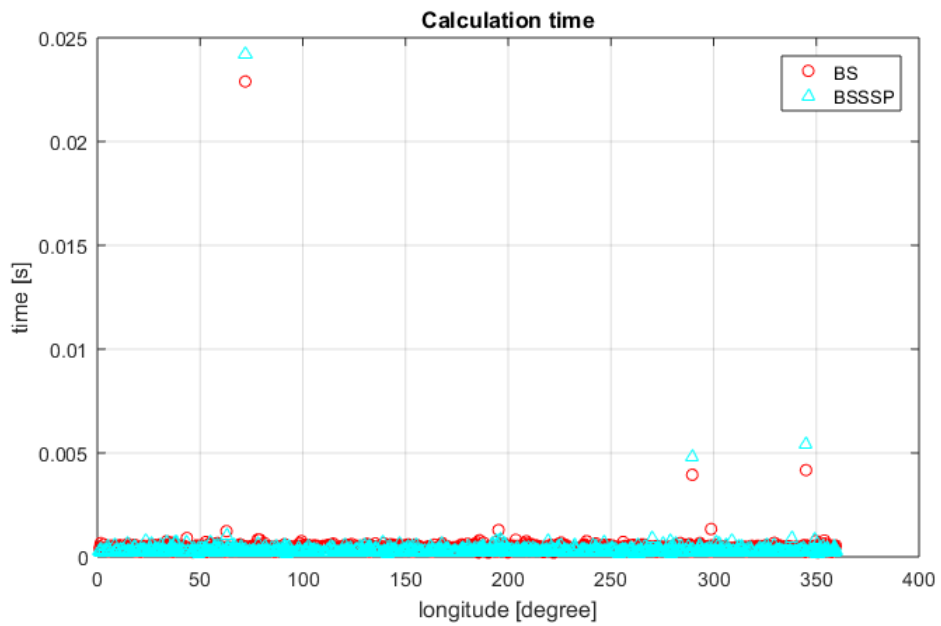
Figure 5.29.: Calculation time vs. longitude, $n_{points} = 1000$, $maxit = 1,000$ iterations, $accuracy_{BS} = 1 \times 10^{-4}$ rd, $accuracy_{BSSSP} = 1 \times 10^{-3}$ rd

can be seen, that the calculation time has no dependency and is somewhat around 0.5 m for BS and 0.3 ms for BSSSP. To show that the outliers happen randomly because of some delays produced by the PC, Figure 5.33 shows another simulation with the same parameters. It is plain to see that it has not the same outliers.
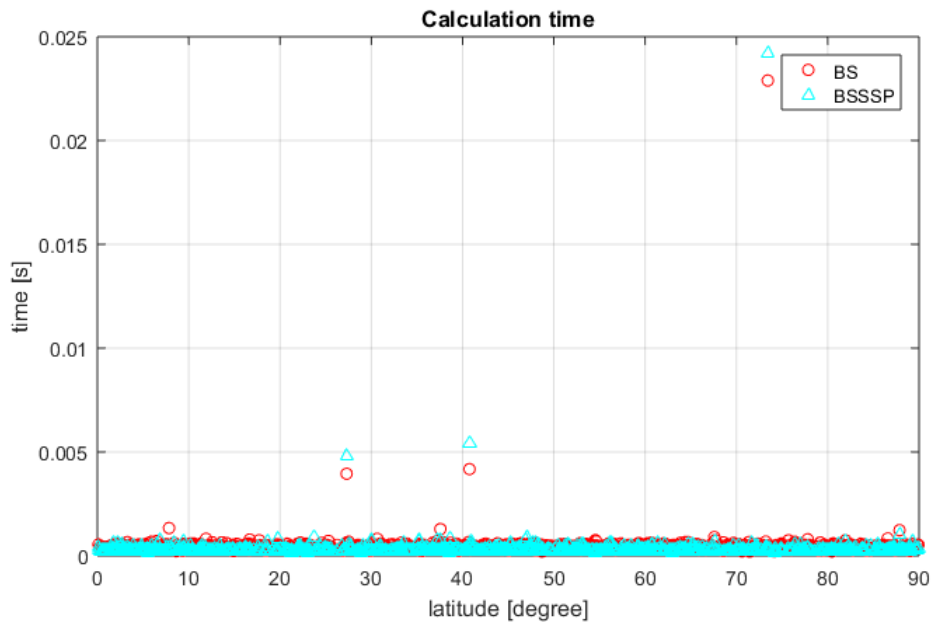
Figure 5.30.: Calculation time vs. latitude, $n_{points} = 1000$, $maxit = 1,000$ iterations, $accuracy_{BS} = 1 \times 10^{-4}$ rd, $accuracy_{BSSSP} = 1 \times 10^{-3}$ rd
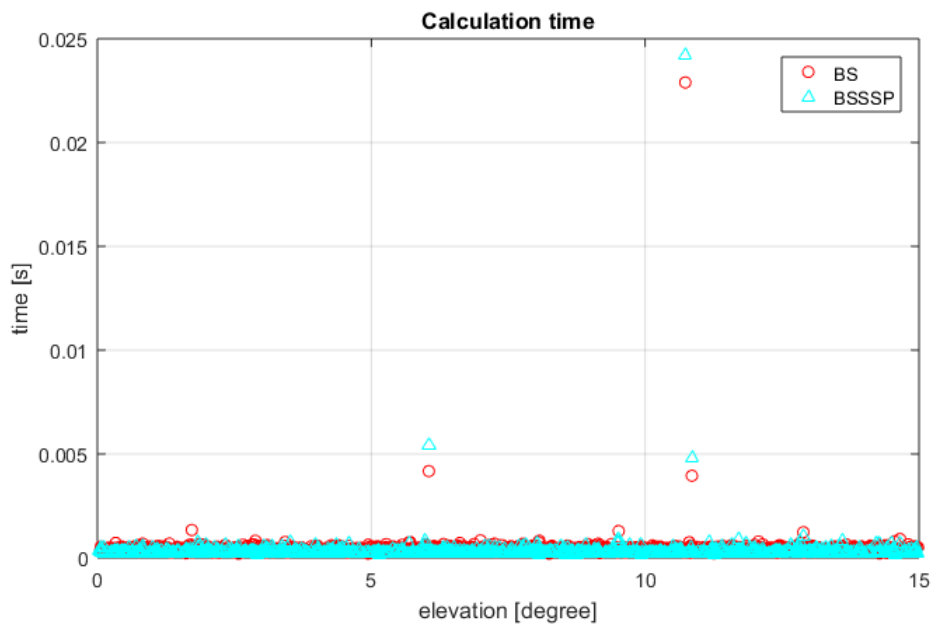
Figure 5.31.: Calculation time vs. elevation, $n_{points} = 1000$, $maxit = 1,000$ iterations, $accuracy_{BS} = 1 \times 10^{-4}$ rd, $accuracy_{BSSSP} = 1 \times 10^{-3}$ rd
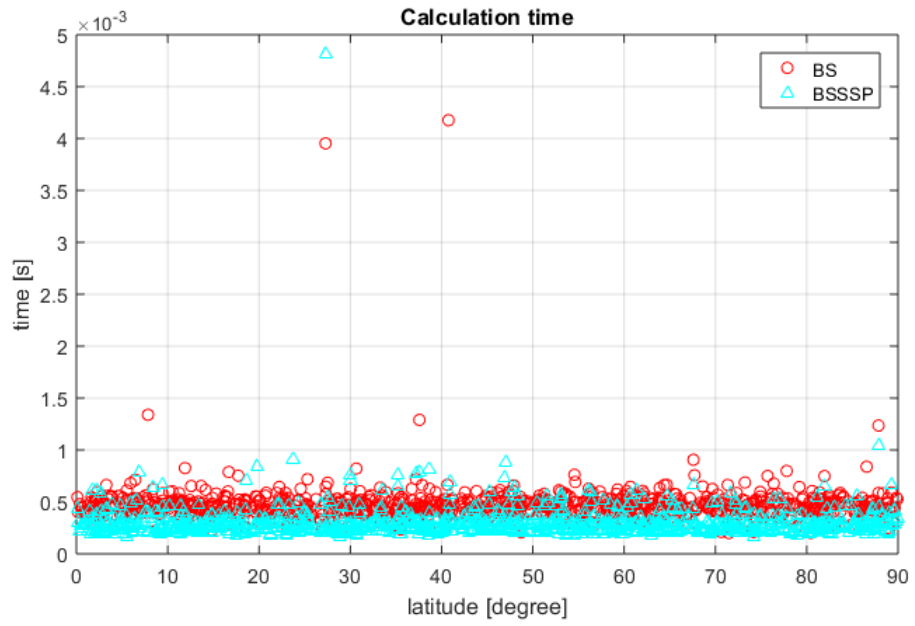
Figure 5.32.: Calculation time vs. latitude, $n_{points} = 1000$, $maxit = 1,000$ iterations, $accuracy_{BS} = 1 \times 10^{-4}$ rd, $accuracy_{BSSSP} = 1 \times 10^{-3}$ rd, zoomed in
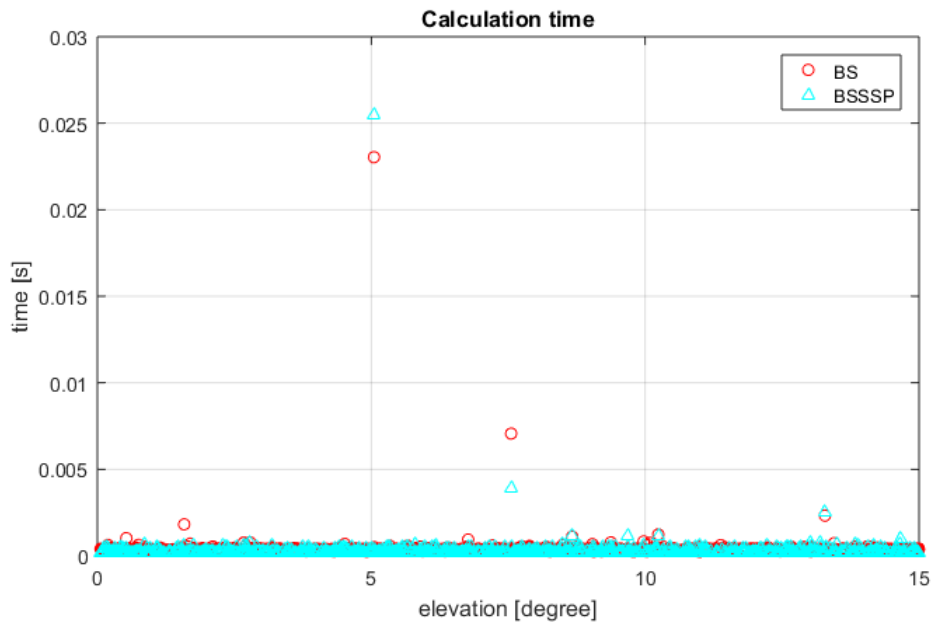
Figure 5.33.: Calculation time vs. latitude for another simulation, $n_{points} = 1000$, $maxit = 1,000$ iterations, $accuracy_{BS} = 1 \times 10^{-4}$ rd, $accuracy_{BSSSP} = 1 \times 10^{-3}$ rd

5.2.4. Histograms of BS vs. BSSSP

To proof, that the result of the Monte Carlo simulation from section 5.2.3 are no coincidence, this section shows three histograms of the signal path difference SP_{diff} of three single simulations. All three histograms reflect simulation results with the same accuracies and maximum number of iterations. For a closer look at BSSSP, an additional histogram with a smaller bin size of the first simulation is shown.

$$
\begin{aligned}
maxit &= 1,000 \, \text{iterations} \\
accuracy_{BS} &= 1 \times 10^{-4} \, \text{rad} \\
accuracy_{BSSSP} &= 1 \times 10^{-3} \, \text{rd}
\end{aligned}
$$

Figures 5.34, 5.35 and 5.37 show histograms for $n_{points} = 1,000$ and Figure 5.36 shows a histogram for $n_{points} = 10,000$. In the figures 5.34, 5.35 and 5.36 all reflection points calculated with BSSSP have a SP_{diff} lower than 0.5 m. For BS on the contrary only on third of the calculated reflection points has a SP_{diff} lower than 0.5 m. Figure 5.37 shows a histogram for $n_{points} = 1000$ with a smaller bin spacing. It shows that SP_{diff} for BSSSP is actually less than 18 cm. However, for the histogram of BSSSP a similar distribution as for BS was expected. Instead, the histogram of BSSSP does not show any form of distribution. Similar to SS_{calc} and SP_{diff}, there is no other explanation for this effect, than a possible implementation error.

5.3. Discussion

The objective of chapter 5 was to evaluate the methods SG, BS and BSSSP with respect to their performance to calculate a reflection point with the WGS 84 as earth model. The determining factors for the evaluation are a short calculation time and to fulfil the accuracy criteria $SP_{diff} < 10$ m. Already at the beginning of the evaluation, it turned out that SG requires more calculation time than BS and BSSSP. Additionally, SG has big shortcomings concerning small satellite elevation angles. It is not able, to calculate them with a reasonable given number of iterations and therefore does not achieve the required accuracy. A more detailed comparison of BS and BSSSP showed, that BSSSP is more precise than BS. Additionally BS is not fully able to fulfil the accuracy criteria. For some reflection points it has a signal path difference of ≈ 12 m. BSSSP on the other hand, has a maximum signal path difference of ≈ 18 cm. Additional histogram plots show, that
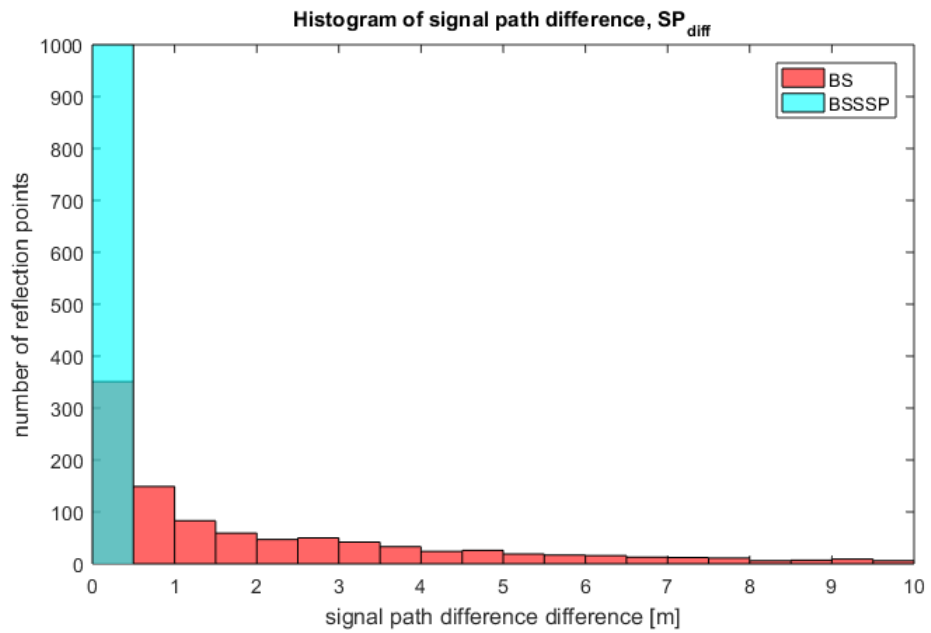
Figure 5.34.: First histogram of the signal path difference for $1,000$ calculated reflection points
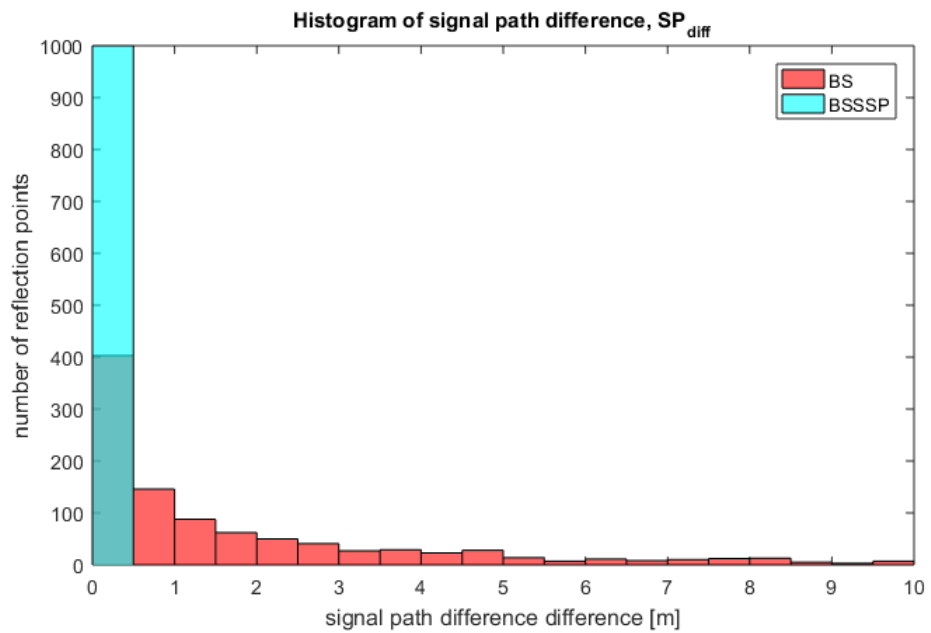
Figure 5.35.: Second histogram of the signal path difference for $1,000$ calculated reflection points
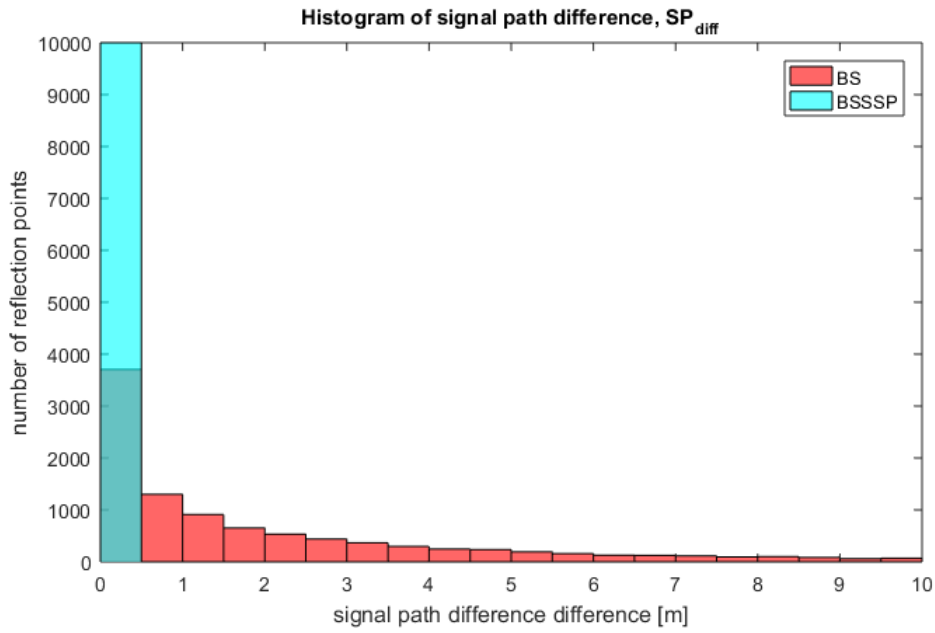
Figure 5.36.: Third histogram of the signal path difference for 10,000 calculated reflection points
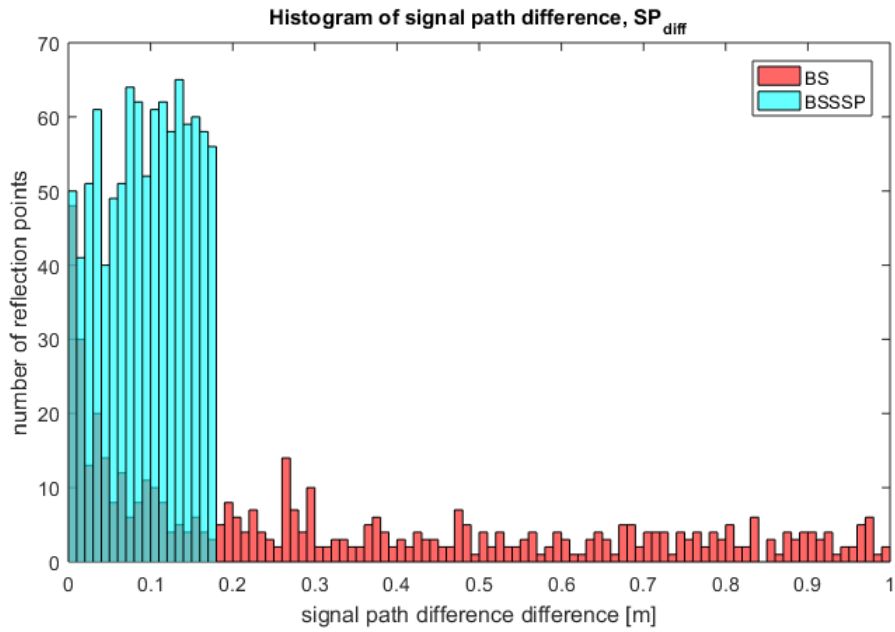
Figure 5.37.: First histogram of the signal path difference for 1,000 calculated reflection points with smaller bin spacing

other simulations with the same parameters for accuracy result similar accurateness of the reflection point calculation for BS and BSSSP. Also for a higher number of reflection points. Concerning the calculation time, BS requires $\approx 0.5\,\mathrm{ms}$ and BSSSP $\approx 0.3\,\mathrm{ms}$. Since it can not be said, if BS or BSSSP is faster on-board a satellite, both methods must be tested on satellite hardware.

In addition to statements on computational accuracy and speed of the methods, the evaluation showed that the computational accuracies of BS and BSSSP have certain dependencies. The accuracy of BS shows a latitude dependency due to the use of a calculation plane defined by T, R and M (see section 4.7). Therefore, the reflection point calculation of BS is more precise for reflection points located at the equator or at the poles. The path length difference for both methods is shortest for small satellite elevation angles. This is because, the smaller the elevation angle the less is the deviation between SP_d and SP_r. For a satellite elevation angle of $0\,°$, SP_d would be equal to SP_r. The continuous dependency without variance of SS_{calc} and SP_{diff} of BSSSP can not be explained. The same goes for the histogram of BSSSP, which does not look like the expected distribution. The reason for this behaviour might be an implementation error of BSSSP or a rounding error. Therefore, for BSSSP, despite its good results, further investigation beyond the scope of this thesis is necessary.

6. Conclusion

The objective of this thesis was to find methods to calculate the reflection point for a snapshot of the measurement constellation with the WGS 84 as earth model for the GNSS-R mission PRETTY. This was done in order to investigate, how a real time on board calculation of the reflection point will perform. Before the actual reflection point calculation, the influence of the atmosphere on the refraction of an electromagnetic signal was investigated. This was done in order to clarify, if this influence must be taken into account for the reflection point calculation. Afterwards, several different methods for the reflection point calculation have been introduced, described and investigated concerning their feasibility. Finally, three of the introduced methods were evaluated with regard to their accuracy and performance. The conclusion chapter now sums up the results and gives a recommendation which method should be used for PRETTY. In addition, some points that the reader should be aware of are noticed and an outlook on how to proceed with the reflection point calculation is given.

6.1. The calculation of the reflection point

6.1.1. Influence of the atmosphere on the refraction of an electromagnetic signal and its associated effects on the reflection point calculation

To investigate the influence of the atmosphere on the refraction of an electromagnetic signal (see chapter 3), a model of the atmosphere, consisting of individual layers of atmosphere with certain heights and a constant reflection indices for each layer, was created. In order to evaluate how much the atmosphere influences the refraction of an electromagnetic signal, a non-refracted and a refracted signal, both reflected at the earth surface, were simulated and compared for two earth models. The first model was

an assumed flat Earth with parallel layers of atmosphere and the second one was a spherical Earth with radially bent layers of atmosphere. The evaluation for both earth model was done with regard to the position of the reflection point and the path length difference between the non-refracted and the refracted signal. Since the spherical earth model is the more realistic one and therefore has more significance, following the maximum values of the results for this model for two height step sizes are stated.

Height step size: 0.5 km

  Distance between reflection points: $\approx 647\,\mathrm{m}$
  Path length difference: $\approx 1.1\,\mathrm{m}$

Height step size: 5 km

  Distance between reflection points: $\approx 813\,\mathrm{m}$
  Path length difference: $\approx 3.3\,\mathrm{m}$

As can be easily seen, a higher height step size results higher deviations. Both have maximum path length differences up to the metre range. Since the maximum allowed path length difference for the reflection points calculation is 10 m, the impact of the influence of the atmosphere on the refraction of an electromagnetic signal on the reflection point calculation can only be clarified in relation to the signal path difference of the results of the reflection point calculation. Since a higher height step size results less precise calculations, the results of the calculation with $h_{step} = 500\,\mathrm{m}$ are recommended for the comparison with the results of the reflection point calculation.

6.1.2. Evaluated methods for the reflection point calculation

The following three calculation methods for the reflection point calculation were evaluated in chapter 5.

- *Ellipsoidal Earth* (henceforward: SG), described in section 4.2.3, MAT-LAB code from Gleason and Gebre-Egziabher (2009)
- *Binary Search for an ellipsoid* (henceforward: BS), described in section 4.3
- *Binary Search for a spheroid enhanced with satellite sub-point calculation* (henceforward: BSSSP), described in section 4.3 and 4.8

The evaluation was done with a Monte Carlo simulation with true reflection points randomly distributed over the earth surface as start values. Out of

these start values the satellite positions have been calculated and out of the satellite positions the calculation methods calculated the reflection points. The distance between the true and the calculated reflection points, the signal path differences between the signal path of the calculated and the true reflection points and the required computing times were evaluated. This evaluation showed, that SG is not able to reach the same accurateness as BS and BSSSP for small satellite elevation angles. For higher satellite elevations, SG achieves the same accurateness as BS does, but SG requires much more calculation time (SG: $> 2\,\mathrm{s}$, BS and BSSSP: $\approx 0.5\,\mathrm{ms}$). Therefore, the main evaluation was done for BS and BSSSP. However, it cannot be ruled out that an improved SG algorithm can achieve the same accuracy as BS within the same calculation time.

The comparison of BS and BSSSP showed that BSSSP is more accurate and requires a lower accuracy criterion than BS. This means, BSSSP can calculate a more precise reflection point within a shorter calculation time than BS. Following, some values of the results of the comparison between BS and BSSSP are stated. The mean values and the standard deviations of the signal path differences are calculated out of a simulation consisting of $1,000$ true reflection points and the parameters of section 5.2.4.

BS:
Maximum distance between reflection points:	$\approx 22\,\mathrm{km}$
Mean value of the signal path difference:	$\approx 2\,\mathrm{m}$
Standard deviation of the signal path difference:	$\approx 2.6\,\mathrm{m}$
Calculation time:	$\approx 0.5\,\mathrm{ms}$

BSSSP:
Distance between reflection points:	$\approx 2\,\mathrm{km}$
Mean value of the signal path difference:	$\approx 10\,\mathrm{cm}$
Standard deviation of the signal path difference:	$\approx 5\,\mathrm{cm}$
Calculation time:	$\approx 0.3\,\mathrm{ms}$

According to the characteristics of a Gaussian distribution, $95\,\%$ of the reflection points calculated with BS have a signal path difference lower than $\approx 7.2\,\mathrm{m}$ ($2\,\mathrm{m} + 2 \cdot 2.6\,\mathrm{m} = 7.2\,\mathrm{m}$). Therefore, BS fulfils the required accurateness for the signal path difference ($< 10\,\mathrm{m}$). According to the histogram, all reflection points calculated with BSSSP are within the accuracy required for the signal path difference. However, the distance between the reflection points and the signal path difference of BSSSP show a continuous behaviour without variance that can not be explained conclusively. There is no explanation why the histogram of BSSSP does not show a distribution

neither. According to the mean value and the standard deviation of the signal path difference, the histogram of BSSSP should look like a declining exponential function (like the histogram of BS does). It is suspected that the reason for this behaviour is an undiscovered implementation or rounding error.

6.1.3. Conclusion on the reflection point calculation

The method SG is not able to calculate the reflection point within an acceptable calculation time with a satisfying accuracy. BS and BSSSP require acceptable low calculation times for the reflection point calculation and calculate the reflection point within the required accuracy. Since the refraction of the atmosphere influences the signal path difference within around 1 m, the influence of the atmosphere on the refraction of an electromagnetic signal can be neglected for BS and BSSSP.

Although, BSSSP delivers very promising results, it is assumed that BSSSP has problems with an implementation error or a rounding error. Possible sources for the implementation error could be the algorithm that calculates the satellite sub-point, the Binary Search algorithm of BSSSP or the calculation of the satellite positions out of the true reflection points. Since BS seems to work well, it could also be that some idiosyncrasy of the calculation of the satellite positions in combination with the BSSSP algorithm results a rounding error, which only occurs for BSSSP. Since neither an implementation nor a rounding error could be detected so far, BSSSSP has to be further investigated.

The method BS is recommended to calculate the reflection point on-board the PRETTY mission. Because, it is able to calculate the reflection point within the required accuracy with an acceptable low calculation time. Since satellite hardware differ strongly to a PC, further testing on satellite hardware with a special focus on the calculation time is strongly recommended.

6.2. Notes and Outlook

All calculations in this thesis were performed for a spherical Earth or the WGS 84 as model for the Earth. Since the WGS 84 models the Earth as an ellipsoid of rotation with a plane surface, but the earth surface is uneven, it

is mentioned here that other (more precise) models of the Earth are available too. One for example is the geoid (EGM 96) related to the WGS 84. As stated in Hofmann-Wellenhof, Lichtenegger, and Collins (2001, chapter 10.2.4), the geoid is a bumpy surface which should represents the actual shape of the Earth. Note, the EGM 96 is still a model. To obtain the real altitudes of the earth surface mission like PRETTY are used. The deviation between the WGS 84 and the EGM 96 is called geoid undulation and is given in Department of defense World Geodetic System 1984 (2000, p. 6.2.3) with a standard deviation of $\approx 30\,\mathrm{m}$ and maximum values between $\approx -107\,\mathrm{m}$ and $\approx 85\,\mathrm{m}$. Since the calculation of the EGM 96 is very complex using spherical harmonics and its standard deviation to the WGS 84 is about $30\,\mathrm{m}$, it is not recommended to use the EGM 96 on board a satellite. However, it would be well suited for a more accurate estimation of the accuracies achieved by the reflection point calculation methods evaluated in this thesis. EGM 96 would also be suitable for the on ground post processing of the measurement data obtained from PRETTY, to determine the altitudes of the gauged reflection points. Furthermore, it should be pointed out here that the inaccuracy of the earth model must be taken into account when performing calculations using an earth model.

Due to the conclusions and notes mentioned above, the next steps concerning the calculation of the reflection point should be as follows.

- Further investigated concerning the errors generating the unexpected and unexplainable behaviour of BSSSP is recommended.
- A performance analysis of BS on the satellite hardware.
- Maybe, an investigation of BS with the EGM 96 as earth model to obtain more precise information on the accuracy of BS.
- The investigation of the delay of an electromagnetic signal caused by the ionosphere.

When the error of BSSSP has been found, the last three steps can be performed for BSSSP too.

A. Program codes

A.1. Main program: Influence of atmosphere on refraction, flat Earth

```
%% Influence of atmosphere on refraction, flat Earth
% This program calculates the refraction of an electromagnetic
    wave propagating trough the earth atmosphere for an assumed
    flat Earth. The wave is emitted at a transmitter satellite,
    reflected by the earth surface and than received from a
    receiver satellite. The purpose of the program is to
    investigate the influence of the refraction on the path
    length, the siganl emission angle and the position of the
    reflection point. Therefore, a non refracted signal with a
    given signal emission angle is emitted from the transmitter
    satellite, reflected from the earth surface and received from
    the receiver satellite. Than a refracted signal is emitted
    from the transmitter satellite with the same signal emission
    angle as the non refracted signal. The refracted signal will
    not hit the receiver satellite at the same position as the non
    refracted signal. Hence, the singal emission angle of the
    refracted signal is changed until it hits the receiver
    satellite at the same position as the refracted signal does.
    The path length, the signal emission angle and the position of
    the reflection point are compared.
%
%
% Josef Bauchinger, TU Graz, 01031012
%
% 12.1.2018
%
%% Program Code

clear all;
close all;

% ——determination of parameters——
```

A. Program codes

```matlab
h_T = 20000;                          % heigth transmitter
    satellite [km]
h_R = 600;                            % heigth reeiver sat [km]
h_natmos = 100;                       % height of neutral
    atmmosphere [km]
h_ionos_start = 60;                   % start height of ionosphere
    [km]
h_ionos_end = 2000;                   % height of ionosphere [km]
h_0 = 0;                              % height surface earth [km]
x_T = 0;                              % horizontal distance
    transmitter satellite [km]
theta_T_input = [1,20,40,60,85];      % signal emission angle
    transmitter satellite [degree]
theta_T = deg2rad(theta_T_input);     % convert degree to radian
nele_theta_T = numel(theta_T);
nu = 1.57542e9;                         % GPS L1-frequency [Hz]

% ---get electron density distribution---
fileID = fopen('Ne_Graz_60km_5km_2000km.txt','r');
%source: https://omniweb.gsfc.nasa.gov/vitmo/iri2012_vitmo.html
% file format:
%   1st column:    atmospheric height [km]
%   2nd column:    electron density [1/m^3]
%   3rd column:    Ne to NmF2
Ne_file = fscanf(fileID,'%f %f',[3 inf]);
fclose(fileID);
Ne = (Ne_file(2,:))';

% ---get height step size---
h_step = (Ne_file(1,2)-Ne_file(1,1));   % [km]

% ---calculate the refraction indices for the atmosphere
    (n_atmos), the neutral atmosphere (n_natmos) and the
    ionosphere (n_Gion)---
%--determine the height vector--
% -earth surface to transmitter satellite-
% above the ionosphere is no refractioin -> only one step to h_T
h = [h_0:h_step:h_ionos_end,h_T]';   % [km]

% --calculate the refraction indices--
[n_atmos,n_natmos,n_Gion] = n_calculation
    (h,Ne,nu,h_natmos,h_ionos_start,h_ionos_end);

% ---determine vectors for path calculation---
% this are empty vectors in which to store the calculation results
% --height vectors--
% -transmitter satellite to earth surface-
% above the ionosphere is no refractioin -> only one step to h_T
```

```matlab
h1 = [h_T,h_ionos_end:-h_step:h_o]';      % [km]

% -earth surface to receiver satellite-
h2 = (0:h_step:h_R)';                     % [km]

% --refraction indices--
% -transmitter satellite to reflection point-
% the last element is only required for the spherical earth
n1 = flipud(n_atmos(1:end-1));

% -reflection point to receiver satellite-
n2 = n_atmos(1:numel(h2)-1);


%% Calculation for the non refracted signal

% ---calculate the horizontal distances ---
% -transmitter satellite to refelction point-
x_in = (h_T-h_o)*tan(theta_T) + x_T;      % [km]

% -reflection point to receiver satellite-
x_R = (h_R-h_o)*tan(theta_T) + x_in;      % [km]

% ---calculate the path lengths--
% -transmitter satellite to reflection point-
PL_TS = (h_T-h_o)./cos(theta_T);          % [km]

% -reflection point to receiver satellite-
PL_SR = (h_R - h_o)./cos(theta_T);        % [km]

% -total non refracted path length-
PL = PL_TS + PL_SR;                       % [km]


%% Calculation for the refracted signal

% -step size for the variation of the signal emission angle-
theta1_step_input = 0.005;                % [degree]
theta1_step = deg2rad(theta1_step_input);

% -accuracy within the refracted signal has to hit the position
%    of the cube satellite for the non refracted signal-
accuracy = 0.001;                         % [km]

% ---calculation of the rafracted path--
for l = 1:numel(theta_T)
    [x1(:,l),x2(:,l),theta1(:,l),theta2(:,l),PL1(:,l),PL2(:,l),
    iterations(:,l)] = refracted_path_flat_earth
```

```
    (h1,h2,n1,n2,x_T,theta_T(l),theta1_step ,x_R(l),accuracy);
end

% ——calculation of required results——
% —horizontal distances—
% —transmitter satellite to reflection point—
x_S_diff = abs(x_in − x1(end ,:));

% —reflection point to cube satellite—
x_R_diff = abs(x_R − x2(end ,:));

% ——calculation of whole path length——
% —transmitter satellite to reflection point—
PL_TSrefracted = sum(PL1);

% —reflection point to receiver satellite—
PL_SRrefracted = sum(PL2);

% —whole refracted path length
PL_refracted = PL_TSrefracted + PL_SRrefracted;

% —difference between  non refracted and refracted path length—
PL_diff = abs(PL − PL_refracted);
```

A.1.1. Function: Calculation refraction index

```
%% Calculation of refraction indices
% This funciton calculates the refraction index of the neutral
    atmosphere and of the ionosphere. As well as it combines both
    refraction indices to the refraction index of the atmosphere.
%
% Input:
%   h...                height vector of atmosphere,
%   Ne...               electron density vector,
%   nu...               frequency of the electromagnetic wave,
%   h_natmos...         height of neutral atmosphere,
%   h_ionos_start...    start height of ionosphere,
%   h_ionos_end...      end height of ionosphere,
%
% Output:
%   n_atmos...          refraction index of the atmosphere,
%   n_natmos...         refraction index of the neutral
    atmosphere,
%   n_Gion...           refractino indes of the ionosphere,
%
%
% Josef Bauchinger, TU Graz, 01031012
```

```matlab
%
% 12.1.2018
%
%% Function code
function [n_atmos,n_natmos_mod,n_Gion_mod] = ...
    n_calculation(h,Ne,nu,h_natmos,h_ionos_start,h_ionos_end)

% —check the input—
if nargin < 6
    disp('n_calculation ERROR: Not enough input arguments');
    return
end

% ——find elements of zone boundary——
bele_natoms = find(h==h_natmos);
bele_ionos_start = find(h==h_ionos_start);
bele_ionos_end = find(h==h_ionos_end);

% ——calculate the refraction index of the neutral atmosphere
%   (n_natmos)——
% the calculation is done according to ITU recommendations ITU–R
%   P.453−13 and ITU–R P.835−6

% —calculate temperature (T), atmospheric pressure (p) and water
%   vapour pressure (p_w)—
% see ITU–R P.835−6
% −transform geometric heights to geopotential heights−
% until geometric heights of 86 km geopotential heights are
%   required for the calculation
bele_geop = find(h < 86.001,1,'last');
h_geop = 6356.766*h(1:bele_geop)./(6356.766+h(1:bele_geop));

% −find elments of calculation steps of T and p−
ele11 = find(h_geop < 11.001,1,'last');
ele20 = find(h_geop < 20.001,1,'last');
ele32 = find(h_geop < 32.001,1,'last');
ele47 = find(h_geop < 47.001,1,'last');
ele51 = find(h_geop < 51.001,1,'last');
ele71 = find(h_geop < 71.001,1,'last');
ele84 = find(h_geop < 84.853,1,'last');
ele86 = find(h_geop < 86.001,1,'last');
ele91 = find(h < 91.001,1,'last');
ele100 = find(h < 100.001,1,'last');

% −calculate T in [K]−
T = zeros(ele100,1);
T(1:ele11) = 288.15 − 6.5*h_geop(1:ele11);
T(ele11+1:ele20) = 216.65;
```

```matlab
T(ele20+1:ele32) = 216.65 + (h_geop(ele20+1:ele32)-20);
T(ele32+1:ele47) = 228.65 + 2.8*(h_geop(ele32+1:ele47)-32);
T(ele47+1:ele51) = 270.65;
T(ele51+1:ele71) = 270.65 - 2.8*(h_geop(ele51+1:ele71)-51);
T(ele71+1:ele84) = 214.65 - 2*(h_geop(ele71+1:ele84)-71);
T(ele84+1:ele91) = 186.8673;
T(ele91+1:ele100) = 263.1905 - ...
    sqrt(1-((h(ele91+1:ele100)-91)/19.9429).^2);

% -calculate p in [hPa]-
p = zeros(ele100,1);
p(1:ele11) = 1013.25 * (288.15./T(1:ele11)).^(-34.1632/6.5);
p(ele11+1:ele20) = 226.3226 *
    exp(-34.1632*(h_geop(ele11+1:ele20)-11) ./ T(ele11+1:ele20));
p(ele20+1:ele32) = 54.7498 *
    (216.65./T(ele20+1:ele32)).^(34.1632);
p(ele32+1:ele47) = 8.680422 *
    (228.65./T(ele32+1:ele47)).^(34.1632/2.8);
p(ele47+1:ele51) = 1.109106 *
    exp(-34.1632*(h_geop(ele47+1:ele51)-11) ./ T(ele47+1:ele51));
p(ele51+1:ele71) = 0.6694167 *
    (270.65./T(ele51+1:ele71)).^(-34.1632/2.8);
p(ele71+1:ele84) = 0.03956649 *
    (214.65./T(ele71+1:ele84)).^(-34.1632/2.0);
pa0 = 95.571899;
pa1 = -4.011801;
pa2 = 6.424731e-2;
pa3 = -4.789660e-4;
pa4 = 1.340543e-6;
p(ele84+1:ele100) = exp(pa0 + pa1*h(ele84+1:ele100) +
    pa2*h(ele84+1:ele100).^2 + pa3*h(ele84+1:ele100).^3 +
    pa4*h(ele84+1:ele100).^4);

% -calculate p_w in [hPa]-
p_w_rhoo = 7.5; % [g/m^3]
p_w_ho = 2;     % [km]
p_w_rho = p_w_rhoo*exp(-h(1:ele100)/p_w_ho);
p_w = p_w_rho.*T/216.7;

% --calculate n_atmos--
N_natmos = zeros(numel(h),1);
N_natmos(1:ele100) = 77.6e-6./T.*(p+4810*p_w./T);
n_natmos = 1 + N_natmos;

% ---calculate the refraction index of the ionosphere (n_Gion)---
N_Gion = zeros(numel(h),1);
N_Gion(bele_ionos_start:bele_ionos_end) = ...
    40.3*Ne./h(bele_ionos_start:bele_ionos_end)/nu^2;
```

```
n_Gion = 1+ N_Gion;

% ——calculate the refraction index of the atmosphere (n_atmos)——
n_atmos = 1 + N_natmos + N_Gion;
% the second to last element has to be one, because it is theone
    between the end of the ionosphere and the GNSS satellite
n_atmos(end−1) = 1;

% ——modify n_natmos and n_Gion for output——
n_natmos_mod = n_natmos(1:bele_natoms);
n_Gion_mod = n_Gion(1:bele_ionos_end);
```

A.1.2. Function: Calculation refracted path for flat Earth

```
%% Calculation of refracted path for flat Earth
% This funciton calculates the path of the refracted signal for
    the flat earth model
%
% Input:
%   h1...            height vector transmitter satellite to
    reflection point,
%   h2...            height vector reflection point to receiver
    satellite,
%   n1...            refraction indices vector transmitter
    satellite to reflection
%   point,
%   n2...            refraction indices vector reflection point to
    receiver,
%   satellite,
%   x_T...           horizontal position of transmitter satellite,
%   theta_T...       signal emission angle,
%   theta1_step...   step size to meet required accuracy,
%   x_R...           horizontal distance transmitter satellite to
    receiver satellite
%   for non refracted signal,
%   accuracy...      difference between horizontal distance to
    receiver
%   satellite of refracted and non refracted path
%
% Output:
%   x1...            horizontal distances vector transmitter
    satellite to
%   reflection point,
%   x2...            horizontal distances vector reflection point
    to
%   receiver satellite,
```

A. Program codes

```
%   theta1...        refraction angles vector transmitter
    satellite to reflection
%   point,
%   theta2...        refraction angles vector reflection point to
    receiver
%   satellite,
%   PL1...           path lenght vector transmitter satellite to
    reflection point,
%   PL2...           path lenght vector reflection point to
    receiver satellite,
%   iterations...    number of iterations for calculation,
%
%
% Josef Bauchinger, TU Graz, 01031012
%
% 12.1.2018
%
%% Function code
function [x1,x2,theta1,theta2,PL1,PL2,iterations] =
    refracted_path_flat_earth
    (h1,h2,n1,n2,x_T,theta_T,theta1_step, x_R,accuracy)

% ---check the input---
if nargin < 9
    disp('refracted_path ERROR: Not enough input arguments');
    return
end

% ----determine vectors for path calculation----
% this are empty vectors in which to store the calculation
    results in

% ---horizontal distance vectors---
% -transmitter satellite to reflection point-
x1 = zeros(size(h1));                    % [km]
% horizontal position of transmitter satellite
x1(1) = x_T;

% -reflection point to receiver satellite-
x2 = zeros(size(h2));                    % [km]

% ---refraction angles---
% -transmitter satellite to reflection  point---
theta1 = zeros(numel(h1)-1,1);          % [rad]

% -reflection point to receiver satellite-
theta2 = zeros(numel(h2)-1,1);          % [rad]
```

```matlab
% ---path length vectors---
% -transmitter satellite to reflection point-
PL1 = zeros(size(theta1));              % [km]

% -reflection point to receiver satellite-
PL2 = zeros(size(theta2));              % [km]

% ---calculation of refracted path---
% -set start signal emission angle-
theta1(1) = theta_T;

% -set iterations to 1-
iterations = 1;

% ---calculate the refracted path---
while 1
    % -transmitter satellite to reflection point-
    for l = 1:numel(h1)-2
        x1(l+1) = tan(theta1(l))*(h1(l)-h1(l+1)) + x1(l);
        theta1(l+1) = asin(n1(l)*sin(theta1(l))/n1(l+1));
        PL1(l) = (h1(l)-h1(l+1))/cos(theta1(l));
    end
    % calculation of x1(end) and PL1(end) because the for-loop
    has one
    % step too less
    x1(end) = tan(theta1(end))*(h1(end-1)-h1(end)) + x1(end-1);
    PL1(end) = (h1(end-1)-h1(end))/cos(theta1(end));

    % -reflection point to receiver satellite-
    x2(1) = x1(end);
    theta2(1) = theta1(end);
    for l = 1:numel(h2)-2
        x2(l+1) = tan(theta2(l))*(h2(l+1)-h2(l)) + x2(l);
        theta2(l+1) = asin(n2(l)*sin(theta2(l))/n2(l+1));
        PL2(l) = (h2(l+1)-h2(l))/cos(theta2(l));
    end
    % calculation of x2(end) and PL2(end) because the for-loop
    has one
    % step too less
    x2(end) = tan(theta2(end))*(h2(end)-h2(end-1)) + x2(end-1);
    PL2(end) = (h2(end)-h2(end-1))/cos(theta2(end));
    % calculation of the difference between the point where the
    non
    % refracted and the
    % refracted signal would hit the receiver satellite
    x_diff2 = x_R - x2(end);

    % check if the refracted signal meets the receiver satellite
```

```
    at the
% same point as
% the non refracted signal does,
 if abs(x_diff2)  < accuracy
      break
 elseif imag(x_diff2) ~= 0
      theta1_step = theta1_step/2;
      theta1(1) = theta_T + theta1_step;
 elseif x_diff2 < accuracy
      theta1_step = theta1_step/2;
      theta1(1) = theta_T + theta1_step;
 elseif x_diff2 > 0
      theta1(1) = theta1(1) + theta1_step;
 end

% loop counter to prevent infinite loop
 if iterations > 100000
      disp('refracted_path_flat_earth ERROR: to much
 iterations');
      break
 end
 iterations = iterations + 1;
end
```

A.2. Main program: Influence of atmosphere on refraction, spherical Earth

```
%% Influence of atmosphere on refraction, spherical Earth
% This program calculates the refraction of an electromagnetic
   wave propagating trough the earth atmosphere for an assumed
   spherical Earth. The wave is emitted at a transmitter
   satellite, reflected by the earth surface and than received
   from a receiver satellite. The purpose of the program is to
   investigate the influence of the refraction on the path
   length, the signal emission angle and the position of the
   reflection point. Therefore, a non refracted signal with a
   given signal emission angle is emitted from the transmitter
   satellite, reflected from the earth surface and received from
   the receiver satellite. Than a refracted signal is emitted
   from the transmitter satellite with the same signal emission
   angle as the non refracted signal. The refracted signal will
   not hit the receiver satellite at the same position as the non
   refracted signal. Hence, the singal emission angle of the
   refracted signal is changed until it hits the receiver
   satellite at the same position as the refracted signal does.
```

    The path length, the signal emission angle and the position of
    the reflection point are compared.
```
%
%
% Josef Bauchinger, TU Graz, 01031012
%
% 12.1.2018
%
%% Begin programm
clear all;
close all;

% ——determination of parameters——
r_0 = 6371;                          % radius earth [km]
h_T = 20000;                         % height transmitter
    satellite [km]
h_R = 600;                           % height receiver satelllite
    [km]
h_natmos = 100;                      % height of neutral
    atmmosphere [km]
h_ionos_start = 60;                  % start height of ionosphere
    [km]
h_ionos_end = 2000;                  % height of ionosphere [km]
h_0 = 0;                             % height surface earth [km]
x_T = 0;                             % horizontal distance
    transmitter satellite [km]
theta_T_input =
    [1,2,3,4,5,6,7,8,9,10,11,12,13,13.5,13.9,13.95,13.97]; %
    signal emission angle transmitter satellite [degree]
theta_T = deg2rad(theta_T_input);    % convert degree to radian
nele_theta_GNSS = numel(theta_T);
f = 1.57542e9;                       % GPS L1-frequency [Hz]


r_T = r_0 + h_T;
r_R = r_0 + h_R;

% ——get electron density distribution——
fileID = fopen('Ne_Graz_60km_5km_2000km.txt','r');
%source: https://omniweb.gsfc.nasa.gov/vitmo/iri2012_vitmo.html
% file format:
%   1st column:    atmospheric height [km]
%   2nd column:    electron density [1/m^3]
%   3rd column:    Ne to NmF2
Ne_file = fscanf(fileID,'%f %f',[3 inf]);
fclose(fileID);
Ne = (Ne_file(2,:))';

% ——get height step size——
```

A. Program codes

```matlab
h_step = (Ne_file(1,2)-Ne_file(1,1));    % [km]

% ---calculate the refraction indices for the atmosphere
    (n_atmos), the neutral atmosphere (n_natmos) and the
    ionosphere (n_Gion)---
%--determine the height vector--
% -earth surface to transmitter satellite-
% above the ionosphere is no refraction -> only one step to h_T
h = [h_0:h_step:h_ionos_end,h_T]';    % [km]

% --calculate the refraction indices--
[n_atmos,n_natmos,n_Gion] = n_calculation
    (h,Ne,f,h_natmos,h_ionos_start,h_ionos_end);

% ---determine vectors for path calculation---
% this are empty vectors in which to store the calculation results
% --height vectors--
% -transmitter satellite to earth surface-
% above the ionosphere is no refraction -> only one step to h_T
h1 = [h_T,h_ionos_end:-h_step:h_0]';            % [km]
r1 = h1 + r_0;

% -earth surface to receiver satellite-
h2 = (0:h_step:h_R)';                       % [km]
r2 = h2 + r_0;

% --refraction indices--
% -transmitter satellite to reflection point-
n1 = flipud(n_atmos);

% -reflection point to receiver satellite-
n2 = n_atmos(1:numel(h2));


%% Calculation for the non refracted signal

% ---calculate the incidence angle---
% -at reflection point-
theta_in = asin(sin(theta_T)*r_T/r_0);

% -at receiver satellite-
theta_R = asin(sin(theta_in)*r_0/r_R);

% ---calculate location angle---
% -for reflection point-
phi_S = theta_in - theta_T;

% -for receiver satellite-
```

```matlab
phi_R = phi_S + theta_in − theta_R ;

% −−−−calculate the horizontal distances−−−−
% −transmitter satellite to reflection point−
x_S = r_o∗phi_S ;

% −reflection point to recevier satellite−
x_R = r_o∗phi_R ;

% −−−−calculate the path lengths−−−−
% −transmitter satellite to reflection point−
PL_TS = sqrt(r_T^2 + r_o^2 − 2∗r_T∗r_o∗cos(phi_S)) ;

% −reflection point to reeiver satellite
pl_SR = sqrt(r_R^2 + r_o^2 − 2∗r_R∗r_o∗cos((phi_R−phi_S))) ;

% −total non refracted path length−
PL = PL_TS + pl_SR ;


%% Calculation for the refracted signal

% −step size for the variation of the signal emission angle−
theta1_step_input = 0.005;           % [degree]
theta1_step = deg2rad(theta1_step_input) ;

% −accuracy within the refracted signal has to hit the position
    of the cube satellite for the non refracted signal−
accuracy = 0.001;                       % [km]

% −−−−calculation of the rafracted path−−−−
for l = 1:numel(theta_T)
    fprintf('theta_GNSS: %0.2 f\n',theta_T_input(l)) ;
    [x1(:,l),x2(:,l),theta1(:,l),theta2(:,l),PL1(:,l),PL2(:,l),
    iterations(:,l)] = refracted_path_spherical_earth
    (r1,r2,n1,n2,x_T,theta_T(l),theta1_step,x_R(l),
    r_o,r_T,accuracy) ;
end

% −−−−calculation of required results−−−−
% −−horizontal distances−−
% −transmitter satellite to reflection point−
x_Sdiff = abs(x_S − x1(end,:)) ;

% −reflection point to receiver satellite−
x_Rdiff = abs(x_R − x2(end,:)) ;

% −−calculation of whole path length−−
```

131

```
% −transmitter satellite to reflection point−
PL_TSrefracted = sum(PL1);

% −reflection point to receiver satellite−
PL_SRrefracted = sum(PL2);

% −whole refracted path length
PL_refracted = PL_TSrefracted + PL_SRrefracted;

% −difference between  non refracted and refracted path length−
PL_diff = abs(PL − PL_refracted);
```

A.2.1. Function: Calculation refracted path for spherical Earth

```
%% Calculation of refracted signal for spherical Earth
% This funciton calculates the path of the refracted signal for
    the spherical earth  model
%
% Input:
%   r1...           radius vector transmitter satellite to
    reflection point,
%   r2...           radius vector reflection point to receiver
    satellite,
%   n1...           refraction indices vector transmitter
    satellite to reflection
%    point,
%   n2...           refraction indices vector reflection point to
    receiver satellite,
%   x_T...          horizontal position of transmitter satellite,
%   theta_T...      signal emission angle,
%   theta1_step...  step size to meet required accuracy,
%   x_R...          horizontal distance transmitter satellite to
    receiver satellite
%   for non refracted signal,
%   r_0...          radius of spherical earth,
%   r_T...          orbit radius of transmitter satellite,
%   accuracy...     difference between horiziontal distance to
    receiver
%    satellite of refracted and non refracted path
%
% Output:
%   x1...           horitontal distances vector trasmitter
    satellite to
%    reflection point,
%   x2...           horizontal distances vector reflection point
    to
```

```matlab
%    receiver
%    satellite ,
%    theta1 ...        refraction angles vector transmitter
    satellite to reflection
%    point,
%    theta2 ...        refraction angles vector reflection point to
    receiver
%    satellite ,
%    PL1...            path lenght vector transmitter satellite to
    reflection point ,
%    PL2...            path lenght vector reflection point to
    receiver satellite ,
%    iterations ...    number of iterations for calculation ,
%
%
% Josef Bauchinger , TU Graz , 01031012
%
% 12.1.2018
%
%% Function code
 function [x1,x2,theta1 ,theta2 ,PL1,PL2, iterations ] =
    refracted_path_spherical_earth
    (r1,r2,n1,n2,x_T,theta_T ,theta1_step , x_R,r_0 ,r_T , accuracy )

% —check the input—
 if nargin < 11
     disp ('refracted_path ERROR: Not enough input arguments');
     return
 end

% ——check if signal hits the earth——
% maximum signal emission angle of transmitter satellite , if
    theta_T is higher the signal misses the earth , theta_T_max =
    13.9805 degree = 0.244 rd
 theta_T_max = asind ( r_0/r_T );
 if theta_T >= theta_T_max
     theta_T = theta_T_max − 0.002;
     % −0.002 to avoid rounding errors
 end

% ——determine vectors for path calculation ——
% this are empty vectors in which to store the calculation
    results in
% —refraction angles—
% −transmitter satellite to reflection point−
 beta1 = zeros ( size ( r1 ));             % [rad]

% −reflection point to receiver satellite −
```

A. Program codes

```matlab
beta2 = zeros(size(r2));              % [rad]

% ---horizontal distance vectors---
% -transmitter satellite to reflection point-
x1 = zeros(size(r1));                 % [km]

% -reflection point to receiver satellite-
x2 = zeros(size(r2));                 % [km]

% ---angles after refraction---
% -transmitter satellite to reflection point-
theta1 = zeros(numel(beta1)-1,1);     % [rad]

% -reflection point to receiver satellite-
theta2 = zeros(numel(beta2)-1,1);     % [rad]

% ---angles between horizontal distances---
% -transmitter satellite to reflection point-
phi1 = zeros(size(beta1));            % [rad]

% -reflection point to receiver satellite-
phi2 = zeros(size(beta2));            % [rad]

% ---path length vectors---
% -transmitter satellite to reflection point-
PL1 = zeros(size(theta1));            % [km]

% -reflection point to receiver satellite-
PL2 = zeros(size(theta2));           % [km]

% ----calculation of refracted path----
% -set start signal emission angle-
beta1(1) = theta_T;
%in a height of 20000 km n1(1) = n1(2) so theta1(1) = theta_T
x1(1) = x_T;              % horizontal position of transmitter
    satellite

% -set iterations to 1-
iterations = 1;

% ---calculate the refracted path---
while 1
    % -transmitter satellite to reflection point-
     for l = 1:numel(r1)-1
         % calculation of refraction angles for reflection point
    and transmitter satellite
         beta1(l+1) =
    asin(sin(beta1(l))*n1(l)*r1(l)/(n1(l+1)*r1(l+1)));
```

```matlab
    % calculation of angle after refraction
    theta1(l) = asin(sin(beta1(l))*n1(l)/n1(l+1));        %
Snell's law
    % calculation of angle between transmitter satellite and
reflection point
    phi1(l+1) = beta1(l+1) - theta1(l) + phi1(l);
    % calculation of horizontal distance between transmitter
satellite - reflection point
    x1(l+1) = r_0*phi1(l+1);
    % calculation of path length
    PL1(l) = sqrt(r1(l)^2 + r1(l+1)^2 - ...
        2*r1(l)*r1(l+1)*cos(phi1(l+1)-phi1(l)));        %cosine
rule
 end

% -reflection point to receiver satellite -
 beta2(1) = beta1(end);
 phi2(1) = phi1(end);
 x2(1) = x1(end);
 for l = 1:numel(r2)-1
    % calculation of refraction angles for reflection point
and receiver satellite
    beta2(l+1) =
asin(sin(beta2(l))*n2(l)*r2(l)/(n2(l+1)*r2(l+1)));
    % calculation of angle after refraction
    theta2(l) = asin(sin(beta2(l+1))*n2(l+1)/n2(l));
%Snell's law
    % calculation of angle between receiver satellite and
reflection point
    phi2(l+1) = beta2(l) - theta2(l) + phi2(l);
    % calculation of horizontal distance between receiver
satellite - reflection point
    x2(l+1) = r_0*phi2(l+1);
    % calculation of path length
    PL2(l) = sqrt(r2(l)^2 + r2(l+1)^2 - ...
        2*r2(l)*r2(l+1)*cos(phi2(l+1)-phi2(l)));
    % cosine rule
 end
 x_Rdiff = x_R - x2(end);

% check if the refracted signal meets the receiver satellite
at the same point as the non refracted signal does
 if abs(x_Rdiff) < accuracy
    break
 elseif imag(x_Rdiff) ~= 0
    theta1_step = theta1_step/2;
    beta1(1) = theta_T + theta1_step;
 elseif x_Rdiff < accuracy
```

135

```matlab
        theta1_step = theta1_step /2;
        beta1(1) = theta_T + theta1_step;
    elseif x_Rdiff > 0
        beta1(1) = beta1(1) + theta1_step;
    end

    % loop counter to prevent infinite loop
    if iterations > 100000
        disp('refracted_path_spherical_earth ERROR: to much
    iterations');
        break
    end
    iterations = iterations + 1;
end
```

A.3. Main program: Reflection point calculation (Monte Carlo simulation)

```matlab
%% Reflection point calculation
% This program calculates the difference between a supposed ture
    reflection point and the calculated reflecion points. Out of
    the true reflection points the satellite positions(R,T) for
    given elevations of the satellites are calculated. Out of the
    satellite positions the calculated reflection point is
    calculated by the use of the method Binary Search and the
    method of Scott Gleason.
%
% Josef Bauchinger, 4.12.2017
%
%% Program Code
clear all;
close all;



% ——parameters——
% —WGS84—
% define the semimajor and the semiminor axis for the WGS 84
WGS = wgs84Ellipsoid;
WGS84_a = WGS.SemimajorAxis;
WGS84_b = WGS.SemiminorAxis;
WGS84_eps = WGS.Eccentricity;
WGS84_f = 1/WGS.InverseFlattening;
M = [0,0,0]';       % centre of the Earth
n = 18; %number of grid points of the WGS 84 model
```

```matlab
% ——reflection points——
% —number of refelction points—
n_points = 1000;

% —define the orbit height of the satellites—
h_R = 600e3;      % [m]
h_T = 20000e3;    % [m]
% define semi axis of orbits
a_R = WGS84_a + h_R;
b_R = WGS84_b + h_R;
a_T = WGS84_a + h_T;
b_T = WGS84_b + h_T;


% ——define accuracy of calculation——
% maximum number of itterations for calculation of reflection
    point
maxit = 1000;
% accuracy of Binary Search
accuracy_BS = 0.00001;      % [rad]
% accuracy of Binary Search
accuracy_BSSSP = 0.001;      % [rad]
% accuracy of Scott Gleason
accuracy_SG = 5;          % [m]


% ——declare storage space——
long_deg = NaN(1,n_points,'double');
lat_deg = NaN(1,n_points,'double');
ele_deg = NaN(1,n_points,'double');
S_true = NaN(3,n_points,'double');
S_SG = NaN(3,n_points,'double');
S_BS = NaN(3,n_points,'double');
S_BSSSP = NaN(3,n_points,'double');


% ——define reflection point (S) locations and the elevation of
    the satellites——
% The definition uses rand to generate randomly distributed
    reflection points—
% generate different random numbers each time MATLAB is started
rng('shuffle');
% longitude 0 - 360 degree, start at Greenwich
long_deg = rand(1,n_points)*360;      % [degree]
% latitude +90 degree, start at equator, northern hemisphere
lat_deg = rand(1,n_points)*90;          %[degree]
```

A. Program codes

```matlab
% define satellite elevations between 0 and 15 degree
ele_deg = rand(1,n_points);        % [degree]


% -convert degree to rad-
long = deg2rad(long_deg);
lat = deg2rad(lat_deg);
ele = deg2rad(ele_deg);




% ---calculate grid nods of modelled earth and orbits---
[xE,yE,zE] = ellipsoid(0,0,0,WGS84_a,WGS84_a,WGS84_b,n);




% ---calculation of coordinates of true reflection point and
    satellite
% positions---
[S_true,R,T,N] = RefPt2SatPosRand ...
    (long,lat,ele,WGS84_a,WGS84_b,WGS84_eps,a_R,b_R,a_T,b_T);




% ---calculation of reflection point---
for k = 1:numel(lat)
    % --display calculation step-
    fprintf('calculation step: %i of %i \n',k,numel(lat));


    % ---calculate reflection point with Scott Gleason---
    fprintf('SG\n');
    tic;
    [S_SG(:,k),count_SG(k)] = ScottGleason
    (R(:,k),T(:,k),WGS84_a,WGS84_b,WGS84_f,WGS84_eps,
    accuracy_SG,maxit);
    time_SG(1,k) = toc;


    % ---calculate reflection point with Binary Search---
    fprintf('BS\n');
    tic;
    [S_BS(:,k),count_BS(k)] = BinarySearch
    (R(:,k),T(:,k),WGS84_a,WGS84_a,WGS84_b, accuracy_BS,maxit);
    time_BS(1,k) = toc;


    % ---calculate reflection point with Binary Searc plus
```

```
      Satellite  Sub
      % Point —
       fprintf('BSSSP\n\n');
       tic ;
       [S_BSSSP(:,k),count_BSSSP(k),count_SSP(k)] =
      BinarySearchSatelliteSubPoint
      (R(:,k),T(:,k),WGS84_a,WGS84_b,WGS84_eps,
      accuracy_BSSSP,maxit);
       time_BSSSP(1,k) = toc ;
end
```

```
%% Save  results
save('RefPtCalc20180318_x.mat',
    'S_true','S_BS','S_SG','S_BSSSP','R','T','long_deg','lat_deg',
    'ele_deg','count_BS','count_SG','count_BSSSP','time_BS','time_SG',
    'time_BSSSP','count_SSP');
```

A.3.1. Function: Scott Gleason

```
%% Scott  Gleason
% function  [S] = RT2S_Example1(R,T)
%
% Input:
% R = Receiver  Position  ECEF
% T = GPS  Satellite  Position  ECEF
%   a,b = semi  axis  of  spheroid  (Josef  Bauchinger)
%   f = flattening  of  spheroid  (Josef  Bauchinger)
%   eps = numerical  eccentricity  of  spheroid  (Josef  Bauchinger)
%   accuracy = accuracy  of  calculation  (Josef  Bauchinger)
%   maxit = maximum  number  of  iterations  (Josef  Bauchinger)
% Output:
% S = specular  point  position  ECEF
% iterations = number  of  iterations  needed  (Josef  Bauchinger)
%
%
%
% Copyright  2006  Scott  Gleason,  GNU  GPL
% Adjusted  by  Josef  Bauchinger,  13.3.2018
%
function  [S,iterations] =
    ScottGleason(R,T,a,b,f,eps,accuracy,maxit)

% —check  the  input  (Josef  Bauchinger)—
if  nargin < 8
    disp('ERROR SG: not  enough  input  arguments');
```

```matlab
    return
end

% Initial specular point guess, on the surface directly below R
r = earth_radius(R,a,b,f,eps); %(Josef Bauchinger)
Rmag = norm(R);
Stemp = R*(r/Rmag);
S = Stemp;

% misc
correction = 10000;
%tol = 0.001;      % convergence tolerance, meters
iterations = 0;
rad2deg = 180/pi;
K = 10000;     % correction gain

while correction > accuracy %(Josef Bauchinger)
    iterations = iterations + 1;

  % Take derivatives
  S2R_unit = (R - S)./norm(R-S);
  S2T_unit = (T - S)./norm(T-S);
  % calculate correction direction
  dXYZ = S2R_unit + S2T_unit;

  % apply raw correction
  Stemp = S + K*dXYZ;

  % constrain to Earth surface
  r = earth_radius(Stemp,a,b,f,eps);
  Stemp = (Stemp./norm(Stemp))*r;

  % watch real correction magnitudes, should continually decrease
  correction_temp = abs(norm(S-Stemp));
  correction(iterations) = correction_temp;

  % update estimate of specular point
  S = Stemp;

  % adjust gain based on correction, i.e. if we are getting
    closer, lower correction gain
  if(correction_temp > 10)
    K = 10000;
  else
    K = 1000;
  end
```

```matlab
   if(iterations > maxit)
        disp('ERROR SG: more than maxit iterations'); %(Josef
     Bauchinger)
       break;
   end

end
```

A.3.2. Function: Binary Search for an ellipsoid

```matlab
%% Binary Search for reflection point calculatioin
% This program calculates the reflection point (S) out of two
    given satellite positions (R and T) and the semiaxis of an
    ellipsoid by the use of the Binary Search method for a given
    accuracy.
%
% Input:
%   R ... position of the receiver satellite
%   T ... position of the transmitter satellite
%   a ... 1st semiaxis
%   b ... 2nd semiaxis
%   c ... 3rd semiaxis
%   accuracy ... accuracy
%   maxit ... maximum number of iterations
%
% Output:
%   S_calc ... calculated reflection point
%   count ... number of iterations
%
% Josef Bauchinger, 20.11.2017
%
%% Program Code
 function [S_calc,iterations] =
     BinarySearch(R,T,a,b,c,accuracy,maxit)

% ---check the input---
 if nargin < 7
     disp('ERROR: not enough input arguments');
     return
end

% ---determinate the position right between the two satellites
     (P_BS) and the boundaries for Binary Search---
P_BST = T;
P_BSR = R;
P_BS = R + (P_BST-P_BSR)/2;
dir_BS = P_BS/norm(P_BS);
```

```
% The position (P_BS) is equal to the vector between the centre
    of the Earth and the position in the middle of the two
    satellites and therefore is equal to the direction of the
    straight line (dir_P_BS).

% ---intersect the vector with the earth surface - first guessed
    reflection point (S)---
[S1,S2] = CutStraightWithOrbit([0,0,0]',dir_BS,a,b,c);
S_calc = S1;
% The function "cut_straightwithorbit" returns two positions
    because a straight intersects at two positions with a
    rotational ellipsoid. S1 is the point of intersection in
    positiv direction and S2 in negativ direction. [0,0,0] is the
    centre of the Earth and the space point of the straight line.

% ---calculate reflection angles---
theta_ref = acos((R-S_calc)'*(P_BS-S_calc) /
    (norm(R-S_calc)*norm((P_BS-S_calc))));
theta_in = acos((T-S_calc)'*(P_BS-S_calc) /
    (norm(T-S_calc)*norm((P_BS-S_calc))));
% theta_ref = abs(theta_ref);
% theta_in = abs(theta_in);
% theta_in and theta_red are the incoming and reflected angle at
    the reflection point. At the reflection point, this two angles
    have to be equal to fulfil Snell's law.

% ---determine if angles are equal, otherwise move S---
iterations = 0; %set iteration counter to 0
while abs(theta_ref - theta_in) > accuracy
    % The criterion to perform another loop is, that the
    difference between the incoming and the reflected angle is
    bigger than the accuracy.
    iterations  = iterations + 1;

    if theta_ref < theta_in
        P_BSR = P_BS;
        P_BS = P_BS + (P_BST-P_BSR)/2;
        % If the incoming angle is bigger than the reflected, the
    estimated reflection point has to be moved towards the the
    transmitter satellite.
    elseif theta_in < theta_ref
        P_BST = P_BS;
        P_BS = P_BS - (P_BST-P_BSR)/2;
        % If the relfected angle is bigger than the incoming, the
    estimated reflection point has to be moved towards the
    receiver satellite.
    else
        disp('ERROR BS: angles equal');
```

```matlab
        break
    end

    dir_BS = P_BS/norm(P_BS);
    [S1,S2] = CutStraightWithOrbit([0,0,0]',dir_BS,a,b,c);
    S_calc = S1;
    theta_ref = acos((R-S_calc)'*(P_BS-S_calc) / ...
    (norm(R-S_calc)*norm((P_BS-S_calc))));
    theta_in = acos((T-S_calc)'*(P_BS-S_calc) / ...
    (norm(T-S_calc)*norm((P_BS-S_calc))));
    % theta_ref = abs(theta_ref);
    % theta_in = abs(theta_in);
    % The new reflection point and angles are calculated.

    if iterations > maxit
        disp('ERROR BS: more than maxit iterations');
        break
        % Check if the calculation takes too long.
    else
        continue
    end
end
```

A.3.3. Function: Binary Search for a spheroid enhanced with satellite sub point calculation

```matlab
%% Binary Search for reflection point calculatioin
% This program calculates the reflection point (S) out of two
    given satellite positions (R and T) and the semiaxis of a
    ellipsoid by the use of the Binary Search method. Additionally
    a value for the accuracy is added to ensure a finite
    calculation.
%
% Input:
%   R ... position of the receiver satellite
%   T ... position of the transmitter satellite
%   a ... 1st semiaxis
%   b ... 2nd semiaxis
%   eps ... eccentricity of spheroid
%   accuracy ... accuracy
%   maxit ... maximum number of iterations
%
% Output:
%   S_calc ... calculated reflection point
%   count ... number of iterations
%
% Josef Bauchinger, 15.02.2018
```

```matlab
%
%% Program Code
function [S_calc,iterations,count_SSP] =
    BinarySearchSatelliteSubPoint(R,T,a,b,eps,accuracy,maxit)

% —check the input—
if nargin < 7
    disp('ERROR BSSSP: not enough input arguments');
    return
end


% —determinate the position right between the two satellites
    (P_BS)—
P_BST = T;
P_BSR = R;
P_BS = R + (P_BST-P_BSR)/2;

% —calculate sub point of P_BS —> first esstimated reflection
    point (S)—
[long_PBS,lat_PBS,count_SSP] =
    SatelliteSubPoint(P_BS(1),P_BS(2),P_BS(3),a,b,eps);
[S_calc] = longlat2xyz(long_PBS,lat_PBS,a,eps);

% —calculate reflection angles—
theta_ref = acos((R-S_calc)'*(P_BS-S_calc) /
    (norm(R-S_calc)*norm((P_BS-S_calc))));
theta_in = acos((T-S_calc)'*(P_BS-S_calc) /
    (norm(T-S_calc)*norm((P_BS-S_calc))));
% theta_in and theta_ref are the incoming and reflected angle at
    the reflection point. At the reflection point, this two angles
    have to be equal to fulfil Snell's law.

% —determine if angles are equal, otherwise move S—
iterations = 0; %set iteration counter to 0
while abs(theta_ref − theta_in) > accuracy
    % The criterion to perform another loop is, that the
    difference between the incoming and the reflected angle is
    bigger than the accuracy.
    iterations   = iterations + 1;

    if theta_ref < theta_in
        P_BSR = P_BS;
        P_BS = P_BS + (P_BST-P_BSR)/2;
        % If the incoming angle is bigger than the reflected, the
    estimated reflection point has to be moved towards the the
    transmitter satellite.
        elseif theta_in < theta_ref
```

```
    P_BST = P_BS;
    P_BS = P_BS - (P_BST-P_BSR)/2;
    % If the relfected angle is bigger than the incoming, the
estimated reflection point has to be moved towards the
receiver satellite.
 else
    disp('ERROR BSSSP: angles equal');
    break
 end

 [long_PBS,lat_PBS,count_SSPloop] =
 SatelliteSubPoint(P_BS(1),P_BS(2),P_BS(3),a,b,eps);
 [S_calc] = longlat2xyz(long_PBS,lat_PBS,a,eps);
 count_SSP = count_SSP + count_SSPloop;

 theta_ref =  acos((R-S_calc)'*(P_BS-S_calc) /
 (norm(R-S_calc)*norm((P_BS-S_calc))));
 theta_in = acos((T-S_calc)'*(P_BS-S_calc) /
 (norm(T-S_calc)*norm((P_BS-S_calc))));
 % The new reflection point and angles are calculated.


 if iterations > maxit
    disp('ERROR BSSSP: more than maxit iterations');
    break
    % Check if the calculation takes too long.
 else
    continue
 end
end
```

A.3.4. Function: Calculate satellite positions out of true reflection point

```
%% Calculate Satellite position out of reflection point
% This program calculates the positions of the receiver and
    transmitter satellite out of a given reflection point and the
    elevation and orbital height of the satellites. The direction
    from the reflection point to the satellites is randomly
    calculated.
%
% Input:
%   long ... longitude, vector where each element is a longitude
%   lat ... latitude, vector where each element is a latitude
%   ele ... elevation of the satellites
%   aE ... semimaor axis of the earth model
%   bE ... semiminor axis of the earth model
```

A. Program codes

```matlab
%   epsE... numerical eccentricity of the earth model
%   aR... semimaor axis of the orbit of the receiver satellite
%   bR... semiminor axis of the orbit of the receiver satellite
%   aT... semimaor axis of the orbit of the transmitter satellite
%   bT... semiminor axis of the orbit of the transmitter satellit
%
% Output:
%   S... postion of true reflection point, matrix where each row
%   is a
%   position
%   R... position of the receiver satellite, matrix where each
%   row is a
%   position
%   T... position of the transmitter satellite, matrix where each
%   row is a
%   position
%   N... direction of the surface normal, matrix where each row
%   is a
%   direction
%
% Josef Bauchinger, 3.12.2017
%
%% Proram Code
function [S,R,T,N] =
    RefPt2SatPosRand(long,lat,ele,aE,bE,epsE,aR,bR,aT,bT)

% —check the input—
if nargin < 10
    disp('ERROR: not enough input arguments');
    return
end


% —calculation of [x,y,z] of S out of long and lat—
S = longlat2xyz(long,lat,aE,epsE);


% —calculate surface normal on refelction point—
N = SurfnormEllipsoid(S,aE,aE,bE);


% —calculate direction to satellites—
% —direction A with zero elevation—
dir_A = zeros(size(N));
dir_A(2,:) = -N(3,:);
dir_A(3,:) = N(2,:);
% norm DirA
norm_dirA = sqrt(sum(dir_A.^2));
```

```matlab
norm_dirA = repmat(norm_dirA,3,1);
dir_A = dir_A./norm_dirA;

% −direction B orthogonal to direction A and N−
dir_B = cross(N,dir_A);
% norm DirB
norm_dirB = sqrt(sum(dir_B.^2));
norm_dirB = repmat(norm_dirB,3,1);
dir_B = dir_B./norm_dirB;

% −calculate random direction vector Dir out of DirA and DirB−
% calculate random length in direction A and B
leng_A = −1 +(1+1).*rand(1,numel(dir_A(1,:)));
leng_A = repmat(leng_A,3,1);
leng_B = −1 +(1+1).*rand(1,numel(dir_B(1,:)));
leng_B = repmat(leng_B,3,1);
% calculate direction vector Dir
dir = leng_A.*dir_A + leng_B.*dir_B;
% norm Dir
norm_dir = sqrt(sum(dir.^2));
norm_dir = repmat(norm_dir,3,1);
dir = dir./norm_dir;

% −direction with given elevation−
ele = repmat(ele,3,1);
dir_R = N.*sin(ele)+dir.*cos(ele);
dir_T = N.*sin(ele)−dir.*cos(ele);

% −−calculate position of satellites −−
[R1,R2] = CutStraightWithOrbit(S,dir_R,aR,aR,bR);
[T1,T2] = CutStraightWithOrbit(S,dir_T,aT,aT,bT);

R = R1;
T = T1;
```

A.3.5. Function: Satellite sub point

```matlab
%% Calculate the satellite sub point version 1
% This function calculates the satellite sub point for a spheroid
    given by a and b.
%
% Input:
%   xS, yS, zS...        cartesian coordinates of satellite
%   a...                 1st semiaxis
%   b...                 2nd semiaxis
%   eps...               eccentricity of spheroid
%
```

A. Program codes

```matlab
% Output:
%   longSP, latSP...      longitude and latitude of the satellite
%   subpoint
%   in [rad]
%
% Josef Bauchinger, 25.01.2018
%
%% Program Code
function [longSP,latSP,iterations] = ...
    SatelliteSubPoint(xS,yS,zS,a,b,eps)

% ---check the input---
if nargin < 6
    disp('ERROR: not enough input arguments');
    return
end

% ---calculate longitude---
longSP = atan2(yS,xS);

% ---calculate latitude---
% see https://www.celestrak.com/columns/v02n03/
R = sqrt(xS^2+yS^2);

lat_st = atan2(zS,R);

lati = lat_st;
accuracy = deg2rad(5e-6);
iterations = 0;

C = 1/sqrt(1-eps^2*sin(lati)^2);
latSP = atan((zS+a*C*eps^2*sin(lati))/R);
while abs(latSP-lati) > accuracy
    iterations = iterations + 1;
    lati = latSP;

    C = 1/sqrt(1-eps^2*sin(lati)^2);

    latSP = atan2((zS+a*C*eps^2*sin(lati)),R);

    if iterations > 100
        disp('ERROR satsubpt1: too many iterations');
        break
    end
end
```

A.3.6. Function: Cut straight with orbit

```
%% Intersection of a straight line and an ellipsoid
% This function calculates the intersection point of a straight
    line and the surface of an ellipsoid. The maths behind this
    funciton is to insert the equation of straight line into the
    equation of the ellipsoid.
%
% Input:
%    S... space point of straight line, matrix where each column is
    a space
%    point
%    r... direction of straight line, matirx where each column is a
%    direction vector
%    a  ... 1st semiaxis
%    b  ... 2nd semiaxis
%    c  ... 3rd semiaxis
%
% Output: coordinates of intersection point [x,y,z]
%
% Josef Bauchinger, 4.12.2017
%
%% Program Code
function [I1,I2] = CutStraightWithOrbit(S,r,a,b,c)

% —check the input—
if nargin < 5
    disp('ERROR cut_straightwithorbit: not enough input
    arguments');
    return
end


% —check for row or column vector—
size_S = size(S);
size_r = size(r);
if size_S(1) ~= 3
    disp('ERROR cut_straightwithorbit: wrong size of space point
    matrix S');
end
if size_r(1) ~= 3
    disp('ERROR cut_straightwithorbit: wrong size of direction
    matrix r');
end


% —intermediate calculation—
A = b^2*c^2*r(1,:).^2 + a^2*c^2*r(2,:).^2 + a^2*b^2*r(3,:).^2;
```

```
B = 2*b^2*c^2*S(1,:).*r(1,:) + 2*a^2*c^2*S(2,:).*r(2,:) +
    2*a^2*b^2*S(3,:).*r(3,:);
C = b^2*c^2*S(1,:).^2 + a^2*c^2*S(2,:).^2 + a^2*b^2*S(3,:).^2 -
    a^2*b^2*c^2;
k1 = (-B + sqrt(B.^2-4*A.*C))/(2*A);
k2 = (-B - sqrt(B.^2-4*A.*C))/(2*A);


% --calculate coordinates--
% The intersection point with index 1 is the one in the positiv
    direction.
% The interesction point with index 2 is the one in the negativ
    direction.
% For both intersection points the direction is specified from
    the space
% point.
x1 = S(1,:) + k1.*r(1,:);
y1 = S(2,:) + k1.*r(2,:);
z1 = S(3,:) + k1.*r(3,:);
I1 = [x1;y1;z1];

x2 = S(1,:) + k2.*r(1,:);
y2 = S(2,:) + k2.*r(2,:);
z2 = S(3,:) + k2.*r(3,:);
I2 = [x2;y2;z2];
```

A.3.7. Function: Calculate surface normal

```
%% Surface normal on ellipsoid
% This function calculates the surface normal on a given point
    (S) on an ellipsoid.
%
% Input:
%   S ... points on ellipsoid, each column is a position vector
%   a ... 1st semiaxis
%   b ... 2nd semiaxis
%   c ... 3rd semiaxis
%
% Output:
%   N ... normed surface normal (direction of surface normal)
%         to plot it regarded to S don't forget to add S to N
    (like Nplot = S + N)
%
% Josef Bauchinger, 4.12.2017
%
%% Begin Code
function [N] = SurfnormEllipsoid(S,a,b,c)
```

```matlab
% ---check the input---
if nargin < 4
    disp('ERROR: not enough input arguments');
    return
end


% ---check size of S---
size_S = size(S);
if size_S(1) ~= 3
    disp('ERROR: wrong size of position matrix S');
    return
end


% ---calculate surfac normal---
% generate Matrix with gradient function for ellipsoid
gradientMatrix = repmat([2/a^2;2/b^2;2/c^2],1,numel(S(1,:)));
% calculate surface normals
N = S.*gradientMatrix;
% norm the surface normals
normN = sqrt(sum(N.^2));
normN = repmat(normN,3,1);
N = N./normN;
```

A.3.8. Function: Convert longitude and latitude to x, y and z

```matlab
%% Transform longitude and latitude into cartesian coordinates
% This function calculates the [x,y,z] position of a point on a
%   spheroid surface by input of the geodetic longitude and the
%   latitude.
%
% Input:
%   long ... longitude, vector where each element is a longitude
%   lat ... latitude, vector where each element is a latitude
%   a ... 1st semiaxis
%   eps ... numerical eccentricity
%
% Output:
%   S... position of reflection point in cartesian coordinates
%   [x,y,z]
%
% Josef Bauchinger, 4.12.2017
%
%% Program Code
```

A. Program codes

```matlab
function [S] = longlat2xyz(long,lat,a,eps)

% ---check the input---
if nargin < 4
    disp('ERROR: not enough input arguments');
    return
end


% ---check for row or column vector---
size_long = size(long);
size_lat = size(lat);
if size_long(1) ~= 1
    long = long';
end
if size_lat(1) ~= 1
    lat = lat';
end

% ---calculate the coefficients C1 and C2---
C1 = 1./sqrt(1-eps^2.*sin(lat).^2);
C2 = C1.*(1-eps^2);

% ---calculate x,y,z and S---
x = a.*C1.*cos(lat).*cos(long);
y = a.*C1.*cos(lat).*sin(long);
z = a.*C2.*sin(lat);

S = [x;y;z];
```

List of Figures

List of Tables

Nomenclature

$\bar{C}_{2,0}$ normalized second degree zonal gravitational coefficient

ϵ numerical eccentricity of an ellipse of an ellipsoid

μ Earth's gravitational constant

ν frequency of the GNSS signal

ω_E truncated angular velocity of the Earth

$\overrightarrow{MS_{calc}}$ vector between the centre of the Earth and the calculated reflection point

$\overrightarrow{MS}$ vector between the centre of the Earth and the true reflection point

$\overrightarrow{S_{calc}R}$ vector between the calculated reflection point and the receiver satellite

$\overrightarrow{SR}$ vector between the true reflection point and the receiver satellite

$\overrightarrow{SS_{calc}}$ vector between the true and the calculated reflection point

$\overrightarrow{TR}$ vector between the transmitter and the receiver satellite

$\overrightarrow{TS_{calc}}$ vector between the transmitter satellite and the calculated reflection point

$\overrightarrow{TS}$ vector between the transmitter satellite and the true reflection point

ϕ and λ angles used to perform a coordinate transformation from geocentric coordinates to Cartesian coordinates

ρ density of atmosphere

ρ_0 standard ground level water vapour density

θ_{in} angle of incidence at the reflection point

θ_{ref} reflected angle at the reflection point

θ_{Tmax} maximum signal emission angle at the transmitter satellite for the spherical earth model related to nadir

$\theta_{Trefracted}$ superelevated signal emission angle at transmitter satellite for the refracted signal

θ_R angle of incidence at the receiver satellite for the non refracted signal

θ_T signal emission angle at transmitter satellite for the non refracted signal related to nadir

φ and λ angles used to perform a coordinate transformation from geodetic coordinates toe ECEF Cartesian coordinates

a, b and c semi axes of an ellipsoid

$accuracy_{BSSSP}$ accuracy / stopping criteria for the method BSSSP

$accuracy_{BS}$ accuracy / stopping criteria for the method BS

$accuracy_{SG}$ accuracy / stopping criteria for the method SG

c speed of light in vacuum

e linear eccentricity of an ellipse of an ellipsoid

ele elevation of the transmitter and the receiver satellite over the horizontal plane of the true reflection point

f flattening of an ellipse of an ellipsoid

h height above the earth surface

h height difference to the WGS 84 surface

h' geopotential height above earth surface

h_0 scale height above earth surface

h_R altitude of the receiver satellite

h_{step} height step size for the boundaries between the layers of the atmosphere

h_T altitude of the transmitter satellite

hd_R horizontal distance to the receiver satellite for the non refracted signal for the spherical earth model

$hd_R refracted$ horizontal distance to the receiver satellite for the refracted signal for the spherical earth model

hd_S horizontal distance to the reflection point for the non refracted signal for the spherical earth model

$hd_S refracted$ horizontal distance to the reflection point for the refracted signal for the spherical earth model

hd_{Rdiff} difference between the refracted and the non refracted horizontal distance from the transmitter satellite to the receiver satellite for the spherical earth model

hd_{Sdiff} difference between the refracted and the non refracted horizontal distance from the transmitter satellite to the reflection point for the spherical earth model

hd_T horizontal distance to the transmitter satellite for the spherical Earth

K update gain for *Scott Gleason*

maxit   maximal number of iterations a method is allowed to need for the reflection point calculation

n refraction index

N_e electron density of atmosphere

N_S surface normal on earth surface at true reflection point

n_{atmos} refraction index of the atmosphere

n_{Gion} group refraction index of the ionosphere

n_{ion} refraction index of the ionosphere

n_{natmos} refraction index of the neutral atmosphere

n_{points} number of calculated reflection points

N_{Scalc} surface normal on earth surface at calculated reflection point

p atmospheric pressure

p_w water vapour pressure of the atmosphere

P_{BS} point on $\overrightarrow{TR}$ for the method BS

PL total path length for the non refracted signal

PL_{diff} difference between the refracted and the non refracted total path length

$PL_{SRrefracted}$ path length from the reflection point to the receiver satellite for the refracted signal

PL_{SR} path length from the reflection point to the receiver satellite for the non refracted signal

$PL_{TSrefracted}$ path length from the transmitter satellite to the reflection point for the refracted signal

PL_{TS} path length from the transmitter satellite to the reflection point for the non refracted signal

$PLrefracted$ total path length for the refracted signal

R position of the receiver satellite

r_R radius of circular receiver satellite orbit

r_T radius of circular transmitter satellite orbit

r_0 average earth radius for the Earth modelled as a sphere

S position of the true reflection point / specular point

S' improved reflection point for *Scott Gleason*

S_n estimated reflection point for *Scott Gleason*

SP_d direct signal path from the transmitter to the receiver satellite

SP_r true earth-reflected signal path from the transmitter to the receiver satellite

SP_{diff} difference between the signal path of the signal reflected at the calculated reflection point and the signal path of the signal reflected at the true reflection point $(SP_r - SP_{rcalc})$

SP_{diff} signal path difference between the true reflected signal path (SP_r) and the calculated reflected signal path (SP_{rcalc})

SP_{rcalc} calculated earth-reflected signal path from the transmitter to the receiver satellite

SS_{calc} distance between the true and the calculated reflection point

T position of the transmitter satellite

T_{atmos} absolute temperature of the atmosphere

$theta_{Trefracted}$ signal emission angle for the refracted signal related to nadir

v speed of light in a specific medium

x_R horizontal distance to receiver satellite for the non refracted signal for the flat earth model

x_S horizontal distance to reflection point for the non refracted signal for the flat earth model

x_T horizontal distance to transmitter satellite for the flat earth model

x_{Rdiff} difference between the refracted and the non refracted horizontal distance from the transmitter satellite to the receiver satellite for the flat earth model

$x_{Rrefracted}$ horizontal distance to receiver satellite for the refracted signal for the flat earth model

x_{Sdiff} difference between the refracted and the non refracted horizontal distance from the transmitter satellite to the reflection point for the flat earth model

$x_{Srefracted}$ horizontal distance to reflection point for the refracted signal for the flat earth model

BS   abbreviation for the method *Binary Search for an ellipsoid*

BSSSP abbreviation for the method *Binary Search for a spheroid enhanced with satellite sub-point calculation*

ECEF Earth Centered Earth Fixed coordinates

EGM 96 geoid related to WGS 84

ESA   European Space Agency

FE   Finite elements

GNSS Global Navigation Satellite System

GNSS-R Global Navigation Satellite System Reflectometry

M   centre of the Earth

nadir plumb line direction of the satellite

PARIS Passive Reflectometry and Interferometry System

PRETTY Passive REflectomeTry and dosimeTrY

PRN   pseudo random noise

SG   abbreviation for the method *Ellipsoidal Earth* from Scoot Gleason

SNR   signal to noise ratio

TEC   total electron count of ionosphere

WGS 84 World Geodetic System 1984

Bibliography

Alizadeh, Mahdi M. et al. (2013). "Ionospheric Effects on Microwave Signals". In: *Atmospheric Effects in Space Geodesy* (cit. on pp. 9, 13, 14).

Bronstein, Ilja N. et al. (2008). *Taschnbuch der Mathematik*. German. 7th ed. Harri Deutsch. ISBN: 978-3-8171-2007-9 (cit. on pp. 21, 22).

CliffsNotes (2016). *Geometrical Optics*. URL: https://www.cliffsnotes.com/study-guides/physics/light/geometrical-optics (cit. on p. 28).

Department of defense World Geodetic System 1984 (2000). *DEPARTMENT OF DEFENSE WORLD GEODETIC SYSTEM 1984. Its Definition and Relationships with Local Geodetic Systems*. Tech. rep. National Imaginary and Mapping Agency (cit. on p. 117).

Fischer, Gerd (2017). *Lernbuch Lineare Algebra und Analytische Geometrie*. German. 3rd ed. Springer Spektrum. ISBN: 978-3-658-18190-1 (cit. on p. 18).

Gleason, Scott and Demoz Gebre-Egziabher (2009). *GNSS Applications and Methods*. German. 1st ed. Artech House. ISBN: 978-1-59693-329-3 (cit. on pp. 2, 3, 62, 63, 65, 81, 83, 114).

GrindGIS (2017). *A to Z About Active and Passive Remote Sensing*. URL: http://grindgis.com/remote-sensing/active-and-passive-remote-sensing (cit. on p. 3).

Hakim, Gregory (2017). *Introduction to atmosperic sciences*. URL: https://atmos.washington.edu/~hakim/301/climo_sounding.png (cit. on p. 13).

Heise, Stefan (2002). "Rekonstruktion dreidimensionaler Elektronendichteverteilungen basierend auf CHAMP-GPS-Messungen". Doctor Thesis. FU Berlin, Geowissenschaften (cit. on pp. 9, 10, 13, 14).

Hofmann-Wellenhof, Bernhard, Klaus Legat, and Manfred Wieser (2003). *Navigation*. 1st ed. Springer-Verlag Wien. ISBN: 3-211-00828-4 (cit. on p. 10).

Hofmann-Wellenhof, Bernhard, Herbert Lichtenegger, and James Collins (2001). *GPS. Theory and Practice*. English. 1st ed. Springer-Verlag Wien. ISBN: 3-211-83534-2 (cit. on p. 117).

Hofmann-Wellenhof, Bernhard, Herbert Lichtenegger, and Elmar Wasle (2008). *GNSS*. English. 1st ed. Springer-Verlag Wien. ISBN: 978-3-211-73012-6 (cit. on pp. 24, 25).

International Terrestrial Reference Frame (2005). *ITRF2005*. URL: http://itrf.ensg.ign.fr/ITRF_solutions/2005/ITRF2005.php (cit. on p. 25).

ITU-R P.453 (2017). *The radio refractive index: its formula and refractivity data. Recommendation ITU-R P.453-13*. Tech. rep. ITU-R Radiocommunication Sector of ITU (cit. on p. 10).

ITU-R P.835 (2017). *Reference standard atmospheres. Recommendation ITU-R P.835-6*. Tech. rep. ITU-R Radiocommunication Sector of ITU (cit. on pp. 11, 13, 34).

Jales, Philip (2012). "Spaceborne Receiver Design for Scatterometric GNSS Reflectometry". Doctor Thesis. Surey Space Center (cit. on pp. 53, 60–64).

Kelso, T. S. (2014). *Orbital Coordinate Systems, Part III*. URL: https://www.celestrak.com/columns/v02n03/ (cit. on pp. 77, 78, 104).

Knuth, Donald E. (1998). *The Art of Computer Programming. Volume 3: Sorting and Searching*. 2nd ed. ISBN: 0-201-89685-0 (cit. on p. 28).

Kostelecký, J., J. Klokocník, and C.A. Wagner (2005). "Geometry and accuracy of reflecting points in bistatic satellite altimetry". In: *Journal of Geodesy* 79 (cit. on p. 4).

Lang, Christian and Norbert Pucker (2005). *Mathematische Methoden in der Physik*. German. 2nd ed. Spektrum. ISBN: 978-3-8274-1558-5 (cit. on pp. 19, 20, 22).

Leick, Alfred (1990). *GPS Satellite Surveying*. English. 1st ed. John Wiley and Sons. ISBN: 0-471-81990-5 (cit. on p. 26).

Mangum, Jeffrey G. and Patrick Wallace (2015). *Atmospheric refractive electromagnetic wave bending and propagation delay*. Tech. rep. The Astronomical Society of the Pacific (cit. on p. 16).

Martin-Neira, M. (1993). "A Passive Reflectometry and Interferometry System (PARIS): Application to Ocean Altimetry". In: *ESA Journal* 17 (cit. on pp. 2, 3, 60, 61).

NASA (2012). *International Reference Ionosphere - IRI-2012*. URL: https://omniweb.gsfc.nasa.gov/vitmo/iri2012_vitmo.html (cit. on pp. 14, 33, 34, 36, 43).

Olivik, S. et al. (2005). *Position of Reflecting Points in Bistatic Satellite Altimetry: Theoretical Solutions for Ellipsoid*. Tech. rep. Czech Technical University in Prague (cit. on pp. 69, 72).

PoleCATS (2017). *Electron density section*. URL: https://rexuscats.wikispaces.com/Science (cit. on p. 15).

Theis, Christian and Winfried Kernbichler (2002). "Grundlagen der Monte Carlo Methoden". German. URL: https://itp.tugraz.at/MML/MonteCarlo/MCIntro.pdf (cit. on pp. 29, 30).

Wickert, Jens (2016). "GNSS reflectometry: Introduction and recent developments". English. URL: ftp://ftp.gfz-potsdam.de/pub/GNSS/workshops/gnss4swec/Summer_School/D1/7_Wickert_Reflect.pdf (cit. on p. 4).

Wikimedia Commons (2004). *Wikimedia Commons*. URL: https://commons.wikimedia.org/wiki/Main_Page (cit. on pp. 26, 29, 71).

Zhu, Yongchao (2017). *GNSS Reflectometry for Sea Ice Detection*. TU Berlin. URL: http://www.gnss.tu-berlin.de/menue/studium_und_lehre/aktuelle_doktorandenprojekte/gnss_reflectometry_for_sea_ice_detection/ (cit. on p. 4).